

**THE ROLE OF DYNAMIN-RELATED PROTEINS IN  
VACUOLE BIOGENESIS IN FISSION YEAST**  
*(Schizosaccharomyces pombe)*

A thesis presented in partial fulfilment of the requirements for  
the degree of

Master of Science  
in  
Biochemistry

At Massey University, Palmerston North,  
New Zealand.

**Sarah Ruth R thlisberger**

**2008**

## ABSTRACT

Dynamins are GTPases concerned with membrane tubulation and scission (Praefcke and McMahon, 2004). In the fission yeast, *Schizosaccharomyces pombe*, the dynamin-related proteins (DRPs) Vps1 and Dnm1 act redundantly in peroxisome biogenesis (Jourdain *et al.*, 2008) but nothing is known about their other cellular roles. Fission yeast cells contain ~20 small, spherical vacuoles that undergo fission or fusion in response to environmental signals (Bone *et al.*, 1998). *S. pombe* cells lacking Vps1 had smaller vacuoles with reduced capacity for fusion in response to hypotonic stress but enhanced fission in response to hypertonic conditions. Unlike wild type, *vps1* $\Delta$  vacuoles showed no change in diameter in response to temperature stress. Vps1-Cgfp localised to the vacuolar membrane both in living cells and in isolated vacuoles. *vps1* $\Delta$  cells showed close to wild type levels of vacuole protein processing and normal actin organisation and endocytosis. Overexpression of Vps1 caused a global transformation of vacuoles from spherical to tubular. Spherical vacuoles were restored by repression of *vps1* expression or by induction of vacuole fusion. Tubulation was blocked in the presence of GTP $\gamma$ S and in a *vps1* mutant that lacked the entire GTPase domain. Vacuole tubulation was more extensive in the absence of a second DRP, Dnm1. The absence of Dnm1 abolished the hyper fission phenotype of *vps1* $\Delta$ , whereas overexpression of Dnm1 induced vacuole fission. These results are consistent with a model of vacuole fission in which Vps1 creates a tubule of an appropriate diameter for subsequent scission by another DRP. Preliminary evidence suggests that Dnm1 serves the latter role.

## ACKNOWLEDGEMENTS

There are many people I would like to thank. Firstly, I owe a big thank you to my supervisor Professor Jeremy Hyams, who supported and encouraged me the whole way through. I could not have imagined having a better supervisor! You have made me a pombe fan for life. Thank you to Dr Isabelle Jourdain for being such a great “little boss” and putting up with all my questions. You have taught me so many things. Thank you! Also, thanks to Chad for providing endless entertainment (sometimes at your expense) and practical help.

I gratefully acknowledge financial support from a Massey University Masterate scholarship.

Finally, I would like to thank my family and friends, wherever they are. Thanks to Bruce and Brenda for being my adoptive parents in New Zealand. To John, Raich, Ant, Dave and Lolita in Wellington: Thank you for your moral support and for all the fun times we spent together. A special thanks to John who helped me in my battle against Word. To Edilson, thank you for being with me each step of the way and for making me laugh in times of stress. I couldn't have done it without you. Lastly, to my parents, who have always given the best of themselves and encouraged me to do my best in all matters of life. To them I dedicate this thesis.

## ABBREVIATIONS

CDCFDA: 5[6]-Carboxy-2',7'-Dichlorofluorescein Diacetate

CPY: Carboxypeptidase Y

DAPI: 4', 6-diamidino-2-phenylindole

DIC: Differential interference contrast

DMSO: Dimethylsulfoxide

DNA: Deoxyribonucleic acid

dNTP: Deoxyribonucleotide triphosphate

DRP: Dynamin-related protein

EDTA: Ethylenediaminetetraacetic acid

EMM: Edinburgh minimal medium

GED: GTPase effector domain

GFP: Green fluorescent protein

GTP: Guanosine triphosphate

Lat-A: Latrunculin A

LB: Luria-Bertani medium

MSA: Minimal supporting agar

MT: Microtubule

*nmt1*: No message in thiamine

OD: Optical density

PBS: Phosphate buffered saline

PCR: Polymerase chain reaction

PEG: Polyethylene glycol

PH: Pleckstrin homology domain

PRD: Proline-rich domain

SH3: Src 3 homology

TBZ: Thiabendazole

Vps: Vacuolar protein sorting

# TABLE OF CONTENTS

	<b>Page</b>
<b>TITLE PAGE</b>	<b>i</b>
<b>ABSTRACT</b>	<b>ii</b>
<b>ACKNOWLEDGEMENTS</b>	<b>iii</b>
<b>ABBREVIATIONS</b>	<b>iv</b>
<b>TABLE OF CONTENTS</b>	<b>v</b>
<b>LIST OF FIGURES</b>	<b>viii</b>
<b>LIST OF TABLES</b>	<b>x</b>
<b>1. INTRODUCTION</b>	<b>1</b>
1.1. THE DYNAMIN SUPERFAMILY	2
1.1.1. Dynamin-related proteins in yeast	3
1.2. DYNAMIN FUNCTION	5
1.2.1. Endocytosis	5
1.2.2. The Golgi complex	7
1.2.3. Peroxisome biogenesis	8
1.2.4. Mitochondrial Division	9
1.2.5. Vacuoles	10
1.2.6. Membrane Tubulation	12
1.2.7. Dynamin GTPase Activity	13
1.3. PROJECT AIMS	15
<b>2. MATERIALS AND METHODS</b>	<b>16</b>
2.1. MOLECULAR BIOLOGY	17
2.1.1. FISSION YEAST PLASMIDS	17
2.1.2. OLIGONUCLEOTIDE PRIMERS	18
2.1.3. POLYMERASE CHAIN REACTION (PCR)	19
2.1.3.1. Standard PCR	19
2.1.3.2. PCR using Expand™ High Fidelity (Roche)	19
2.1.3.3. PCR product purification	20

2.1.4. PLASMID ISOLATION	20
2.1.5. <i>S. pombe</i> DNA ISOLATION	20
2.1.6. DNA QUANTIFICATION	21
2.2. YEAST STRAINS AND CULTURES	21
2.2.1. MEDIA	21
2.2.1.1. Standard rich medium (YES)	21
2.2.1.2. Edinburgh minimal medium (EMM)	21
2.2.1.3. Minimal supporting agar (MSA)	22
2.2.2. YEAST TRANSFORMATION	22
2.2.3. STRAINS	23
2.2.4. GROWTH	24
2.2.4.1. <i>S. pombe</i> growth	24
2.2.4.2. Overexpression of genes under the control of the <i>nmt1</i> promoter	25
2.2.5. FISSION YEAST CLASSICAL GENETICS	25
2.2.5.1. Genetic crosses	25
2.2.5.2. Random spore analysis (RSA)	26
2.3. CELL BIOLOGY	26
2.3.1. STAINING	26
2.3.1.1. Nuclear staining	26
2.3.1.2. Cell wall staining	27
2.3.1.3. Actin staining	27
2.3.1.4. Microtubule immunofluorescence	27
2.3.2. DRUGS	28
2.3.2.1. Latrunculin A	28
2.3.2.2. TBZ	28
2.3.3. VACUOLES	29
2.3.3.1. FM4-64	29
2.3.3.2. CDCFDA	29
2.3.3.3. Vacuole fusion and fission	30
2.3.4. MICROSCOPY AND ANALYSIS	30
2.3.4.1. Electron microscopy	30
2.4. BIOCHEMISTRY	30
2.4.1. CARBOXYPEPTIDASE Y (CPY) ANALYSIS	30
2.4.2. VACUOLE ISOLATION	31

2.4.3. WESTERN BLOT	31
<b>3. RESULTS</b>	<b>33</b>
3.1. VPS1 IN FISSION YEAST	34
3.1.1. Vps1 sequence and domains	34
3.1.2. Vps1 characterisation	34
3.2. VPS1 AND VACUOLE MORPHOLOGY	43
3.2.1. Loss of Vps1 affects vacuole size but not vacuole function	43
3.2.2. Vps1 is involved in vacuole fusion and fission	45
3.2.3. Vps1 is present at the vacuole membrane	47
3.2.4. Overexpression of Vps1 results in vacuole tubulation whilst overexpression of Dnm1 results in vacuole fission	49
3.2.5. Tubular vacuoles are microtubule and actin dependent	52
3.2.6. Vps1 GTPase activity is required for vacuole morphology	56
<b>4. DISCUSSION</b>	<b>59</b>
4.1. Vps1 has different functions in <i>S. pombe</i> and <i>S. cerevisiae</i>	60
4.2. Vps1 is involved in vacuole fission and fusion	61
4.3. Dnm1 acts together with Vps1	62
4.4. Vps1 tubulates vacuoles	63
4.5. GTP hydrolysis by Vps1 is necessary for tubule formation and vacuole fission	63
4.6. The microtubule and actin cytoskeletons regulate tubular vacuoles	64
4.7. A model for vacuole fission in fission yeast	65
<b>5. CONCLUSIONS AND FUTURE PERSPECTIVES</b>	<b>67</b>
<b>6. APPENDICES</b>	<b>70</b>
6.1. PLASMID MAPS	71
6.1.1. pREP41 Vector	71
6.1.2. pREP41-Ngfp Vector	71
6.2. STOCK SOLUTIONS	72
6.3. MANUSCRIPT	73
<b>7. BIBLIOGRAPHY</b>	<b>95</b>

## LIST OF FIGURES

	<b>Page</b>
Figure 1.1. Domain structure of the dynamin superfamily	2
Figure 1.2. Dynamins are involved in many cellular processes	5
Figure 1.3. EM image showing vesiculation at the plasma membrane	6
Figure 1.4. Peroxisomes in dynamin deletion mutants	8
Figure 1.5. Mitochondria in a dynamin mutant	9
Figure 1.6. Dnm1p is arranged as an asymmetric ring around mitochondria	10
Figure 1.7. The balance between vacuole fusion and fission in <i>S. pombe</i>	11
Figure 1.8. Localisation of Vps1p-GFP around the vacuole	11
Figure 1.9. Dynamin-mediated tubulation	12
Figure 2.1. Constructs made in this study	18
Figure 3.1. Vps1 protein sequence alignment	35
Figure 3.2. <i>vps1Δ</i> is slightly temperature sensitive at 36°C	36
Figure 3.3. Vps1 is not required for vacuolar protein sorting	38
Figure 3.4. Vps1 is not required for endocytosis	39
Figure 3.5. Actin patches in <i>vps1Δ</i> are polarised to the growing cell tips, but are more sensitive to Lat-A	40
Figure 3.6. <i>vps1Δ</i> is more resistant to Lat-A	42
Figure 3.7. The absence of Vps1 does not exacerbate an actin phenotype	43
Figure 3.8. Vps1 controls vacuole size	44
Figure 3.9. The dynamin-related proteins Vps1 and Dnm1 are involved in vacuole morphology	46
Figure 3.10. Overexpression of Ngfp-Vps1 and Vps1-Cgfp	48
Figure 3.11. Vps1 localises to the vacuole membrane	49



Figure 3.12. Vps1 induces vacuole tubulation	50
Figure 3.13. Tubular vacuoles	51
Figure 3.14. Dnm1 induces vacuole fission	53
Figure 3.15. Tubular vacuoles are microtubule-dependent	54
Figure 3.16. Tubular vacuoles are actin-dependent	55
Figure 3.17. A disrupted cytoskeleton reduces the formation of tubular vacuoles	56
Figure 3.18. Vps1 GTPase activity is required for vacuole tubulation	57
Figure 3.19. GTP $\gamma$ S blocks tubule formation	58
Figure 4.1. A model for vacuole fission in fission yeast	66

## LIST OF TABLES

	<b>Page</b>
Table 1.1. <i>S. cerevisiae</i> and <i>S. pombe</i> notation	3
Table 1.2. Reported functions of the dynamin-related proteins in <i>Saccharomyces cerevisiae</i> and <i>Schizosaccharomyces pombe</i> .	4
Table 2.1. Plasmids used in this study	17
Table 2.2. Primers used in this study	19
Table 2.3. Strains used in this study	23
Table 3.1 Fusion and fission indices	47
Table 3.2. Mean vacuole diameter in cells treated with GTP $\gamma$ S	57
Table 6.1 Salt Stock (50x)	72
Table 6.2. Vitamin Stock (1000x)	72
Table 6.3. Mineral Stock (10,000x)	72
Table 6.4. Supplements added to the media	72

# 1. INTRODUCTION

---

## 1.1. THE DYNAMIN SUPERFAMILY

---

Dynamins are a highly conserved family of large GTPases that are primarily concerned with membrane scission events (Hinshaw, 2000; Praefcke & McMahon, 2004). All dynamins have three conserved domains which distinguish them from other GTPases. These distinctive features are a large N-terminal GTPase domain involved in binding and hydrolyzing GTP, a poorly characterised middle domain and a C-terminal GTPase effector domain (GED), which regulates GTPase activity and protein oligomerization (Figure 1.1). A common characteristic of dynamins is self-assembly and oligomerisation into ordered structures, such as rings and spirals (Hinshaw, 1999). The GTPase, middle and GED domains are all involved in dynamin self-assembly (Smirnova *et al.*, 1999). Classical dynamins have additional targeting domains, such as the Pleckstrin Homology (PH) and proline-rich domains (PRD) (Figure 1.1), which mediate molecular interactions with proteins containing SH3-domains, phospholipids and other components in the cell (Schmid *et al.*, 1998). Some dynamin genes are alternatively spliced to yield a number of different isoforms, which are directed to specific compartments. For example, using a GFP-fusion of dynamin 1, it was found that one splice variant localises to clathrin-coated pits, while another isoform localises to the Golgi (Cao *et al.*, 1998). Thus, targeting information in dynamins may also be provided by regions of alternative splicing.

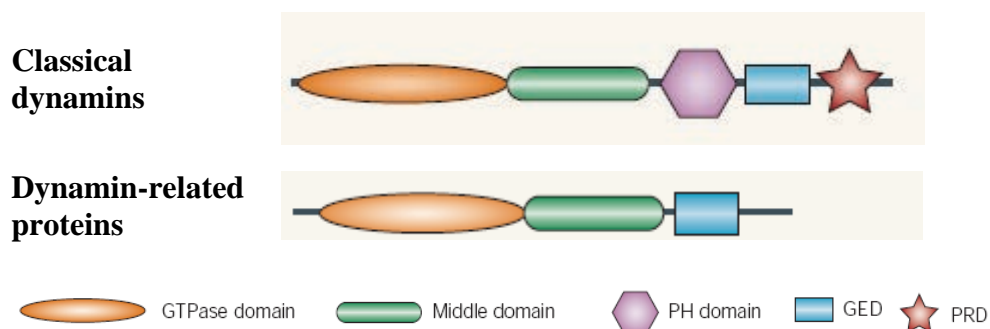


**Figure 1.1. Domain structure of the dynamin superfamily**  
(Praefcke and McMahon, 2004)

The dynamin family includes other unconventional dynamin-related proteins (DRPs) that share high homology with dynamins in their N-terminal GTPase domain but less or no sequence conservation in other regions. These DRPs lack the PRD and PH

domains (Figure 1.1). All superfamily members share a high degree of homology in the first 300-400 amino acids, corresponding to the GTPase domain, and have three highly conserved GTP-binding consensus sites: GXXXXGKS, DXXG and TKXD (Dever *et al.*, 1987; Obar *et al.*, 1990).

### 1.1.1. Dynamin-related proteins in yeast

Yeast has no classical dynamin *per se*, but rather has several dynamin-related proteins, which lack structural elements found in classical dynamins, such as the PH and PRD domains. The budding yeast, *Saccharomyces cerevisiae*, has been one of the main model organisms used to study these DRPs. Budding yeast has three dynamin-related proteins: Mgm1p, Dnm1p and Vps1p. Mgm1p and Dnm1p, are concerned with mitochondrial membrane fusion and fission (Shaw and Nunnari, 2002), as well as an additional role for Dnm1p in peroxisome biogenesis (Kuravi *et al.*, 2006). Vps1p, on the other hand, has a number of cellular roles including vacuolar protein sorting (Vater *et al.*, 1992), growth and endocytosis at high temperatures (Rothman *et al.*, 1990), secretion (Gurunathan *et al.*, 2002; Harsay and Schekman, 2002), peroxisome inheritance (Hoepfner *et al.*, 2001; Vizeacoumar *et al.*, 2006) and actin organization (Yu and Cai, 2004). Like budding yeast, the fission yeast, *Schizosaccharomyces pombe*, also contains three DRPs, two of which, Msp1 (the homologue of Mgm1) and Dnm1, have a mitochondrial function (Guillou *et al.*, 2005). In contrast to budding yeast, not much is known about the role of Vps1 in fission yeast, only that it is involved in peroxisome biogenesis together with Dnm1 (Jourdain *et al.*, 2008).

Gene and protein notation is slightly different between budding yeast and fission yeast; for clarification refer to Table 1.1.

**Table 1.1.** *S. cerevisiae* and *S. pombe* notation

	<i>S. cerevisiae</i>	<i>S. pombe</i>
<b>Gene</b>	<i>VPS1</i>	<i>vps1</i>
<b>Null Mutant</b>	<i>vps1</i> Δ	<i>vps1</i> Δ
<b>Protein</b>	Vps1p	Vps1

**Table 1.2.** Reported functions of the dynamin-related proteins in *Saccharomyces cerevisiae* and *Schizosaccharomyces pombe*.

<b>Dynamin-related proteins</b>	<b>In <i>S. cerevisiae</i></b>	<b>In <i>S. pombe</i></b>
<b>Vps1</b>	vacuolar protein sorting endocytosis/ actin peroxisome biogenesis vacuole fusion and fission	peroxisome biogenesis
<b>Mgm1/Msp1</b>	mitochondrial architecture	mitochondrial architecture
<b>Dnm1</b>	mitochondrial fission peroxisome biogenesis	mitochondrial fission peroxisome biogenesis

## 1.2. DYNAMIN FUNCTION

Dynamin and dynamin-related proteins function in regulating membrane dynamics in diverse cellular processes, such as endocytosis, organelle division and cytokinesis (Praefcke and McMahon, 2004) (Figure 1.2). Although they may be localised to different cellular compartments, dynamins in principle provide similar scission functions.

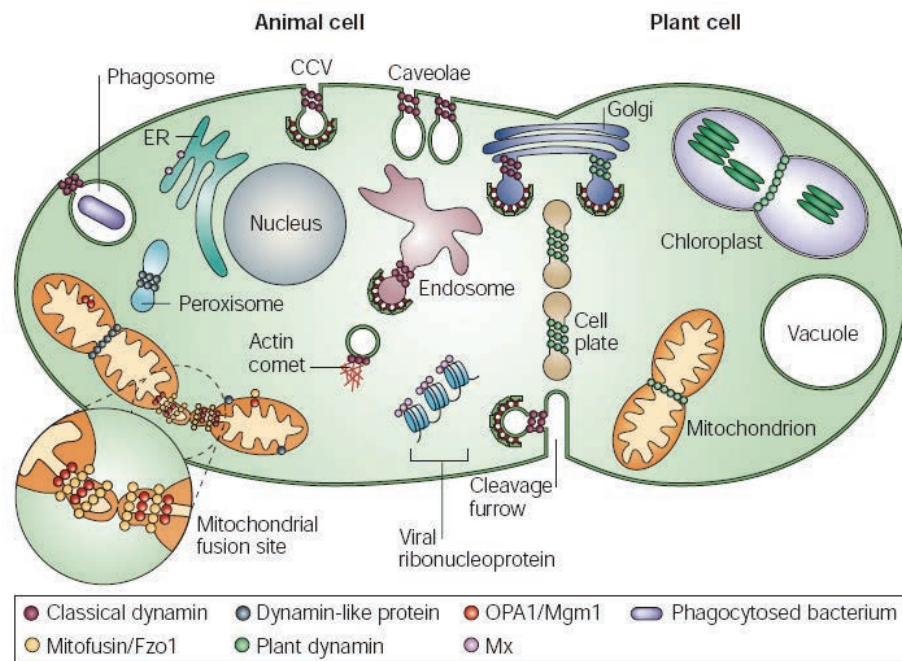


**Figure 1.2. Dynamins are involved in many cellular processes.**  
(Praefcke and McMahon, 2004)

### 1.2.1. Endocytosis

Endocytosis is a process, fundamental to all eukaryotic cells, in which extracellular fluid and molecules are internalised through vesicles formed from the plasma membrane. Evidence for dynamin involvement in endocytosis first came from the temperature-sensitive *shibire* dynamin mutant in *Drosophila*. This mutant exhibits a paralysed phenotype due to impaired endocytic membrane recycling, resulting in the depletion of neurotransmitter-containing vesicles at nerve terminals (Kosaka and Ikeda, 1983a). The mammalian dynamins are 70% identical to *Drosophila* dynamin and are also required for normal endocytosis. Inhibiting dynamin in mammalian cells,

by using anti-dynamin antibodies or by overexpressing a dominant negative dynamin mutant, blocks clathrin-mediated and caveolar endocytosis and results in the accumulation of plasma membrane invaginations that are unable to bud, due to a lack of scission by dynamin (Damke *et al.*, 1994; Henley *et al.*, 1999). This was confirmed by immunolocalising dynamin to clathrin-coated pits and caveolae during endocytosis (Damke *et al.*, 1994; Henley *et al.*, 1999).

Similarly to classical dynamin, Vps1p in budding yeast is also involved in endocytosis, evidenced by the impaired turnover of the membrane receptor protein Ste3p in *vps1Δ* (Yu and Cai, 2004). Endocytosis requires a functional actin cytoskeleton (Gachet and Hyams, 2005) and an additional role for Vps1p in normal actin organization has been shown. Budding yeast *vps1Δ* cells have aggregated and depolarized actin patches, are hypersensitive to the anti-actin drug Latrunculin A and have abnormal bud site selection (Yu and Cai, 2004). This actin effect is not an indirect one, as *vps26Δ* which belongs to the same family of mutants, has no actin phenotype (Yu and Cai, 2004).

It is proposed that dynamin is recruited to sites of endocytosis by proteins such as amphiphysin (David *et al.*, 1996), where it assembles into rings around the necks of clathrin-coated pits or caveolae in order to facilitate the invagination process and mediate fission of vesicles from the plasma membrane (Figure 1.3).

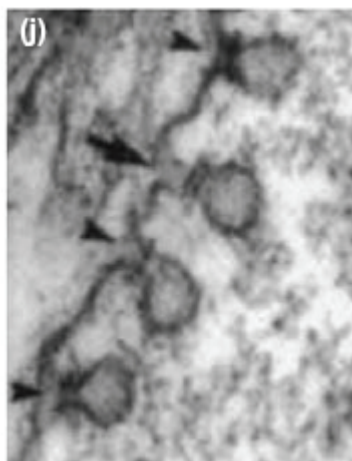


**Figure 1.3.** EM image showing vesiculation at the plasma membrane mediated by the dynamin collar ring (arrows). (Verma and Hong, 2005)



### 1.2.2. The Golgi complex

The formation of clathrin coated vesicles is not restricted to the plasma membrane but also occurs from the trans-Golgi network (Bard and Malhotra, 2006). Therefore it is reasonable to expect that dynamin also functions in vesicle budding from the Golgi complex. This idea was supported by the localisation of a mammalian dynamin GFP-fusion protein to clathrin-coated vesicles at the Golgi (Cao *et al.*, 1998). Additionally, an *in vitro* assay that reconstitutes budding of vesicles from the trans-Golgi network revealed that dynamin depletion, or a dominant negative dynamin mutant, inhibits the formation of vesicles at the Golgi membrane (Jones *et al.*, 1998).

*VPS1* was first identified in *S. cerevisiae* in a screen for vacuolar protein sorting mutants that missort and secrete the vacuolar protein carboxypeptidase Y (CPY) (Rothman *et al.*, 1990; Vater *et al.*, 1992). The CPY sorting defect can be explained by the fact that Vps1p is involved in the formation of vesicles from the Golgi network and their subsequent trafficking to the vacuole (Rothman *et al.*, 1990; Nothwehr *et al.*, 1995). All endosome-bound traffic from the Golgi is diverted to the cell surface in Vps1p mutants (Nothwehr *et al.*, 1995). Vps1p is also implicated in Golgi membrane protein retention (Wilsbach and Payne, 1993). In *vps1Δ* mutants the Kex2p endoprotease, which normally resides in the Golgi, is secreted to the plasma membrane (Wilsbach and Payne, 1993). In agreement with its role at the Golgi, Vps1p is found to be peripherally associated with Golgi membranes (Rothman *et al.*, 1990). Unlike Vps1p, Dnm1p is not required for vacuolar protein sorting (Gammie *et al.*, 1995). However, Dnm1p mutants exhibit delayed turnover of the Ste3p pheromone receptor on the plasma membrane (Gammie *et al.*, 1995). Kinetic analysis revealed that the lag in Ste3p turnover is due to a defect in endosomal trafficking to the vacuole, as opposed to a defect in endocytic internalization (Gammie *et al.*, 1995).

Retrograde transport from the endosome to the Golgi apparatus also requires a functional dynamin. In mammalian cells expressing a dominant negative dynamin mutant, transport of the Shiga toxin from the endosome to the Golgi was inhibited and thus, cytotoxicity declined (Lauvrak *et al.*, 2004). Vps1p also participates in vesicular transport within the secretory pathway. The involvement of Vps1p in membrane-trafficking events was confirmed by a study showing that *vps1Δ* mutants missort

exoglucanase and invertase which are destined for the secretory pathway (Harsay and Schekman, 2002).

### 1.2.3. Peroxisome biogenesis

The mammalian dynamin-related protein Drp1/Dlp1 has been implicated in peroxisome fission. Both the expression of a dominant-negative Dlp1 mutant and silencing of Dlp1 by RNA interference induce elongated peroxisomes which are able to constrict but not divide (Koch *et al.*, 2003; Koch *et al.*, 2004). In agreement with these results, Dlp1 was localised to the peroxisome by subcellular fractionation and fluorescence microscopy (Koch *et al.*, 2003).

The yeast homologues of Dlp1, Vps1p and Dnm1p, are also associated with membrane fission events required for regulating peroxisome abundance in budding yeast and fission yeast (Kuravi *et al.*, 2006; Jourdain *et al.*, 2008). Fluorescence microscopy revealed Vps1p-YFP and Dnm1-GFP transiently colocalise to the peroxisomal membrane (Hoepfner *et al.*, 2001; Kuravi *et al.*, 2006). Budding yeast *vps1Δ* cells were found to have only one or two large peroxisomes, and initially it was proposed that only Vps1p, but not Dnm1p, was involved in regulating peroxisome abundance in budding yeast (Hoepfner *et al.*, 2001). However, later it was shown that *dnm1Δ* cells grown in oleate also have a reduced number of peroxisomes, similar to *vps1Δ* (Kuravi *et al.*, 2006). Furthermore, the *vps1Δ* phenotype is enhanced in the *vps1Δ dnm1Δ* double deletion (Kuravi *et al.*, 2006). Conversely, in fission yeast, Vps1 and Dnm1 have been shown to act redundantly in peroxisome biogenesis (Jourdain *et al.*, 2008). Peroxisomes are normal in fission yeast *vps1Δ* and *dnm1Δ* cells, but they are either absent or morphologically aberrant in the *vps1Δ dnm1Δ* double mutant (Jourdain *et al.*, 2008) (Figure 1.4). However, the precise function of Vps1 remains unclear.

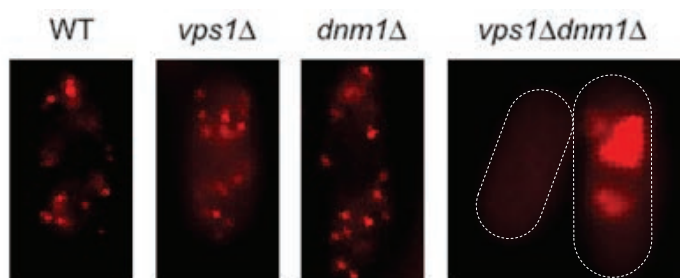


**Figure 1.4.** Peroxisomes in dynamin deletion mutants in *S. pombe* (Jourdain *et al.*, 2008).

#### 1.2.4. Mitochondrial Division

Undoubtedly, the best described role for Dnm1 is in mitochondrial division. Dnm1 is the major orchestrator of mitochondrial outer membrane fission in yeast (Otsuga *et al.*, 1998; Bleazard *et al.*, 1999) and has been the object of many studies. Deletion of the *DNM1* gene in budding yeast resulted in an unfragmented, net-like mitochondrial network (Bleazard *et al.*, 1999) (Figure 1.5). Similarly, fission yeast cells lacking Dnm1 contain mitochondria that are extensively fused (Guillou *et al.*, 2005). Dnm1p acts jointly with Mgm1p, another dynamin-related protein which is involved in the fusion of the mitochondrial inner membrane (Wong *et al.*, 2003). Cells lacking Mgm1p or Dnm1p display fragmented or net-like mitochondria, respectively, but normal mitochondrial morphology is restored in the double mutant *mgm1Δ dnm1Δ* (Sesaki *et al.*, 2003), indicating the existence of an equilibrium between mitochondrial fusion and fission events.

Overexpression of Dlp1 GTPase mutants in mammalian cells induces the collapse of mitochondria into highly reticulated clusters of tubules (Smirnova *et al.*, 1998; Pitts *et al.*, 1999), suggesting that Dlp1 is involved in the maintenance of mitochondrial morphology and that its disruption affects the balance between mitochondrial fusion and fission. Both mammalian Dlp1 and yeast Dnm1p localise *in vivo* to punctate structures on mitochondrial tubules and Dlp1 is also detected together with mitochondria in subcellular fractionations *in vitro* (Smirnova *et al.*, 2001; Shaw and Nunnari, 2002).

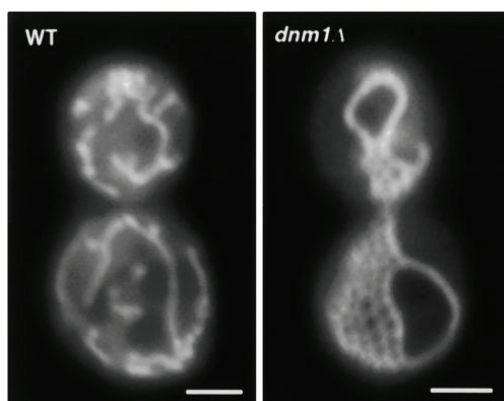


**Figure 1.5.** Mitochondria in budding yeast wild type and *dnm1Δ* cells (Sesaki and Jensen, 1999).

Similarly to other dynamins, Dnm1p hydrolyses GTP and has the ability to self-assemble (Fukushima *et al.*, 2001). Kinetic and structural studies have shown that

Dnm1p self-assembles into rings around the mitochondria, in order to surround, constrict and finally sever mitochondria (Smirnova *et al.*, 2001; Legesse-Miller *et al.*, 2003; Ingerman *et al.*, 2005) (Figure 1.6). Electron microscopy analysis revealed that the mean diameter of Dnm1 spirals is equivalent to the diameter of constricted mitochondria (Ingerman *et al.*, 2005). The relationship between dynamin assembly, GTPase activity and function will be further detailed in 1.2.7.

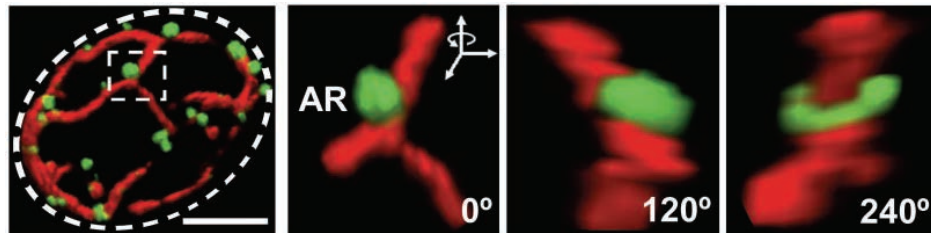


**Figure 1.6.** Dnm1p-EGFP arranged as an asymmetric ring around mitochondria. 3D image of a budding yeast cell expressing Dnm1p-EGFP and mito-RFP visualized from different viewpoints rotated along the indicated axis (Legesse-Miller *et al.*, 2003).

### 1.2.5. Vacuoles

The yeast vacuole plays essential roles in osmoregulation, ion homeostasis (Kim *et al.*, 2005), down-regulation of cell surface proteins (Katzmann and Odorizzi, 2002), and protein and organelle turnover (Klionsky and Ohsumi, 1999). Also, in *S. pombe*, cells detoxify excessive metals, like cadmium, by synthesizing chelators which bind and sequester the ions to the vacuole (Cobbett, 2000).

Most of the genes required for vacuolar biogenesis and protein transport are conserved between fission yeast and budding yeast, indicating that the basic machinery required for vacuolar function is conserved between them. However, vacuolar morphology is different between the two species, as budding yeast has a small number of large vacuoles, while the fission yeast, *Schizosaccharomyces pombe*, has a large number of small vacuoles (Takegawa *et al.*, 2003).

Like most, if not all, organelles, vacuoles are dynamic structures capable of fusing and fragmenting in response to changes in environmental conditions. When cells are under hyperosmotic stress, their vacuoles fragment into numerous small vesicles

(Bone *et al.*, 1998) and the balance is shifted towards fission, with a minimal amount of fusion occurring (Figure 1.7). Conversely, under hypotonic stress the balance is shifted towards fusion and vacuoles fuse to give rise to more voluminous vacuoles (Bone *et al.*, 1998) (Figure 1.7). These vacuole fusion/fission processes act to restore the osmotic equilibrium within the cell, and must be balanced to ensure organelle integrity and to prevent futile cycles of fusion and fission. Dynamins, and dynamin-related proteins, are involved in budding and scission of vesicles from one compartment and in their targeting and fusion with another; therefore they are likely candidates in maintaining the balance between vacuole fusion and fission.

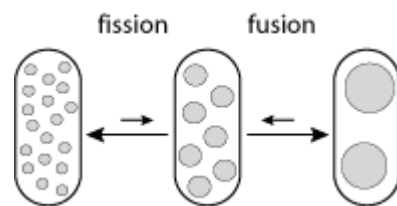


**Figure 1.7.** The balance between vacuole fusion and fission in *S. pombe*

The dynamin-related protein Vps1 is potentially a key player in vacuole membrane events. The *S. cerevisiae vps1Δ* mutant exhibits a class F vacuolar morphology, which is described as having a large central vacuole surrounded by smaller vacuole-like fragments (Raymond *et al.*, 1992). A later study provided evidence for a dual role of the dynamin-related protein Vps1p in fission and fusion at the yeast vacuole (Peters *et al.*, 2004). First, it proposed that Vps1p is part of the vacuole fission machinery, as vacuoles in *vps1Δ* cells are unable to fragment (Peters *et al.*, 2004). Unexpectedly, Vps1p is also essential for vacuole fusion in a cell-free system (Peters *et al.*, 2004). A Vps1-GFP fusion protein localised to the vacuole membrane by fluorescence microscopy (Peters *et al.*, 2004) (Figure 1.8), further supporting its role in vacuole dynamics. However, the role of Vps1 in vacuole dynamics is not clear and there is no evidence of other dynamins being involved.

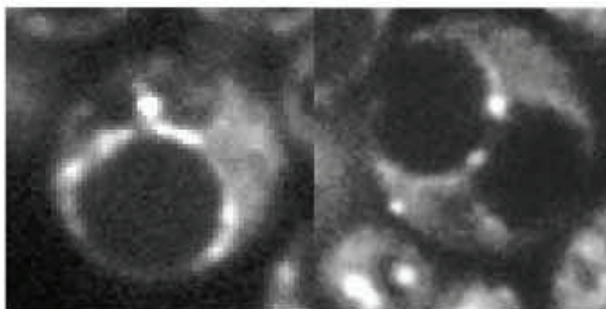


**Figure 1.8.** Localisation of Vps1p-GFP around the vacuole, in living budding yeast cells (Peters *et al.*, 2004).

### 1.2.6. Membrane Tubulation

In plants, during cell plate formation, vesicles are fused to form a latticework of tubules, in the plane of cell division, which contribute to the new plasma membrane and cell wall. The dynamin-related protein phragmoplastin seems to be involved in this process, as its distribution is tightly correlated to the tubulo-vesicular network (Samuels *et al.*, 1995). The self-assembly of phragmoplastin into helical structures suggests a role for this DRP in vesicle tubulation at the newly forming cell plate (Zhang *et al.*, 2000).

Dynamin immunolocalises to tubular invaginations in the plasma membrane of nerve cells (Takei *et al.*, 1995). Tubular structures can be formed *in vitro* by incubating purified dynamin with spherical liposomes (Sweitzer and Hinshaw, 1998; Takei *et al.*, 1998) (Figure 1.9). As seen with conventional dynamins, the dynamin-like protein 1 (Dlp1) also deforms spherical liposomes into elongated tubules *in vitro* (Yoon *et al.*, 2001). Tubulation is enhanced in the presence of GTP $\gamma$ S, a non-hydrolysable form of GTP (Yoon *et al.*, 2001). The same effect is observed with the Dlp1-K38A mutant, which binds, but does not hydrolyse, GTP and therefore is always in the GTP bound state (Yoon *et al.*, 2001). This leads to the idea that dynamin, in its GTP-bound form, binds and tubulates membranes, but once GTP is hydrolysed dynamin is released. The *in vitro* liposome constriction by dynamin can be related to the defined constricted necks of clathrin-coated pits and mitochondria.

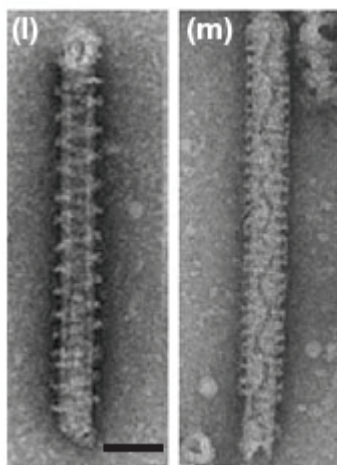


**Figure 1.9.** Tubular structures can be formed by dynamins *in vitro* using lipid nanotubes in the presence of (l) GTP-dynamin and (m) GTP- $\gamma$ -S dynamin. (Verma and Hong, 2005)

### 1.2.7. Dynamin GTPase Activity

Dynamin function is dependent on GTP binding and hydrolysis. Dynamins have low affinities for GTP and high intrinsic rates of GTP hydrolysis. Mutations in the GTP-binding domain abolish dynamin activity. Overexpression of dynamin GTP mutants blocked receptor-mediated endocytosis and caused the accumulation of long tubules at the plasma membrane, due to a failure to constrict and bud endocytic vesicles (Damke *et al.*, 1994; Damke *et al.*, 2001). Overexpression of Vps1p GTPase dead mutants produced the same effects as *vps1Δ*, such as defective vacuolar protein sorting (Vater *et al.*, 1992) and a malfunctioning actin cytoskeleton (Yu and Cai, 2004). A dynamin mutant able to bind, but not effectively hydrolyse GTP, strongly inhibited endocytosis (Marks *et al.*, 2001), suggesting that dynamin is a mechanochemical enzyme that requires GTP hydrolysis for its function and is not simply a molecular switch that is activated by GTP binding.

*In vitro* studies have shown that dynamin exists as a tetramer and self-assembles into rings and spirals (Hinshaw, 1999). The dynamin GTPase effector domain (GED) promotes self-assembly, by interacting with the GTPase domain, and stimulates GTPase activity (Muhlberg *et al.*, 1997). Other functionally diverse molecules, such as microtubules and SH3-domain proteins, interact with dynamin either through its PH domain or its PRD, and can also regulate dynamin GTPase activity (Herskovits *et al.*, 1993; Yoshida and Takei, 2005). GTP binding has been proposed to be sufficient for the self-assembly of Dnm1p into spirals (Naylor *et al.*, 2006). This in turn could stimulate its interaction with the adaptor protein Mdv1p, thus favouring its assembly into fragmentation-competent multimers at the mitochondrial surface (Ingerman *et al.*, 2005; Bhar *et al.*, 2006). A Dnm1p mutant which fails to self-assemble does not undergo mitochondrial division (Ingerman *et al.*, 2005).

Self-assembly stimulates dynamin's basal GTPase activity in a cooperative manner (Tuma and Collins, 1994; Warnock *et al.*, 1996), while GTP hydrolysis drives dynamin disassembly (Warnock *et al.*, 1996); hence dynamin activity is greatly increased when it adopts a helical conformation (Stowell *et al.*, 1999). These helical dynamin structures assemble on, and tubulate, lipid bilayers (Sweitzer and Hinshaw, 1998). Upon GTP addition, the dynamin-tubulated liposomes become constricted and

twisted, confirming that dynamin is capable of generating force (Sweitzer and Hinshaw, 1998; Danino *et al.*, 2004). GTP hydrolysis results in a change in dynamin spiral conformation that can be observed as an increase in helical pitch from approximately 11 nm to 20 nm (Stowell *et al.*, 1999), which is what causes membrane constriction and tubulation. However, there are discrepancies in the literature, as there is another study which states that GTP binding is sufficient for membrane tubulation. In that study, treatment of cells with GTP $\gamma$ S, induced the formation of elongated membrane invaginations that were coated with the dynamin protein (Takei *et al.*, 1995). Membrane constriction, however, is not sufficient for fission (Roux *et al.*, 2006). An *in vitro* study showed that in the absence of membrane tension, dynamin tubulates and constricts but does not cut (Roux *et al.*, 2006). Therefore there may be other factors which cooperate with dynamin to promote membrane fission by contributing to membrane tension.

In summary, it is proposed that dynamin is recruited to its site of action (i.e. the plasma membrane, mitochondria, peroxisome etc.) via interactions with its PRD and PH domains (Shupliakov *et al.*, 1997; Pitts *et al.*, 2004). Dynamin then self-assembles and binds to the lipid bilayer. GTP hydrolysis causes a conformational change in the dynamin helix resulting in constriction and tubulation of the lipid membrane, which may be sufficient for scission.



### 1.3. PROJECT AIMS

---

Dynamins and dynamin-related proteins have been shown to be involved in the maintenance and division of several organelles, such as mitochondria and peroxisomes, and in many cellular processes such as endocytosis and cell plate formation (Figure 1.2). However, there have been few reports on the role of dynamins in vacuole biogenesis.

The main objective of this thesis was to test the hypothesis that the dynamin-related protein Vps1 is involved in vacuole biogenesis in the fission yeast *Schizosaccharomyces pombe*. As Vps1 and Dnm1 in fission yeast act redundantly in peroxisome biogenesis (Jourdain *et al.*, 2008), a second aim was to determine whether Dnm1 acts together with Vps1 in maintaining vacuole homeostasis.

The following questions are addressed in this thesis:

- Is fission yeast Vps1 similar to its budding yeast counterpart?
- Is Vps1 involved in maintaining the balance between vacuole fusion and fission?
- Does Vps1 act together with Dnm1?
- Does Vps1 require its GTPase activity for vacuole biogenesis?

## **2. MATERIALS AND METHODS**

---

## 2.1. MOLECULAR BIOLOGY

### 2.1.1. FISSION YEAST PLASMIDS

**Table 2.1.** Plasmids used in this study

Stock #	Plasmid	Source
V7	pREP41	Y. Gachet
V8	pREP41-Ngfp	D. Mulvihill
V9	pREP41-Cgfp	Y. Gachet
V37	pREP41-Vps1-Cgfp	Lab stock
V64	pREP41-Vps1(untagged)	This study
V67	pREP41-Ngfp-Vps1	This study
V65	pREP41-Dnm1(untagged)	This study
V66	pREP41-Ngfp-Dnm1	This study
V68	pREP41-Vps1-noGTP	This study

The expression vectors used in this study were the pREP41, pREP41-Ngfp and pREP41-Cgfp plasmids (Craven *et al.*, 1998). These vectors are under the control of an attenuated *nmt1* (no message in thiamine) promoter and contain a *LEU2* marker from *S. cerevisiae* which complements *leu1* in *S. pombe*, as well as a yeast origin of replication, *ars1*. The pREP41-Ngfp and pREP41-Cgfp plasmids are based on the pREP41 vector, but have an N-terminal and C-terminal GFP tag respectively.

For creating an untagged Vps1 construct, the 2 kb DNA fragment coding for *vps1* was amplified by polymerase chain reaction (PCR) from *S. pombe* genomic DNA, using primers Vps1Ngfp-F and Vps1Ngfp-R (Table 2.2) (Sigma-Proligo). These two oligonucleotides introduced *NdeI* restriction sites at the 5' and 3' ends of the *vps1* PCR product, which was then digested with the restriction endonuclease *NdeI*. The thiamine-repressible expression vector pREP41 (Craven *et al.*, 1998) (Appendix 6.1.1) was opened by digestion with *NdeI* and the prepared *vps1* PCR product was ligated into the corresponding site.

The pREP41-*dnm1* construct was prepared in the same way, using primers Dnm1-F and Dnm1-R (Table 2.2) which introduced *NdeI* restriction sites at the 5' and 3' ends

of the 2.5 kb *dnm1* fragment. For creating GFP tagged Vps1 and Dnm1 constructs (pREP41-*Ngfp-vps1* and pREP41-*Ngfp-dnm1*) primers Vps1Ngfp-F, Vps1Ngfp-R and Dnm1-F, Dnm1-R (Table 2.2) were used. These primers also introduced *NdeI* restriction sites at the 5' and 3' ends of the amplified DNA fragments and the *vps1* and *dnm1* PCR products were cloned into *NdeI* sites in the pREP41-*Ngfp* plasmid (Appendix 0)

Finally, the pREP41-Vps1-noGTP plasmid was developed, using primers Vps1-NoGTP-F and Vps1Ngfp-R (Table 2.2). These primers amplified the *vps1* gene with a truncation (a.a 1-251) at the N-terminus, which corresponded to the GTPase domain. As described above, the PCR product was ligated into *NdeI* sites in the pREP41 plasmid. All constructs were verified by sequencing (Allan Wilson Centre, Palmerston North, New Zealand).

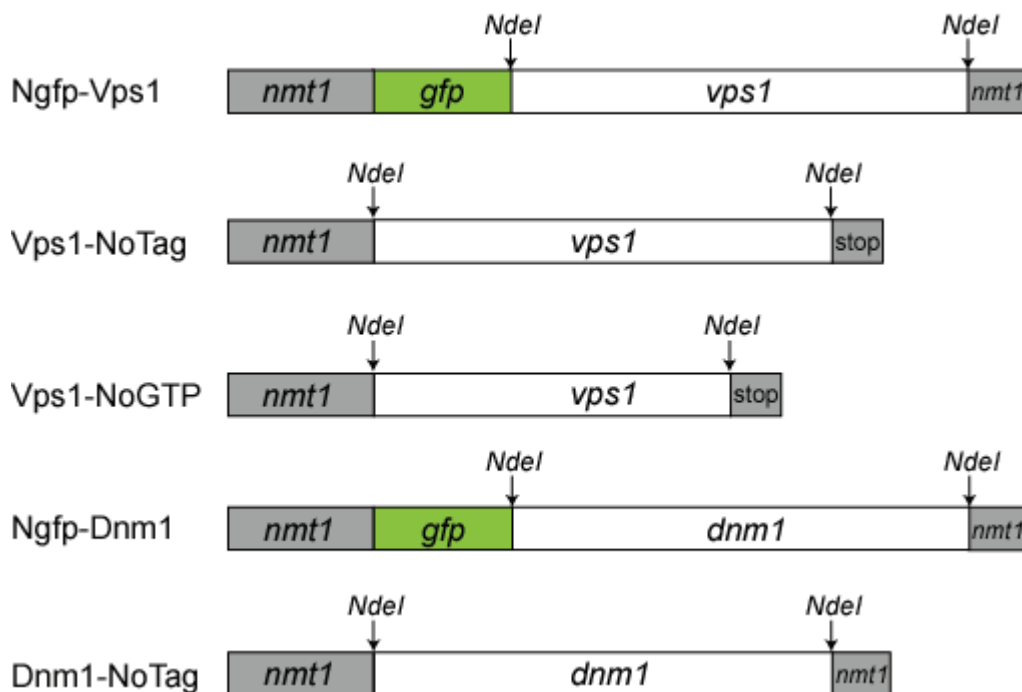


**Figure 2.1** Constructs made in this study

### 2.1.2. OLIGONUCLEOTIDE PRIMERS

Oligonucleotide primers were synthesised by Sigma PROLIGO. Each primer was resuspended in water to a final concentration of 1  $\mu\text{g}/\mu\text{l}$  and stored at  $-20^{\circ}\text{C}$  until

needed. For PCR reactions, primers were used at a final concentration of 2.5 ng/ $\mu$ l. Primers used in this study are shown in Table 2.2.

**Table 2.2.** Primers used in this study

Primer	Sequence (5' - 3')
Vps1Ngfp-F	CATATGGTTAAGCTGATCATGGATCCCTCATTGATTAAAGT TGCAAT
Vps1Ngfp-R	CATATGTTAAACGTTAGACACAATCTCACTTGCCTGTAG
Dnm1-F	CATATGGTTAAGCTGATCATGGAACAACCTATTCCATTGGT GAATCAA
Dnm1-R	GTTCGTTTGTTTTAATAAAGTTGCCAAAAAATTGTATAC
Vps1-NoGTP-F	CATATGGTTATGGCAAATCGCGGTCAAAGGACATCGAAG GGAAG

### 2.1.3. POLYMERASE CHAIN REACTION (PCR)

#### 2.1.3.1. Standard PCR

Each standard PCR reaction contained approximately 1.25 ng of plasmid or 5-10 ng of genomic DNA template, 1 x *Taq* polymerase buffer (1.5 mM MgCl<sub>2</sub>, Roche), 10  $\mu$ M dNTPs, 10 ng/ $\mu$ l of both forward and reverse primers and 0.5 U *Taq* polymerase (Roche). The following PCR program was used:

Initialization	95°C	30 sec	1 cycle
Denaturation	95°C	15 sec	} 30 cycles
Annealing	Variable	30 sec	
Elongation	72°C	2 min	
Final elongation	72°C	7 min	1 cycle
Hold	4°C	Hold	

The optimal annealing temperature depends on the melting temperature of the primers used.

#### 2.1.3.2. PCR using Expand<sup>TM</sup> High Fidelity (Roche)

Each high-fidelity PCR reaction contained approximately 1.25 ng of plasmid or 5-10 ng of genomic DNA template, 1 x Expand<sup>TM</sup> High Fidelity buffer (1.5 mM MgCl<sub>2</sub>,

Roche), 10  $\mu$ M dNTPs, 10 ng/ $\mu$ l of both forward and reverse primers and 3.5 U Expand<sup>TM</sup> High Fidelity enzyme (Roche). The following PCR program was used:

Initialization	95°C	30 sec	1 cycle
Denaturation	95°C	30 sec	} 25 cycles
Annealing	Variable	1 min	
Elongation	68°C	30 sec	
Final elongation	68°C	1 min	1 cycle
Hold	4°C	Hold	

The optimal annealing temperature depends on the melting temperature of the primers used.

#### **2.1.3.3. PCR product purification**

PCR products were purified using the QIAquick<sup>®</sup> PCR purification kit (QIAGEN) and the GENECLAN<sup>®</sup> III Kit (Q-BIOgene) .

#### **2.1.4. PLASMID ISOLATION**

In order to obtain plasmid DNA, *E. coli* was transformed with the desired plasmid and plated on Luria-Bertani (LB) plates with antibiotic selection. After approximately 12 hrs at 37°C, a colony was picked and grown in LB broth. Plasmid DNA was isolated and purified using the QIAprep<sup>®</sup> Spin Miniprep kit and the QIAGEN<sup>®</sup> Plasmid Maxi kit for larger quantities.

#### **2.1.5. *S. pombe* DNA ISOLATION**

For isolating genomic DNA from *S. pombe*, 5 ml of cells at saturation were pelleted and resuspended in 200  $\mu$ l of Winston Juice (2% Triton X-100, 1% SDS, 100 mM NaCl, 10 mM Tris-HCl pH8, 1 mM EDTA). This was transferred to a ribolysis tube containing 300  $\mu$ l of acid-washed glass beads and was ribolysed at 4°C for 20 sec, at power 6.5. Next, 200  $\mu$ l TE (10mM Tris, 1mM EDTA) were added to the preparation, which was then vortexed and centrifuged for 5 min. The supernatant was transferred to a new tube and 200  $\mu$ l of phenol/chloroform were added. This was mixed well by vortexing for 3 minutes and then centrifuged for a few seconds. The supernatant was once again transferred to a new tube and 1 ml of 100% EtOH was added, mixed well

and incubated at -80°C for 1 hr (and up to 24 hr). Following this incubation, the tube was centrifuged for 15 min at 4°C, after which the supernatant was discarded and 500 µl of 70% EtOH were added. The tube was centrifuged again between 5-15 min at 4°C, the supernatant was discarded and the pellet was air dried. Finally, the pellet was resuspended in 200-400 µl TE + RNaseA and if necessary was further purified using a commercial kit (See Section 2.1.3.3). For using in PCR, 1 µl of the purified DNA was sufficient.

### **2.1.6. DNA QUANTIFICATION**

DNA concentrations were measured using the NanoDrop<sup>®</sup> (ND-1000 Spectrophotometer), calibrated with water and blanked appropriately, with the solution which was used for resuspending the DNA sample.

## **2.2. YEAST STRAINS AND CULTURES**

---

### **2.2.1. MEDIA**

All media was prepared according to (Moreno *et al.*, 1991) using distilled water and sterilized by autoclaving at 121°C and 10 psi for 20 minutes. Liquid media was cooled to room temperature before the addition of supplements and inoculation. Solid media was made by adding 2% (w/v) Bacto Agar and was cooled to 50°C and plates poured. Uninoculated plates were stored at 4°C.

#### **2.2.1.1. *Standard rich medium (YES)***

YES is a rich complete medium for *S. pombe* growth, to be used when selection is not required. YES media contained (per litre) 0.5% (w/v) Oxoid yeast extract, 3% (w/v) glucose and amino acid supplements at a final concentration of 225 mg/l (See appendix 6.2 for stock solutions).

#### **2.2.1.2. *Edinburgh minimal medium (EMM)***

EMM is the minimal selective medium most commonly used for *S. pombe* growth. EMM medium contained (per litre) 14.7 mM potassium hydrogen phthalate, 15.5 mM Na<sub>2</sub>HPO<sub>4</sub>, 93.5 mM NH<sub>4</sub>Cl, 2% (w/v) glucose, 2% (w/v) salt stock, 0.1% (w/v)

vitamin stock, 0.01% (w/v) mineral stock, and supplemented with required amino acids at a final concentration of 225 mg/l (See appendix 6.2 for stock solutions).

### **2.2.1.3. Minimal supporting agar (MSA)**

MSA medium is used for crossing and sporulating *S. pombe* strains. MSA agar contained (per litre) 2% (w/v) Bacto Agar, 1% (w/v) glucose, 11 mM Arginine, 7.3 mM  $\text{KH}_2\text{PO}_4$ , 1.7 mM NaCl, 0.83 mM  $\text{MgSO}_4 \cdot 7\text{H}_2\text{O}$ , 0.58 mM  $\text{CaSO}_4 \cdot 2\text{H}_2\text{O}$ , 0.2% (w/v) vitamin stock, 0.01% (w/v) mineral stock and amino acid supplements at a final concentration of 112.5 mg/l (See appendix 6.2 for stock solutions).

## **2.2.2. YEAST TRANSFORMATION**

*S. pombe* cells were transformed with plasmid DNA by the lithium acetate method (Morita and Takegawa, 2004) under sterile conditions. Firstly, cells were counted to ensure they had reached mid-log phase ( $1$  to  $4 \times 10^6$  cells) and were pelleted by spinning at 3000 rpm for 3 min. To wash the cells, the pellet was resuspended in 1 ml lithium acetate (0.1 M Li-Acetate, pH4.9) and centrifuged at 13000 rpm for 2 min. The pellet was then resuspended in 100  $\mu\text{l}$  Li-Acetate/transformation and incubated at 25°C for exactly 1 hour. After the incubation with Li-acetate, 100  $\mu\text{l}$  of cells were added to eppendorf tubes containing 100  $\mu\text{l}$  of PEG (70% PEG 4000), plus the DNA to be transformed (1-3  $\mu\text{g}$  per transformation) and were incubated at 25°C for 1 hour or more. After this incubation, cells were heat-shocked at 42°C for 10 minutes, washed with 100  $\mu\text{l}$  of  $\text{H}_2\text{O}$  and spread onto EMM plates (See section 2.2.1.2) appropriately supplemented. The plates were left at the permissive temperature (generally 25°C) for about 1 week and once colonies were formed they were re-streaked onto fresh EMM plates. Finally, cells were ready for setting up liquid cultures and for analysis.



### 2.2.3. STRAINS

**Table 2.3.** Strains used in this study

Strain	Genotype	Source
MU141	<i>leu1.32, h-</i>	P. Nurse
MU88	<i>vps1::ura4, ura4-D18, leu1.32, h-</i>	Lab stock
MU155	<i>vps1::ura4, ura4-D18, leu1.32, ade6-M210, h+</i>	Lab stock
MU48	<i>Crn1-gfp ::KanMX6, ura4-D18, leu1.32, ade6-</i>	F. Chang
MU157	<i>vps1::ura4, Crn1-gfp ::KanMX6, ura4-D18, leu1.32, h-</i>	Lab stock
MU171	<i>dnm1::kanMX6, leu1.32, ura4-D18, h-</i>	Lab stock
MU205	<i>dnm1::kanMX6, leu1.32, h+</i>	Lab stock
MU159	<i>vps1::ura4, dnm1::kanMX6, leu1.32, h+</i>	Lab stock
MU45	<i>vps34::leu1</i>	Y. Gachet
MU47	<i>for3::KanMX6, leu 1.32, ura4-D18, ade6-M210 h+</i>	Y. Gachet
MU10	<i>myo52::ura4, leu 1.32, ura4-D18, ade6-M210 h-</i>	D. Mulvihill
MU212	<i>nda3-KM311 h-</i>	S. Tournier
MU340	pREP41 in wild type (MU141)	This study
MU341	pREP41- <i>Ngfp</i> in wild type (MU141)	This study
MU92	pREP41- <i>Cgfp</i> in wild type (MU141)	This study
MU342	pREP41- <i>vps1</i> in wild type (MU141)	This study
MU343	pREP41- <i>Ngfp-vps1</i> in wild type (MU141)	This study
MU129	pREP41- <i>vps1-Cgfp</i> in wild type (MU141)	This study
MU333	pREP41- <i>dnm1</i> in wild type (MU141)	This study
MU344	pREP41- <i>Ngfp-dnm1</i> in wild type (MU141)	This study
MU318	pREP41- <i>vps1</i> in <i>vps1Δ</i> (MU88)	This study
MU319	pREP41- <i>Ngfp-vps1</i> in <i>vps1Δ</i> (MU88)	This study
MU130	pREP41- <i>vps1-Cgfp</i> in <i>vps1Δ</i> (MU88)	This study
MU334	pREP41- <i>dnm1</i> in <i>vps1Δ</i> (MU88)	This study
MU320	pREP41- <i>Ngfp-dnm1</i> in <i>vps1Δ</i> (MU88)	This study
MU312	pREP41 in <i>vps1Δ</i> (MU88)	This study
MU302	pREP41- <i>Ngfp</i> in <i>vps1Δ</i> (MU88)	This study
MU133	pREP41- <i>Cgfp vps1Δ</i> (MU88)	This study
MU313	pREP41 in <i>dnm1Δ</i> (MU205)	This study

MU324	pREP41- <i>vps1</i> in <i>dnm1Δ</i> (MU205)	This study
MU322	pREP41- <i>Ngfp-vps1</i> in <i>dnm1Δ</i> (MU205)	This study
MU303	pREP41- <i>Ngfp</i> in <i>dnm1Δ</i> (MU205)	This study
MU368	<i>for3::KanMX6, vps1::ura4, leu 1.32,, ade6-M210</i>	This study
MU374	pREP41- <i>vps1</i> in <i>nda3-KM311</i> (MU212)	This study
MU378	pREP41- <i>vps1</i> in <i>myo52Δ</i> (MU10)	This study
MU381	pREP41- <i>vps1</i> in <i>for3Δ</i> (MU47)	This study
MU385	pREP41- <i>vps1-NoGTP</i> in wild type (MU141)	This study
MU386	pREP41- <i>vps1-NoGTP</i> in <i>dnm1Δ</i> (MU205)	This study

---

## 2.2.4. GROWTH

### 2.2.4.1. *S. pombe* growth

Strains were grown either in standard rich medium YES, or in synthetic minimal medium EMM. EMM is used mainly for selecting auxotrophic markers and for *nmt1* promoter expression (See Section 2.2.4.2). All cultures were grown at the permissive temperature, which is generally 25°C. For experiments at the restrictive temperature (36°C), cells were grown at 25°C for 5 generations (~ 20 hrs) after which they were transferred to 36°C for at least one generation time (~ 4 hrs). For re-isolating strains from frozen cultures at -80°C (in 50% glycerol), cells were streaked onto either YES or EMM plates and incubated for 2-4 days at the permissive temperature. For setting up a liquid culture, firstly a 5 ml mini-culture (YES or EMM) was inoculated with cells taken directly from a plate, and grown for 1-2 days. Cells were then grown in 50 ml of the appropriate medium until they reached mid log phase ( $OD_{600nm} = 0.5-1.0$ ). The optical density (OD) of a culture can be used to measure the concentration of cells, where one OD is the amount of cells required to give 1 ml of culture an optical density of 1 at 600 nm. The following formula is used to calculate the volume of cells needed to set up a large culture from a mini culture (5 ml):

$$\frac{(V_{final} \times OD_{final}) \div 2^{n-1}}{OD_{initial}}$$

n = number of generations of a given strain, in a specific medium and at a specific temperature (e.g. WT= 4 hrs in EMM at 25°C)

For obtaining a growth curve, cell cultures were set up at 25°C and left to grow for 5 generations (~20 hrs), after which the OD<sub>600nm</sub> was measured every hour.

#### 2.2.4.2. *Overexpression of genes under the control of the nmt1 promoter*

The pREP41 plasmids used in this study are thiamine-repressible expression vectors, under the control of an attenuated *nmt1* (no message in thiamine) promoter (Maundrell, 1990). As its name indicates, the *nmt1* promoter is repressed by the addition of thiamine (5-60 μM) to the growth medium. However, the response to thiamine can depend on the protein being expressed and on the sensitivity of the cell to that particular protein. Thus, the concentration and time of incubation with thiamine must be determined for each gene, as their response may be different.

### 2.2.5. FISSION YEAST CLASSICAL GENETICS

#### 2.2.5.1. *Genetic crosses*

Fission yeast is generally haploid, even in the wild. Thus, in order to induce mating, haploid cells must be under conditions of nitrogen starvation and the parental strains must be of opposite mating type ( $h^+$  and  $h^-$ ). For crossing two strains, a loop full of each parental strain was mixed together on a very fresh MSA plate, with a drop of sterile water. The mating plate was then incubated at 25°C, as mating is inherently temperature-sensitive. Successful mating was determined microscopically (under a bench microscope, lens ×40) by observing the formation of zygotes and asci. Once the parental strains mate, they proceed immediately through sporulation, generating a curved, zygotetic ascus. For obtaining diploids (banana-shaped or Z-shaped cells with a long nucleus), the reaction was stopped before the cells entered meiosis, that is, after 8 hr, 12 hr and 24 hr, by replating on YES. If cells were allowed to enter meiosis they sporulated, forming a tetraploid (banana-shaped or Z-shaped cell with 4 spores) which eventually gave rise to 4 different strains.

Diploid:



Tetraploid:



### **2.2.5.2. *Random spore analysis (RSA)***

Random spore analysis allows many spores to be examined, thus facilitating rapid recombination mapping and strain construction. It is easy to do in *S. pombe* because a simple enzyme treatment kills remaining vegetative (unsporulated) cells and releases the spores from their asci, without having an effect on the spores themselves (Forsburg and Rhind, 2006). Using a three day old cross, asci were detected under the light microscope. A 1 ml volume of distilled sterile water was inoculated with a loop full of cells from the mating plate and 220 units/ml of  $\beta$ -glucuronidase were added. The mixture was incubated at 37°C for a few hours (preferably overnight or as long as 2 days). After digestion of the cell wall, cells were centrifuged for 1 min at 13000 rpm, washed twice with sterile water and finally resuspended in 1 ml sterile water. Using a haemocytometer, the number of spores was counted in 10  $\mu$ l of a 10:1 dilution. Between 200-1000 spores/plate were plated out on YES (no selection at this stage). Colonies appeared in 2-5 days, depending on the temperature, and plates were then replica-plated onto EMM for selection of auxotrophic markers. All crosses were verified by auxotrophy and by PCR.

## **2.3. CELL BIOLOGY**

---

### **2.3.1. STAINING**

#### **2.3.1.1. *Nuclear staining***

Hoechst is a fluorescent DNA stain. Hoechst stock solution was prepared as 1 mg/ml in H<sub>2</sub>O and stored in small aliquots at 4°C in the dark. For nuclear staining, 200  $\mu$ l of mid-log phase cells were incubated with 1  $\mu$ l of Hoechst (final concentration of 5  $\mu$ g/ml) for 15 min in the dark. Cells were then washed 3 to 4 times with culture medium and resuspended in a small volume depending on the size of the pellet. Of these cells, 5  $\mu$ l were spotted onto an agarose chamber (2% agarose in medium) and viewed under the fluorescence microscope. It is possible to mix a Hoechst-labelled strain with an unlabelled strain, as the signal does not leak too much from strain A to strain B. Hoechst has an excitation/emission spectrum of 352 nm/461 nm.

### **2.3.1.2. Cell wall staining**

Calcofluor white is a fluorescent brightener used to stain the cell wall (Alfa *et al.*, 1993). A 1 ml aliquot of cells was resuspended in 100  $\mu$ l of calcofluor (5 mg/ml in PEM), and incubated for 30 min in the dark, after which they were washed 3 times in PEM buffer (100 mM Pipes, 1 mM EGTA, 1 mM MgSO<sub>4</sub>, pH6.9). Cells were mounted on a slide and observed under the fluorescence microscope. Calcofluor has an excitation/emission spectrum of 440 nm/ 500-520 nm.

### **2.3.1.3. Actin staining**

Rhodamine-phalloidin is used for staining the actin cytoskeleton. This protocol was adapted from (Marks and Hyams, 1985). Rhodamine-phalloidin stock solution was prepared by resuspending 300 units in 1.5 ml of methanol (6,6 mM) and stored at -20°C, in the dark. For actin staining, 10 ml of cells were fixed in 3.3% paraformaldehyde for 1 hour, washed 3 times with PEM buffer (100 mM Pipes, 1 mM EGTA, 1 mM MgSO<sub>4</sub>, pH6.9) and permeabilized with 1% Triton X-100 for 30 sec. Cells were washed 3 more times with PEM and incubated at 4°C in the dark, for 30 minutes, with 1.5  $\mu$ M Alexa Fluor 488-phalloidin (Molecular Probes). To mount the cells onto a microscope slide, 5  $\mu$ l of cells were applied to a coverslip and mixed with 3  $\mu$ l of DAPI. The cells were then observed under the fluorescence microscope. Rhodamine-phalloidin has an excitation/emission spectrum of 554 nm/573 nm.

### **2.3.1.4. Microtubule immunofluorescence**

For preparing cells for immunofluorescence, cells were fixed in 3.3% Paraformaldehyde (PAF) and 0.2% glutaraldehyde and incubated for 1 hr on a rotary inverter. At the end of the incubation, the cells were centrifuged at 3000 rpm for 2 min and the supernatant discarded. The pellet was then washed twice with PEM (100 mM Pipes, 1 mM EGTA, 1 mM MgSO<sub>4</sub> pH6.9) and resuspended in 500  $\mu$ l of PEMS (1,2 M D-Sorbitol in PEM) plus 2.5 mg Zymolyase (20T) and incubated at 37°C for about 45 min. After this incubation, cell digestion was checked under the microscope and cells were centrifuged and resuspended in 1% Triton X-100 in PEMS to permeabilise the membrane for 30 sec and washed twice with PEM. Glutaraldehyde is a charged molecule that might bind the antigen, so the antibody will be unable to bind. This is why, despite all the washes made before, it has to be quenched. In a universal tube, a few grains of sodium borohydride were mixed with approximately 3 ml of PEM and 500  $\mu$ l of this solution were added to the last pellet. After a few minutes the

cells were centrifuged 3 times and washed in PEM. This procedure was repeated once more, after which the last pellet was incubated with 100  $\mu$ l of PEMBAL blocking buffer (1% (w/v) BSA, 0.1% (w/v) NaN<sub>3</sub>, 100 mM Lysine hydrochloride pH6.9 adjusted to 1 litre with PEM buffer) for 30 min. After this incubation, the cells were centrifuged twice and resuspended in 100  $\mu$ l of primary TAT-1 antibody (provided by Keith Gull) (diluted 1:10 in PEMBAL) for an overnight incubation period. TAT-1 is an anti  $\alpha$ -tubulin from trypanosome that works on most yeast cells. For incubating with the secondary antibody, the cells were washed in PEMBAL several times and then resuspended in 100  $\mu$ l of secondary antibody for at least 5 hrs. Finally, the cells were washed both with PEMBAL and PEM and the pellet resuspended in a small volume of PEM, ready to be observed under the fluorescence microscope.

## **2.3.2. DRUGS**

### **2.3.2.1. Latrunculin A**

Latrunculin A is an actin depolymerising drug. Lat-A treatment was performed by adding 2.4 mM Lat-A to the cells and incubating at 25°C for 15 minutes (Pelham and Chang, 2001). Cells were then fixed in 3.3% paraformaldehyde for 1 hour and stained with Rhodamine-phalloidin for actin visualization (See Section 2.3.1.3). For live-cell imaging of Lat-A treatment, cells were fixed to a coverslip coated with lectin and medium containing 150  $\mu$ M Lat-A was flushed under the coverslip (Castagnetti *et al.*, 2005). Cells were viewed under the fluorescence microscope and time-lapse images were taken every 2 seconds.

### **2.3.2.2. TBZ**

Thiabendazole (TBZ) is an anti-microtubule drug. For microtubule depolymerisation, 1 ml of mid-log phase cells was incubated for 30 min with 300  $\mu$ g/ml of TBZ. As a control, the same concentration of DMSO was used in place of TBZ. To verify complete microtubule depolymerisation cells were subjected to immunofluorescence using the TAT-1 antibody (Section 2.3.1.4).

### 2.3.3. VACUOLES

#### 2.3.3.1. FM4-64

FM4-64 is a red fluorescent dye that is taken up via endocytosis and stains the vacuolar membrane (Vida and Emr, 1995; Gachet and Hyams, 2005). FM4-64 stock solution was prepared as 1 mg/ml in DMSO (1.64 mM) and stored in small aliquots at 4°C in the dark. For FM4-64 vacuole staining, 1 µl of FM4-64 (1.64 mM) was added to 200 µl of mid-log phase cells and incubated in the dark on a rotary inverter at 25°C for 30 min or 1 hour. Cells were then washed twice in medium and resuspended in a small volume.

In order to follow the endocytic uptake of FM4-64, 2 ml of mid-log phase cells were placed on ice for 5 min, after which they were labelled with 10 µl of FM4-64 and chased for given periods of time at room temperature. At times 0, 15 sec, 30 sec, 45 sec, 1 min, 2 min, 5 min, 10 min and 30 min, 100 µl aliquots of cells were taken and fixed in 3.3% Paraformaldehyde for 1 hr. For cell imaging, 5 µl of cells were spotted onto an agarose chamber (2% agarose in medium) and viewed under the fluorescence microscope. FM4-64 has an excitation/emission spectrum of 479 nm/598 nm.

#### 2.3.3.2. CDCFDA

CDCFDA [5(6)-carboxy-2', 7'-dichlorofluorescein diacetate] is a dye that accumulates inside the vacuoles and fluoresces due to the acidic pH in the vacuolar lumen. CDCFDA stock solution was prepared as 1 mg/ml in DMSO (1.89 mM) and stored at -20°C in the dark. A 1 ml volume of mid-log phase cells was prepared for staining by centrifuging and re-suspending the pellet in 1 ml of water or medium. 1 µl of CDCFDA stock solution (at 1.89 mM) was added to the cells and incubated on a rotary inverter at permissive temperature for 30 min in the dark. After this incubation, the cells were pelleted, washed once in medium and resuspended in a small volume. This protocol was adapted from (Alfa *et al.*, 1993; Gachet and Hyams, 2005). To mount the cells onto a microscope slide, 5 µl of cells were spotted onto an agarose chamber (2% agarose in medium) and the cells were then observed under the fluorescence microscope. CDCFDA has an excitation/emission spectrum of 504 nm/530 nm.

### **2.3.3.3. *Vacuole fusion and fission***

For inducing vacuole fusion, 1 ml of cells were washed at least 3 times in water and then re-suspended in water for 2 hours or more before staining with 5  $\mu$ l of FM4-64 or 1  $\mu$ l of CDCFDA for 30 min. For cell imaging, 5  $\mu$ l of cells were spotted onto an agarose chamber (2% agarose in water) and viewed under the fluorescence microscope. On the other hand, for inducing vacuole fission, cells were stained for 30 min with FM4-64 or CDCFDA after which the cells were washed in medium and incubated in 0.4 M NaCl or 1 M Sorbitol for 10 min. For mounting the cells onto a microscope slide, 5  $\mu$ l of cells were spotted onto an agarose chamber (2% agarose in 0.4M NaCl) and observed under the fluorescence microscope.

## **2.3.4. MICROSCOPY AND ANALYSIS**

Live cell imaging was performed in imaging chambers (CoverWell, 20-mm diameter, 0.5-mm deep) (Molecular Probes) filled with 800  $\mu$ l of 2% agarose in EMM and sealed with a 22 x 22-mm glass coverslip. For cell imaging, an Olympus IX71 fluorescence microscope was used with an x100 oil immersion lens, and images were captured with a Hamamatsu ORCA-ER C4742-80 digital charge-coupled device camera (Hamamatsu Corporation). For confocal microscopy, a Leica TCS SP5 microscope and an x63 oil immersion lens were used. Image analysis was carried out using METAMORPH Software (Molecular Devices Corporation).

### **2.3.4.1. *Electron microscopy***

*S. pombe* cells were fixed for electron microscopy in 1% potassium permanganate and pelleted in 20% BSA. This was followed by acetone dehydration, and infiltration and embedding in Procure 812 Epoxy resin. Thin sections for transmission electron microscopy were stained for 1 min in uranyl acetate and 1 min in lead citrate.

## **2.4. BIOCHEMISTRY**

---

### **2.4.1. CARBOXYPEPTIDASE Y (CPY) ANALYSIS**

Vacuolar Carboxypeptidase Y (CPY) missorted to the medium was detected by colony blot assay as previously described (Iwaki *et al.*, 2006). In brief, cells at 0.12 OD<sub>600nm</sub> were spotted onto an EMM plate in contact with a nitrocellulose membrane



and incubated at 25°C for 2 days. After removing cells by washing, the nitrocellulose membrane was subjected to immunodetection of CPY using rabbit polyclonal antibodies against *S. pombe* Cpy1 (1:1000 dilution) (Tabuchi *et al.*, 1997), followed by horseradish peroxidase-conjugated anti-rabbit IgG antiserum (1:5000 dilution) (Promega), and the SuperSignal<sup>®</sup> West Pico Chemiluminescent Substrate (PIERCE).

#### **2.4.2. VACUOLE ISOLATION**

Vacuoles were isolated as previously described (Tabuchi *et al.*, 1997). Cells were grown to an optical density OD<sub>600nm</sub> of 0.5 to 1.0 in 1 litre of EMM, harvested by centrifugation, washed twice with distilled water and resuspended in water for a couple of hours to allow vacuole fusion. After this incubation, cells were labelled with FM4-64 (8.2 µM) for 30 min, centrifuged and resuspended at 100 OD<sub>600</sub> units/ml in 10 mM Tris-HCl (pH7.5) plus 1 M sorbitol. To this suspension, 500 mg of Zymolyase 20T were added, and the mixture was incubated at 30°C for 60 min. Spheroplasts were collected by centrifugation and washed twice with 1 M sorbitol. Further procedures were all carried out on ice. The spheroplast pellet was suspended at 100 OD<sub>600</sub> units/ml in 10 mM morpholineethanesulfonic acid (MES) - Tris (pH6.9) - 0.1 mM MgCl<sub>2</sub> - 12% Ficoll 400 and homogenized by 10 strokes in a Potter homogenizer. The homogenate was placed on a 1 ml cushion of 20% Ficoll and was successively overlaid with 3 ml of 12% Ficoll 400 in 10 mM MES - Tris (pH 6.9) - 0.1 mM MgCl<sub>2</sub>, 2 ml of 8% Ficoll 400 in 10 mM MES - Tris (pH 6.9) - 0.1 mM MgCl<sub>2</sub> - 0.2 M NaCl, and 2 ml of 0.2 M sorbitol in 10 mM MES - Tris (pH 6.9) - 0.5 mM MgCl<sub>2</sub> - 0.2 M NaCl. The discontinuous Ficoll gradient was centrifuged in a SW41Ti rotor (Sorvall) at 100,000 g at 4°C overnight and fractions of 0.5 ml were collected. Vacuoles were collected from the 8% to 0% Ficoll interface. Successful vacuole isolation was determined microscopically and by spotting the fractions onto a nitrocellulose membrane and probing with Anti-CPY antibody (CPY used as a vacuole marker).

#### **2.4.3. WESTERN BLOT**

To begin with, the nitrocellulose membrane was stained with Ponceau Red (in 1% glacial acetic acid) for 5 min or more and then washed with 1% acetic acid until the red background disappeared and the protein bands were clearly visible. The

membrane was then washed with acetic acid 1% until all the red disappeared and was rinsed with 1x PBS (10x Phosphate Buffered Saline contained 1.3 M NaCl, 26.8 mM KCl, 0.1 M Na<sub>2</sub>HPO<sub>4</sub> and 17.6 mM KH<sub>2</sub>PO<sub>4</sub> adjusted to pH7.4). For blocking unspecific sites, the membrane was incubated with 5% (w/v) skim milk (in 1x PBS) at room temperature for 1 hour and then briefly washed in 1x PBS. Next, the membrane was probed with the primary antibody (appropriately diluted in a 1% skim milk solution) for 1 hour at room temperature, and washed 3 times for 5 min each with 1x PBS. The membrane was incubated with the secondary antibody (diluted in a 1% skim milk solution) for 1 hour at room temperature and then washed as before. Visualization was enhanced using the SuperSignal<sup>®</sup> West Pico Chemiluminescent Substrate (PIERCE). The hybridised blot was wrapped in plastic and exposed to a sheet of Medical X-ray film (Kodak) in an X-ray cassette for an appropriate period of time, which varied according to the strength of the signal. The film was developed using a 100 Plus Automatic X-ray film processor (All-Pro Imaging Group) using 100 Plus developer and fixative solutions. For stripping the nitrocellulose membrane, it was incubated in a solution of 7 µl/ml β-mercaptoethanol, 2% SDS and PBS, for 30 min at 50°C. The membrane was then washed many times in PBS before being ready for a new blot.

### **3. RESULTS**

---

### 3.1. VPS1 IN FISSION YEAST

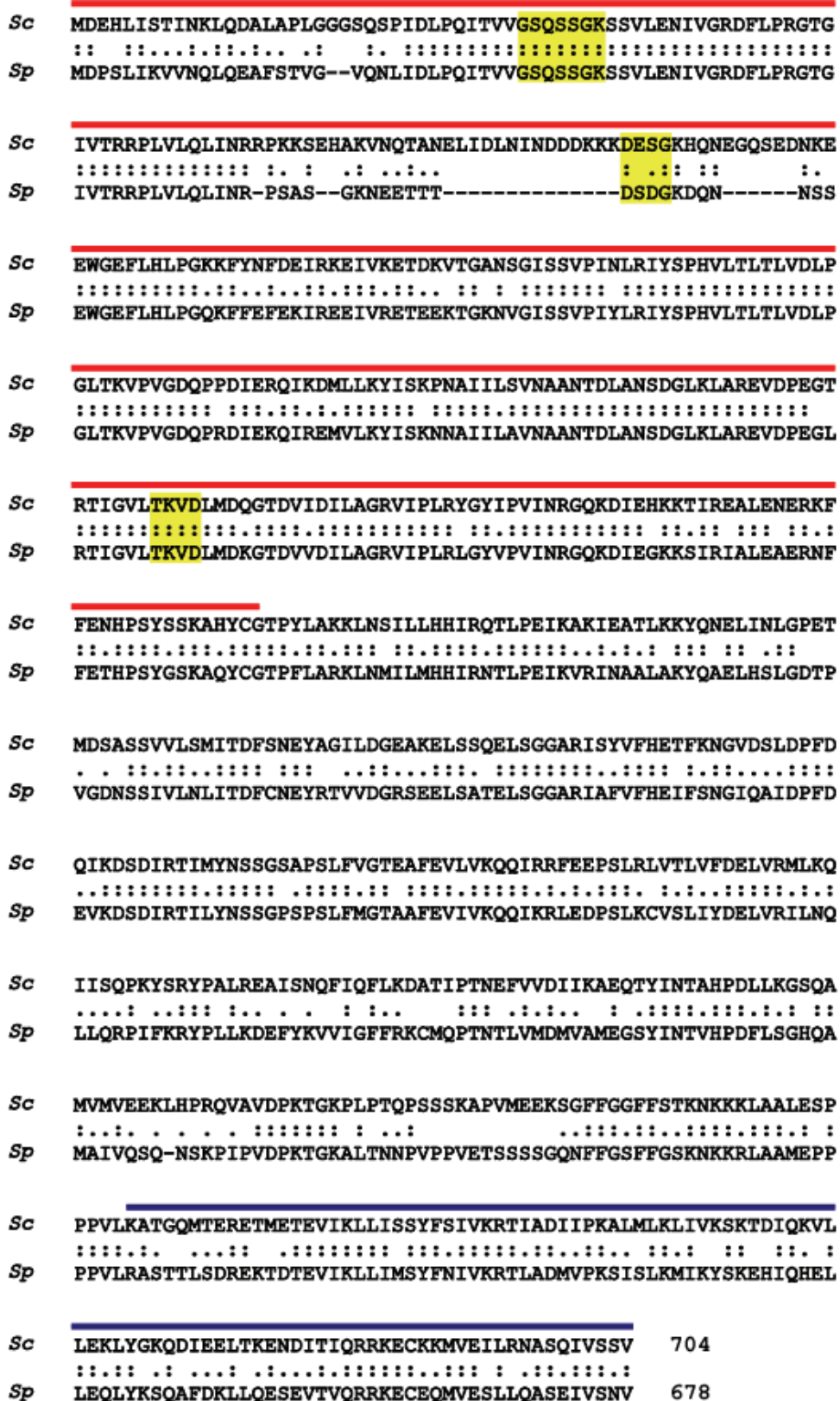
---

#### 3.1.1. Vps1 sequence and domains

The fission yeast gene coding for Vps1 (SPAC767.01c) was identified on the basis of its homology with the *VPS1* gene of *S. cerevisiae* (Vater *et al.*, 1992). Alignment of the Vps1 amino acid sequences from *S. cerevisiae* and *S. pombe* (fission yeast) showed 62.9% sequence identity (Figure 3.1). All dynamins have 3 conserved domains which distinguish them from other GTPases. These distinctive features are a large N-terminal GTPase domain involved in binding and hydrolyzing GTP, a middle domain and a C-terminal GTPase effector domain (GED), which regulates GTPase activity and protein oligomerization. As can be seen in Figure 1, the *S. pombe* Vps1 amino acid sequence has the conserved GTPase, middle and GTP effector domains typical of dynamins, as well as the three consensus GTP-binding motifs GSQSSGKS, DXXG, and TKVD (Dever *et al.*, 1987; Rothman *et al.*, 1990). Altogether, this significant sequence conservation suggests that *S. pombe* Vps1 is a dynamin-related protein, functionally homologous to *S. cerevisiae* Vps1p.

#### 3.1.2. Vps1 characterisation

To gain insight into the role of Vps1 in vacuole biogenesis and function, a *vps1Δ* fission yeast strain developed in a previous study in this lab (Jourdain *et al.*, 2008) was used. As a first step in characterising *vps1Δ*, cell viability at both the permissive (25°C) and the restrictive (36°C) temperatures was tested. In order to do this, wild type and *vps1Δ* colonies were streaked onto YES plates (rich medium) and incubated at both 25°C and 36°C for 3 days. At 25°C the *vps1Δ* mutant grew at a similar rate as the wild type (Figure 3.2 a), whereas at 36°C *vps1Δ* growth was slightly delayed (Figure 3.2 b), similar to the *vps1Δ* mutant in *S. cerevisiae* (Rothman and Stevens, 1986). To obtain a better estimate of the growth rate, growth curves were measured for wild type and *vps1Δ* at both temperatures. For this, cell cultures were set up at 25°C and incubated for 5 generations (~20 hr), after which they were switched to 36°C for at least one generation time (~ 4 hr), or left at 25°C, and the optical density (OD<sub>600nm</sub>) was measured every hour.



GTPase domain

Middle domain

GED domain

Figure 3.1. Protein sequence alignment of *Saccharomyces cerevisiae* Vps1 (Sc) and predicted *Schizosaccharomyces pombe* Vps1 (Sp). The two proteins share 62.9% identity. Red bar: GTPase domain, blue bar: GTP effector domain (GED), yellow boxes: consensus GTP-binding motifs.

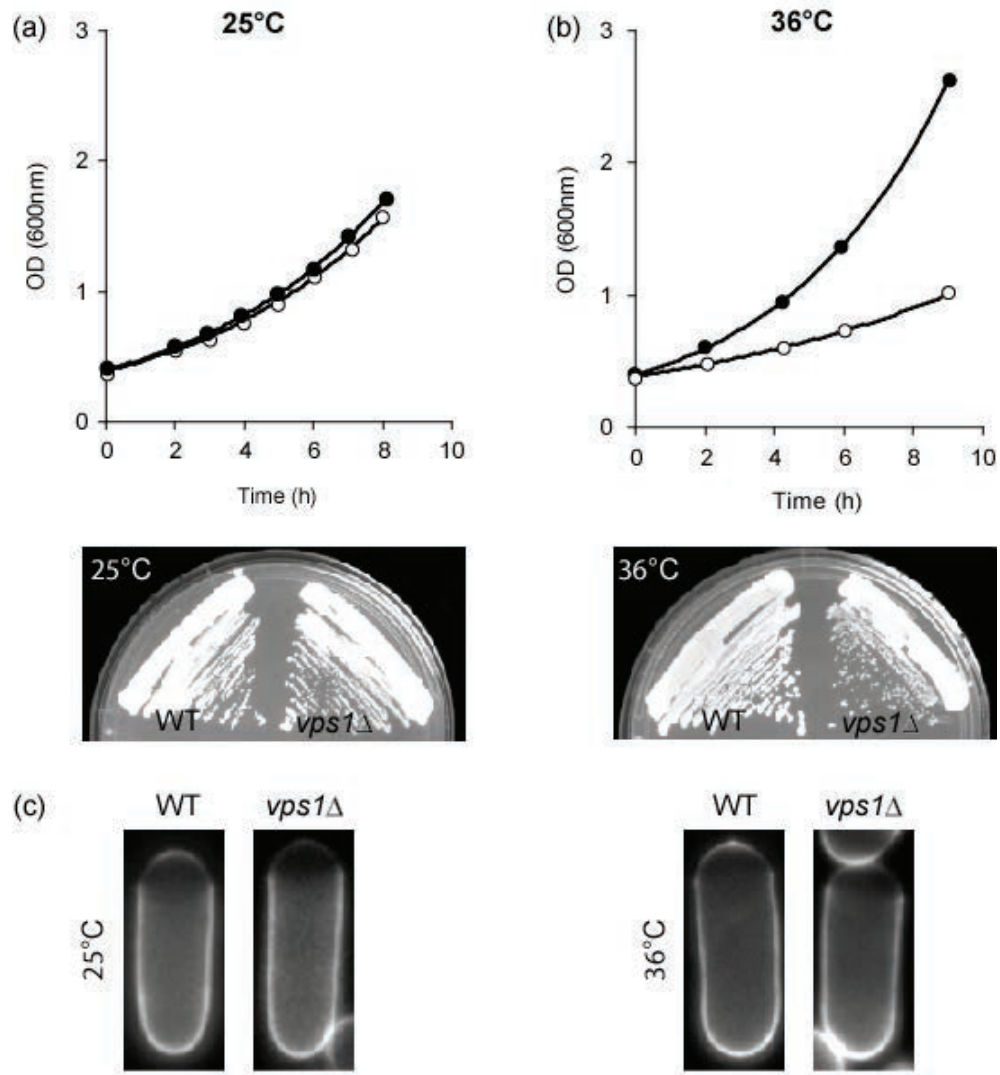


**Figure 3.2. *vps1Δ* is slightly temperature sensitive at 36°C.** The growth phenotype of wild type and *vps1Δ* cells was examined at 25°C and 36°C, by streaking colonies on plates and measuring the optical density ( $OD_{600nm}$ ) of liquid cultures. **(a)** At 25°C *vps1Δ* grew at a similar rate as the wild type, with a 4 hour generation time. **(b)** At 36°C *vps1Δ* growth was slightly delayed with a 6.5 hr generation time as opposed to 3.25 hr in the wild-type. Filled circles: wild type; open circles: *vps1Δ*. **(c)** *vps1Δ* cells have a normal shape and size. Wild type and *vps1Δ* cells were grown at 25°C and 36°C and stained with calcofluor. Bar, 5  $\mu$ m.

At 25°C the *vps1Δ* mutant had the same generation-time as the wild type (4 hr) (Figure 3.2 a), whereas at 36°C its generation-time was double that of the wild type (*vps1Δ*= 6.5 hr; WT= 3.25 hr) (Figure 3.2 b). As determined by staining the cell wall with calcofluor (Figure 3.2 c), the shape and size of *vps1Δ* cells was apparently normal at both the permissive and restrictive temperatures, similar to the wild type. These results indicate that Vps1 is not essential for cell viability, although its absence makes cells temperature-sensitive for growth. Also, loss of Vps1 in fission yeast has

no significant effect on cell morphology, contrary to what is seen in budding yeast (Yu and Cai, 2004), suggesting a functional actin cytoskeleton.

The name Vps stands for vacuolar protein sorting (Rothman and Stevens, 1986). In *S. cerevisiae*, many genes required for vacuolar protein sorting have been identified in several independent screens (Rothman and Stevens, 1986; Raymond *et al.*, 1992; Bonangelino *et al.*, 2002). *vps* mutants have defective membrane trafficking from the prevacuolar compartment to the vacuole. As a result, the vacuolar protease carboxypeptidase Y (CPY) is missorted and secreted from the cell and can then be detected using an anti-CPY antibody in a simple colony blot assay. Sorting of CPY in *vps1Δ* was examined by detecting the secretion of CPY into the growth media by immunoblotting. Wild type cells efficiently sorted CPY to the vacuole and therefore it was not detected in the growth medium (Figure 3.3 a). Surprisingly, *vps1Δ* cells also showed normal vacuolar protein processing as CPY secretion was not detected (Figure 3.3 a). *vps34Δ*, on the other hand, has been reported in fission yeast to secrete high levels of CPY (Takegawa *et al.*, 1995) and was thus used as a positive control (Figure 3.3 a).

To confirm this result, the rate of CPY maturation was determined by pulse-chase analysis, courtesy of Dr Kaoru Takegawa our collaborator in Japan. CPY is processed from the ER- and Golgi-specific precursor form (proCPY) to a mature form (mCPY) by proteases in the vacuole (Tabuchi *et al.*, 1997) and these modifications lead to changes in its apparent molecular mass. During the initial labelling period, proCPY and a small amount of mCPY were produced in wild type cells (Figure 3.3 b). After a 30 min chase, proCPY was almost completely converted to mCPY (Figure 3.3 b). In the *vps1Δ* mutant there was a slight delay in CPY processing, as after 30 min there was still a small amount of proCPY which had not been processed to the mature form (Figure 3.3 b). On a whole, *vps1Δ* exhibited a near normal rate of CPY maturation similar to that seen in the wild type and taken together, these results indicate that Vps1 in fission yeast is not required for vacuolar protein sorting as its name would suggest.

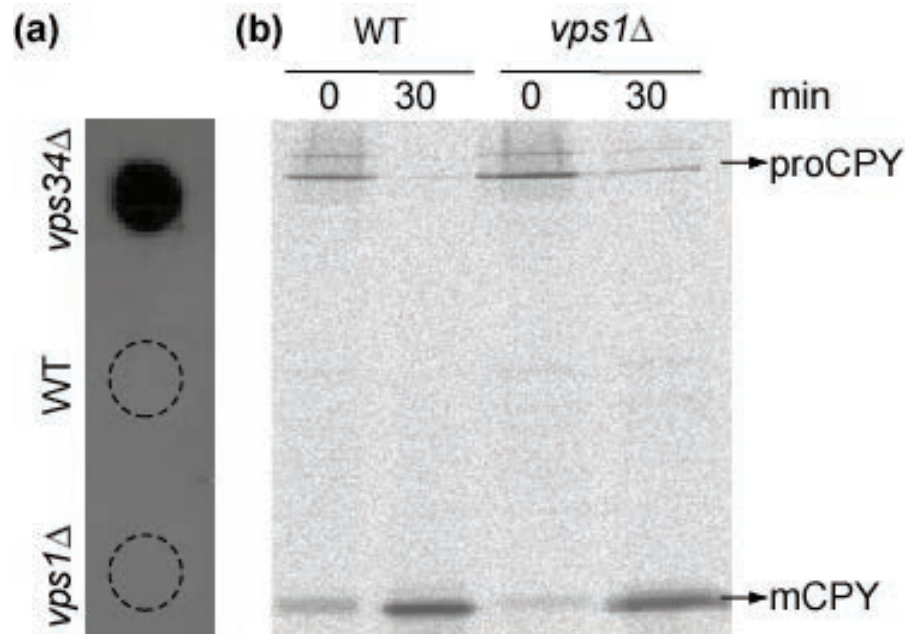


**Figure 3.3. Vps1 is not required for vacuolar protein sorting.** (a) *vps1Δ* does not secrete CPY into the growth medium. Missorted carboxypeptidase Y (CPY) was detected by colony blot assay using an antibody against *S. pombe* CPY. *vps34Δ* was used as a positive control. (b) *vps1Δ* has near normal CPY processing. Wild type and *vps1Δ* strains were pulse-labelled with Express35<sup>S</sup> for 15 min and cold chased for 30 min. The positions of the precursor (proCPY) and the mature (mCPY) forms of CPY are indicated. Figure (b) is courtesy of Dr K. Takegawa.

In other organisms, dynamins have been reported to be involved in endocytosis. The first of these reports was in *Drosophila*, where the temperature-sensitive dynamin mutant *shibire* exhibited a paralytic phenotype due to blocked endocytosis at the presynaptic membranes (Kosaka and Ikeda, 1983b). In *S. cerevisiae*, the dynamin-related protein Vps1 has been also been shown to be involved in endocytosis and actin organisation (Yu and Cai, 2004). In order to assess the role of fission yeast Vps1 in endocytosis, *vps1Δ* cells were incubated with the fluorescent dye FM4-64, which enters fission yeast cells via the endocytic pathway and is transported to the vacuoles (Gachet and Hyams, 2005). To examine the rate of FM4-64 incorporation, wild type and *vps1Δ* cells were labelled with FM4-64 on ice and chased for given periods of time. Initially, FM4-64 stained the cell membrane and after a couple of minutes the fluorescent spots began to move from the cell tips into the interior of the cell until the vacuolar membranes became stained (Figure 3.4). In the *vps1Δ* mutant the rate of FM4-64 endocytic internalization was comparable to that in the wild type and in both cases vacuoles could be visualised from about 30 min (Figure 3.4), suggesting that



there is little difference in the rate of endocytosis in the two strains. However, it was noted that *vps1Δ* cells had smaller vacuoles than the wild type (Figure 3.4), suggesting a role for Vps1 in vacuole morphology rather than in endocytosis.

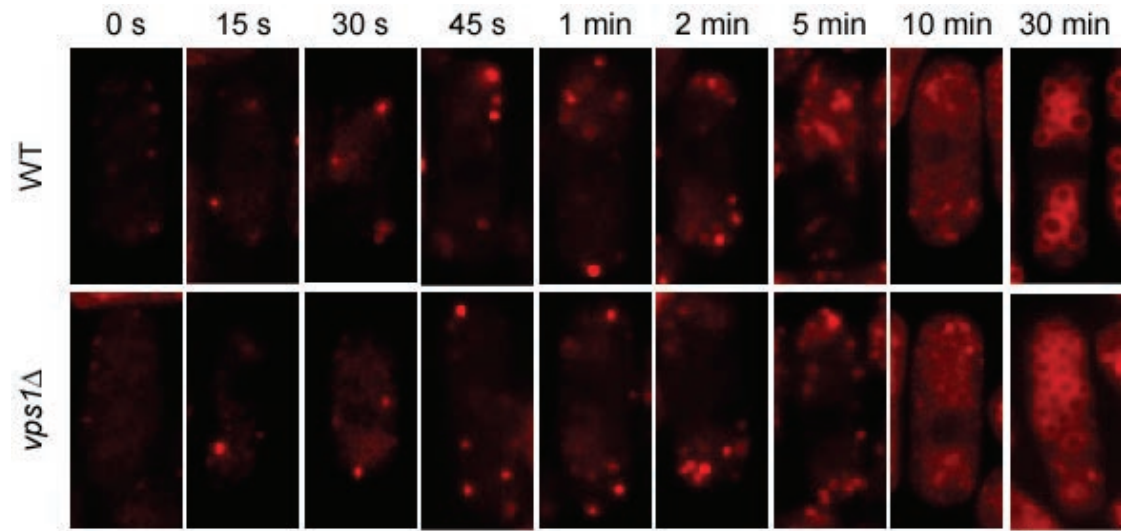


**Figure 3.4. Vps1 is not required for endocytosis.** Wild type and *vps1Δ* cells were labelled with FM4-64 and chased for given periods of times. *vps1Δ* cells have smaller vacuoles than the wild type. Bar, 5 $\mu$ m.

Given that endocytosis requires a functional actin cytoskeleton (Gachet and Hyams, 2005), the next step was to examine actin organisation in *vps1Δ* cells. As endocytosis was normal in *vps1Δ* it was assumed that the actin cytoskeleton would also be normal, as indeed was the case. The actin cytoskeleton in fission yeast is comprised primarily of F-actin patches and cables, as in budding yeast. Both structures can be visualized by rhodamine-phalloidin staining, with the disadvantage that the cells have to be fixed first. Unfortunately, there is no tool available for observing actin cables in live fission yeast cells, although it is possible to visualize live actin patches with coronin-GFP (Crn1-GFP), a protein that binds to, bundles and nucleates F-actin (Pelham and Chang, 2001). As can be seen in Figure 3.5 a, rhodamine-phalloidin staining of the actin cytoskeleton showed no difference between the wild type and *vps1Δ* cells. In both cases the actin patches were polarised to the growing cell tips. Time-lapse microscopy of wild type and *vps1Δ* cells, in which actin patches were visualised using Crn1-GFP, showed no difference in the localization of actin patches or their movement (Figure 3.5 b).

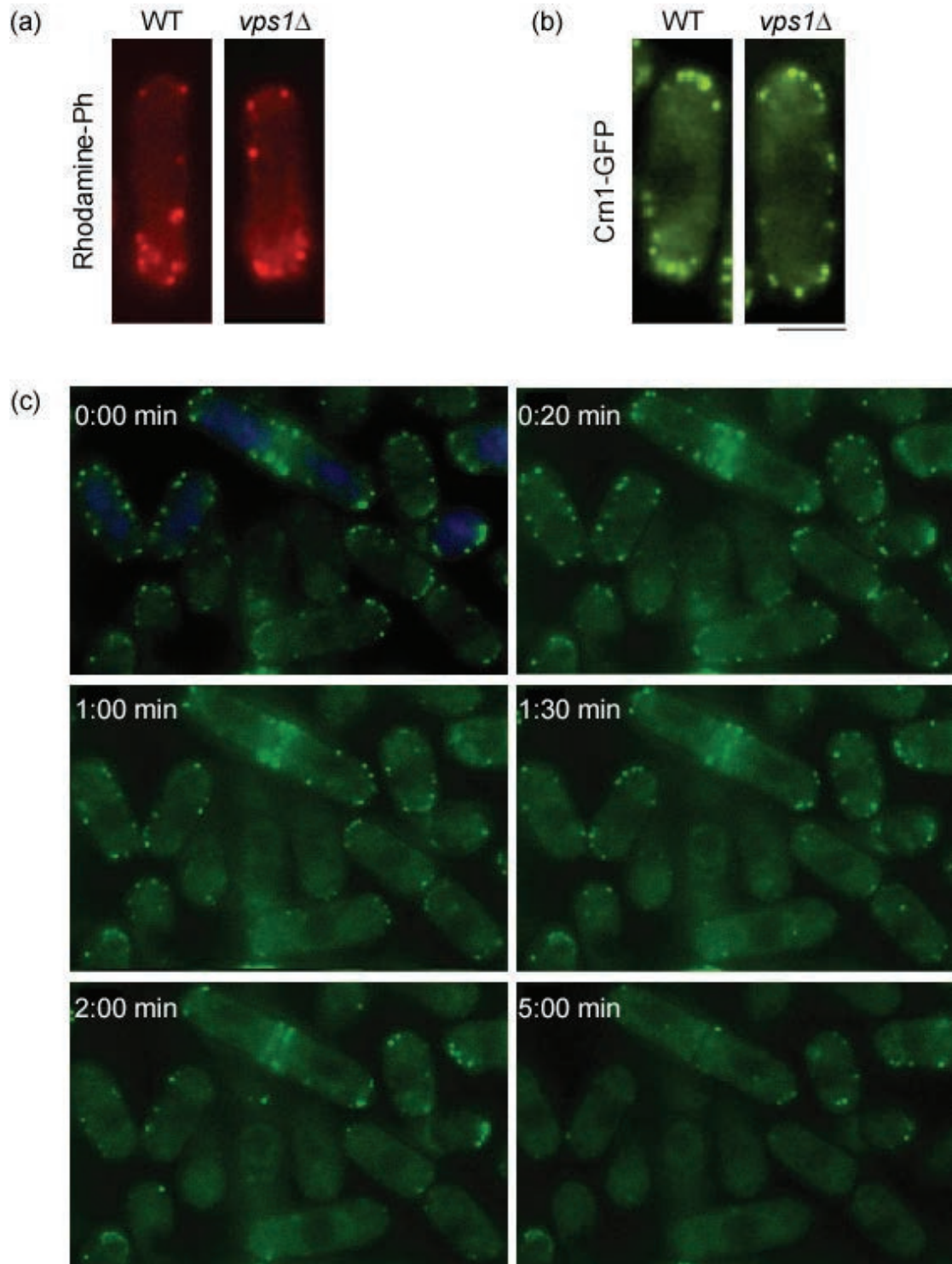


**Figure 3.5. Actin patches in *vps1Δ* are polarised to the growing cell tips, but are more sensitive to Lat-A.** Actin patches are polarised to the cell tips in both wild type and *vps1Δ* cells, shown by (a) rhodamine-phalloidin staining and by (b) tagging actin patches with Crn1-GFP. (c) Time-lapse images of wild type (nucleus stained with Hoescht) and *vps1Δ* cells treated with 75  $\mu$ M Lat-A shows that actin patches in *vps1Δ* cells are more sensitive to the actin depolymerising drug. Bar, 5  $\mu$ m.

Another approach for revealing the integrity of the actin cytoskeleton is the use of drugs affecting actin, such as Latrunculin A (Lat-A). Lat-A causes complete disruption of the actin cytoskeleton, both *in vitro* (Coue *et al.*, 1987) and *in vivo* (Spector *et al.*, 1983), without affecting mitotic spindles and cytoplasmic microtubules. It does this by binding and sequestering actin monomers thus inhibiting actin assembly. The promptness of actin disassembly in yeast cells treated with Lat-A suggests that actin filaments turnover very rapidly in living cells. Differences in Lat-A sensitivities of mutant strains highlight their contribution to cytoskeleton stability. Therefore, wild type and *vps1Δ* cells were washed with 75 μM Lat-A, by perfusion under the coverslip, and time-lapse images were taken every 2 seconds in order to analyse the stability of actin patches. Actin cables are more sensitive to Lat-A than patches and at this concentration of Lat-A both patches and cables are depolymerised (Tournier *et al.*, 2004). Actin patches were followed using Crn1-GFP. Wild type cells were first stained with Hoechst, for later recognition, and mixed with unstained *vps1Δ* cells in order to reduce experimental error between the two strains. Treatment with 75 μM Lat-A caused the disappearance of most actin patches in *vps1Δ* cells within 2 minutes (Figure 3.5 c), whereas actin patches in the wild type (nucleus stained with Hoechst) were more stable, some being still visible after 5 minutes (Figure 3.5 c). The fact that the *vps1Δ* mutant was hypersensitive to Lat-A suggests that Vps1 is required for actin cytoskeleton organization and integrity. A similar situation has been described in *S.cerevisiae* (Yu and Cai, 2004).

In order to confirm this result, a Lat-A halo assay was performed. In this assay, a lawn of cells was spread on a YES plate and small filter disks, permeated with different concentrations of Lat-A, were placed around the plate (Figure 3.6 a). Cells are unable to grow in the presence of Lat-A and thus a halo is formed in the lawn of cells. For a given strain, the halo size increases proportionally to the concentration of Lat-A. As can be seen in Figure 3.6 a, *vps1Δ* cells tolerated higher concentrations of Lat-A than the wild type, as the mean halo sizes of *vps1Δ* were smaller than in the wild type. The sensitivity to Lat-A was quantified as a ratio, in which halo size for wild type was normalized to 1. At 25°C, *vps1Δ* was approximately 10% less sensitive to Lat-A (WT= 1; *vps1Δ*= 0.9), while at 36°C *vps1Δ* was nearly 20% less sensitive (WT= 1; *vps1Δ*= 0.82) (Figure 3.6 b). The increased resistance to Lat-A at 36°C is due to the fact that cytoskeletal polymers are more stable at higher temperatures.

This experiment poses the problem of low reproducibility, hence these results are inconclusive, as the time-lapse experiment suggests that *vps1Δ* is more sensitive to Lat-A while the halo assay indicates the opposite.

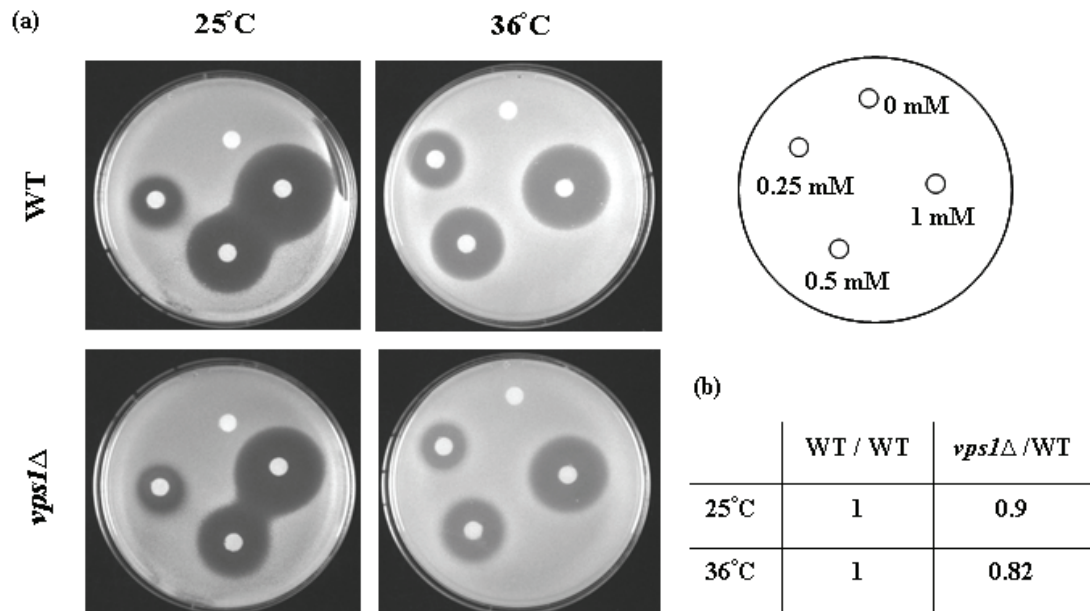


**Figure 3.6. *vps1Δ* is more resistant to Lat-A.** (a) Wild type and *vps1Δ* cells were grown on YES plates and spotted with different concentrations of Lat-A, as described in Materials and Methods. (b) The halo diameters were measured at 0.25, 0.5 and 1 mM LAT-A. The results were quantified as ratios (WT normalised to 1).

To clarify whether Vps1 has a role in actin organization it was examined whether the absence of Vps1 exacerbated the phenotype of the *for3Δ* actin mutant, which lacks actin cables and has delocalized actin patches (Feierbach and Chang, 2001). The *vps1Δ*, *for3Δ* and *vps1Δ for3Δ* double mutant strains were visualized by differential interference contrast (DIC) microscopy and their shape phenotypes quantified (Figure 3.7). *vps1Δ* cells were 100% normal, whereas *for3Δ* cells were either chubby (65%), pear-shaped (28%) or bent (7%) (Figure 3.7). The *vps1Δ for3Δ* double mutant had the same phenotype distribution as *for3Δ* (Figure 3.7) indicating that the absence of Vps1 did not exacerbate the actin phenotype.

Vps1p in budding yeast has been shown to have a number of cellular roles including vacuolar protein sorting (Vater *et al.*, 1992), growth and endocytosis at high

temperatures (Rothman *et al.*, 1990) and actin organization (Yu and Cai, 2004). As in budding yeast, Vps1 in fission yeast is not an essential protein but its absence causes temperature sensitivity. Surprisingly however, Vps1 in fission yeast appears not to be involved in membrane trafficking and vacuolar function, nor does it seem to have a role in actin organisation. The interesting feature which was noted in fission yeast *vps1Δ* cells was the reduction in vacuole size as compared to the wild type; therefore, the following experiments focus on vacuole morphology.

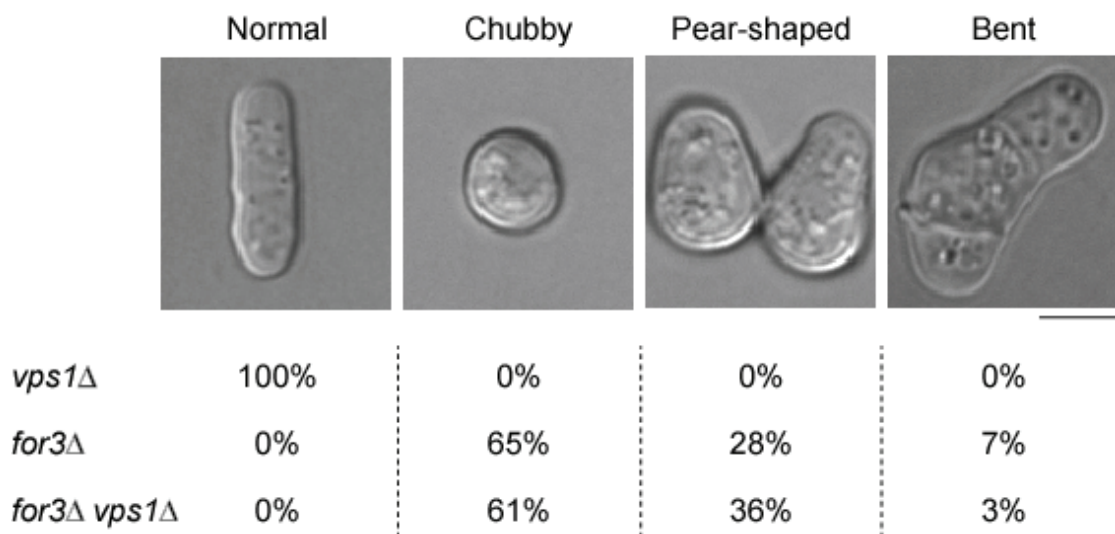


**Figure 3.7. The absence of Vps1 does not exacerbate the shape phenotype of the *for3Δ* actin mutant.** Cells were imaged by DIC microscopy and the percentage of cells in each category (normal, chubby, pear-shaped or bent) was determined. Bar, 5μm.

## 3.2. VPS1 AND VACUOLE MORPHOLOGY

### 3.2.1. Loss of Vps1 affects vacuole size but not vacuole function

To determine the role of Vps1 in vacuole biogenesis in *S. pombe*, vacuoles in wild type and *vps1Δ* cells were labelled with either FM4-64, which stains the vacuolar membrane, or CDCFDA which illuminates the vacuolar lumen (Bone *et al.*, 1998; Takegawa *et al.*, 2003; Gachet and Hyams, 2005) (Figure 3.8 a). Vacuole diameter was ~25% smaller in *vps1Δ* cells than in wild type in minimal medium (EMM; mean internal diameter WT = 0.80 μm; *vps1Δ* = 0.60 μm) (Figure 3.8 a, b). The difference was not as marked in rich medium (YE; mean internal diameter WT = 0.9 μm; *vps1Δ* = 0.8 μm) (Figure 3.8 b) so all further experiments were carried out in EMM.

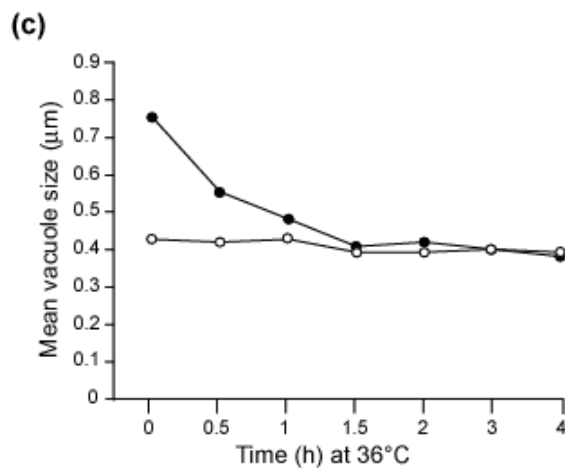
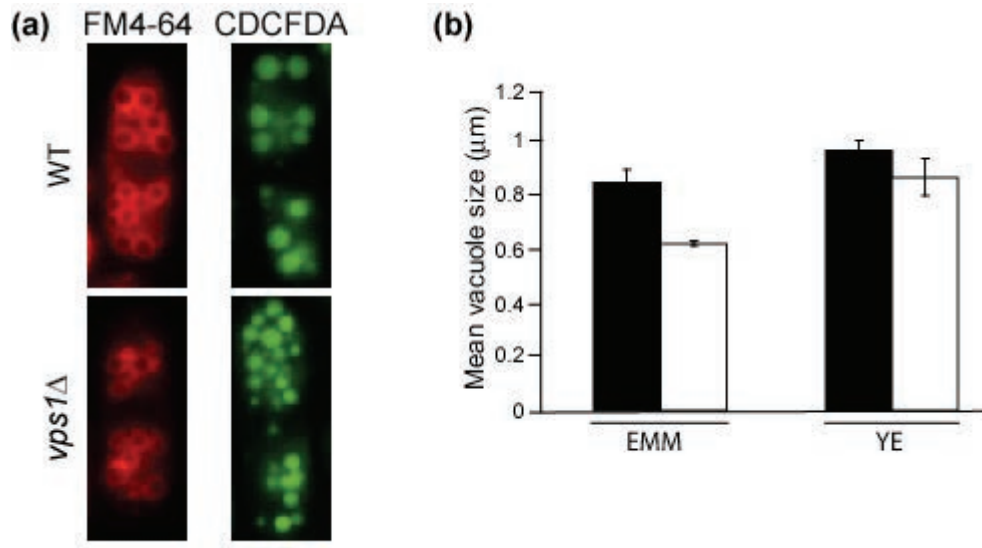


**Figure 3.8. Vps1 controls vacuole size.** (a) *vps1Δ* has small vacuoles. Wild type (WT) and *vps1Δ* cells were labelled with FM4-64 or CDCFDA. Bar, 5μm. (b) The inner diameter of wild type and *vps1Δ* FM4-64 stained vacuoles was measured in cells grown in rich (YE) and minimal (EMM) medium. The difference between wild type and *vps1Δ* vacuoles is more obvious in EMM. Results are the mean of at least two independent experiments. Between 280 and 350 vacuoles were measured in each case.

(c) Time course of vacuole size in wild type (filled circles) and *vps1Δ* cells (open circles) following transfer from 25°C to 36°C. Vacuoles were stained with FM4-64 and their diameter measured. Unlike wild type, *vps1Δ* vacuole size did not change at 36°C.

To investigate whether the temperature sensitivity of *vps1Δ* reflected a vacuole phenotype, both wild type and *vps1Δ* cells were grown at 25°C and transferred to 36°C, after which vacuole size was measured at different time intervals. Wild type vacuoles steadily decreased in size upon shifting the cells to 36°C (from 0.86 to 0.48 μm) (Figure 3.8 c), whilst vacuole size in *vps1Δ* cells remained constant (Figure 3.8 c). This may reflect a failure of *vps1Δ* cells to respond to stress. Even though *vps1Δ* vacuoles were smaller than the wild type, vacuole function appeared to be normal. This is reflected by the normal growth and size phenotype of *vps1Δ* (Figure 3.2 c), normal endocytic uptake of FM4-64 (Figure 3.4, Figure 3.8 a) and vacuole protein



sorting (Figure 3.3). Internal vacuolar homeostasis is also maintained, as indicated by staining with CDCFDA (Figure 3.8 a) which only fluoresces at acidic pH within the vacuole. On a whole, these results indicate that Vps1 in fission yeast plays a role in regulating vacuole size and not vacuole function.

### 3.2.2. Vps1 is involved in vacuole fusion and fission

A vacuole size phenotype can be indicative of a vacuole fusion or fission defect. Vacuole fusion and fission can be followed in living fission yeast cells (Bone *et al.*, 1998) by labelling vacuoles with FM4-64 and incubating cells in distilled water for 2 hr (for fusion) or in 0.4 M NaCl or 1 M sorbitol for 10 min (for fission) (Bone *et al.*, 1998). Vacuole diameter was measured before and after each treatment. In order to reduce error in comparing vacuole fusion and fission efficiencies, a “fusion index” and “fission index” was determined for each strain relative to the size of the control vacuoles. Each value was calculated as a ratio between the initial (control) and the

final (after fusion or fission) vacuole size: 
$$\frac{\text{Mean vacuole diameter}_{\text{final}}}{\text{Mean vacuole diameter}_{\text{initial}}}$$

Following fusion, both wild type and *vps1Δ* showed enlarged vacuoles, although in *vps1Δ* they were approximately 50% smaller than in the wild type (WT = 1.91 μm; *vps1Δ* = 0.91 μm) (Figure 3.9). Thus, *vps1Δ* cells do indeed exhibit a vacuole fusion defect. Under conditions promoting vacuole fission, in both wild type and *vps1Δ* vacuole diameter was substantially reduced (WT = 0.46 μm; *vps1Δ* = 0.39 μm), although in the case of *vps1Δ* vacuole fission was so efficient that this value is almost certainly an underestimate as many vacuoles were too small to be measured accurately (Figure 3.9). To ensure that this result was not an indirect effect of salt-induced stress, the experiment was repeated using 1 M sorbitol and the same effect on vacuole fission was observed (WT = 0.45 μm; *vps1Δ* = 0.37 μm). Thus, quite contrary to the expected function of a dynamin-related protein, Vps1 is important for vacuole fusion but vacuole fission takes place more efficiently in its absence.

Previous studies in this lab have shown that Dnm1, another of the fission yeast dynamin-related proteins, has a role in both mitochondrial fission (Guillou *et al.*,

2005) (Jourdain *et al.*, in preparation) and peroxisome biogenesis (Jourdain *et al.*, 2008). Collaboration between Dnm1 and Vps1 has been shown in these membrane processes. As Vps1 appeared to have a role in regulating the balance between vacuole fusion and fission, it was tested whether Dnm1 was also involved in this process. For this, *dnm1Δ* and the *vps1Δ dnm1Δ* double mutant were labelled with FM4-64 and vacuole fusion and fission were induced (Figure 3.9).

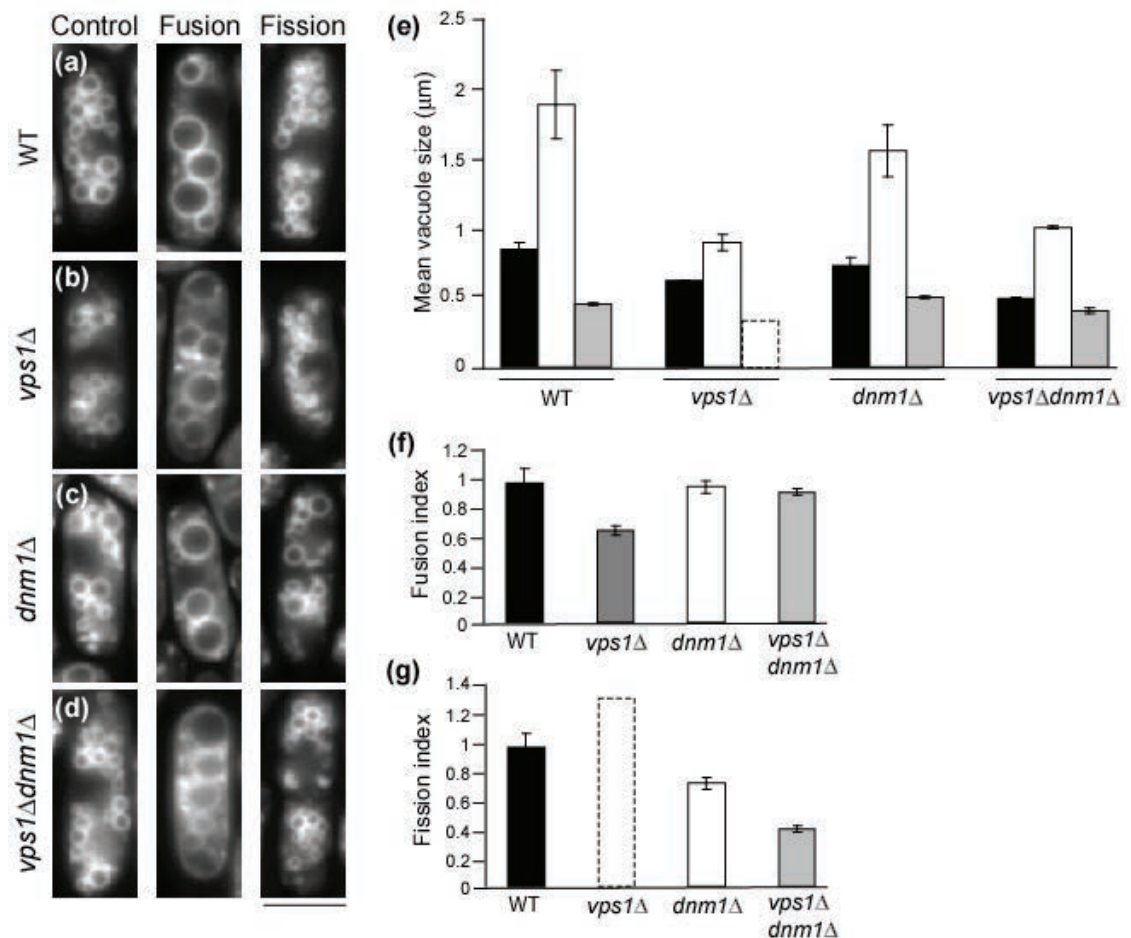


**Figure 3.9. The dynamin-related proteins Vps1 and Dnm1 are involved in vacuole morphology.** Vacuoles in wild type (WT; **a**), *vps1Δ* (**b**), *dnm1Δ* (**c**) and *vps1Δdnm1Δ* cells (**d**) were labelled with FM4-64 and incubated with either EMM (control), water (to examine fusion), or salt (to observe fission). Vacuole diameter was measured in each condition (**e-g**). In (**e**): control vacuole size (black bars), fused vacuoles (white bars) and fragmented vacuoles (grey bars). Fusion and fission indices were normalised to wild type = 1. The higher the index, the more efficient the fusion or fission process. Results are the mean of at least two independent experiments. Between 400 and 450 vacuoles were measured in each condition. Values for *vps1Δ* are shown as dotted bars, as they are likely to be underestimates due to the presence of many vacuoles that were too small to measure accurately. Bar, 5μm.



Vacuole diameter measurements after fusion revealed that the *dnm1Δ* and *vps1Δ dnm1Δ* mutants had fusion values much closer to wild type (WT = 1; *dnm1Δ* = 0.97; *vps1Δ dnm1Δ* = 0.93), than *vps1Δ* (fusion index = 0.6) (Table 3.1). Under fission conditions however, *dnm1Δ* and *vps1Δ dnm1Δ* showed reduced fission efficiencies (WT = 1; *dnm1Δ* = 0.7; *vps1Δ dnm1Δ* = 0.4), whereas fission was enhanced in *vps1Δ* (fission index = 1.27) (Table 3.1). Interestingly, the increased fission index of *vps1Δ* was abolished in the absence of Dnm1 (Figure 3.9 g). Thus, it can be concluded that, as in budding yeast (Peters *et al.*, 2004), Vps1 regulates the balance between vacuole fusion and fission but, in fission yeast, Vps1's role in fission also involves Dnm1.

**Table 3.1** Fusion and fission indices

	Fusion index	Fission index
WT	1	1
<i>vps1Δ</i>	0.66	1.27
<i>dnm1Δ</i>	0.97	0.7
<i>vps1Δ dnm1Δ</i>	0.93	0.44

### 3.2.3. Vps1 is present at the vacuole membrane

If Vps1 has a role at the vacuolar membrane, it should be possible to demonstrate this cytologically. Accordingly, both N- and C-terminally GFP-tagged Vps1 constructs were developed for studying the effects of Vps1 overexpression and observing its localization in the cell. Both Ngfp-Vps1 and Vps1-Cgfp were non-functional in terms of rescuing the vacuole size phenotype of *vps1Δ* (Figure 3.10 a). However, both were able to oligomerize as evidenced by the formation of dots of Vps1 fluorescence, which increased in size relative to the level of expression, as well as showing background cytoplasmic fluorescence (Figure 3.10 b). At a low level of expression (< 20 hr), Vps1-Cgfp localised to small cytoplasmic dots, while at elevated levels of expression (24-36 hr), Vps1-Cgfp was present as large aggregates of fluorescence at the cell poles in interphase cells (Figure 3.10 b). The small dots of Vps1 fluorescence exhibited rapid motility, moving rapidly around the larger Vps1 aggregates as if docking and fusing with them (See Movie 1).

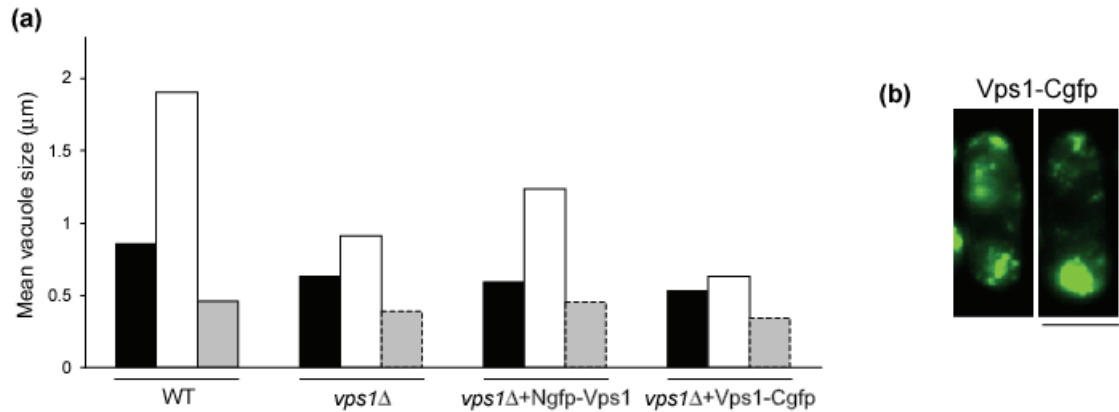


**Figure 3.10. Overexpression of Ngfp-Vps1 and Vps1-Cgfp.** (a) Vacuoles in wild type (WT), *vps1Δ*, *vps1Δ*+Ngp-Vps1 and *vps1Δ*+Vps1-Cgfp cells were labelled with FM4-64 and incubated with either EMM (control, black bars), water (to examine fusion, white bars), or salt (to observe fission, grey bars). Vacuole diameter was measured in each condition. Values shown as dotted bars are likely to be underestimates due to the presence of many vacuoles that were too small to measure accurately. Approximately 400 vacuoles were measured in each condition. (b) Vps1-Cgfp overexpressed in the wild type localised to cytoplasmic dots, which increased in size relative to the level of expression. Bar, 5 µm.

However, in cells containing fused vacuoles Vps1-Cgfp was observed close to, and in many cases following the contours of, the vacuolar membrane (Figure 3.11 a). Therefore, the association of Vps1-Cgfp with isolated vacuoles was examined. Cells were pre-stained with FM4-64 and vacuoles fused in distilled water prior to isolation. Cells were spheroplasted in the presence of sorbitol, broken in a glass-teflon homogeniser and fractions separated on a discontinuous Ficoll gradient. Examination by fluorescence microscopy revealed dots of Vps1 fluorescence, indicating the presence of Vps1 oligomers (Peters *et al.*, 2004), associated with the vacuolar membrane (Figure 3.11 b). Interestingly, Vps1 was present at the vertices, but not the adhering faces, of the apposed vacuole membranes (Figure 3.11 b).

Fractions taken from the vacuole isolation were analysed biochemically by slot blotting onto a membrane and immunoblotting with antibodies against CPY (used as a vacuolar marker) and GFP (Vps1-Cgfp). Both CPY and Vps1-Cgfp were detected in the vacuolar fractions, but not in the cytoplasmic fraction (Figure 3.11 c), thus confirming the cytology findings. It can be concluded that this result indeed reflects the correct association of Vps1 with vacuoles in *S. pombe*, although whether this is exclusive to fused vacuoles is unknown.

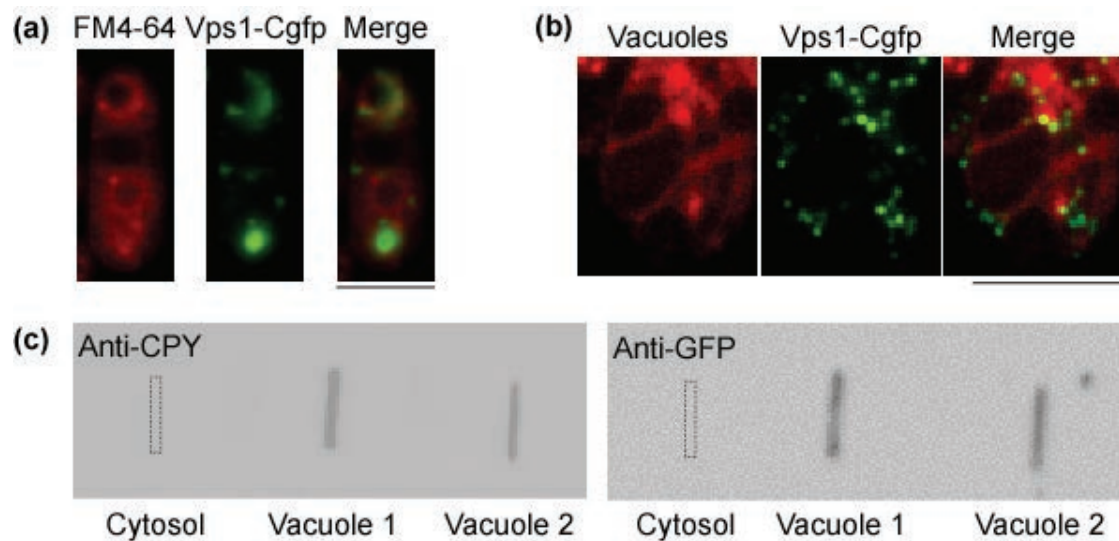


**Figure 3.11. Vps1 localises to the vacuole membrane.** (a) Live cells stained with FM4-64. Vps1-Cgfp is cytoplasmic but also localises to dots, whose size varies with the level of expression, around vacuoles. (b) Isolated vacuoles prestained with FM4-64. Within the vacuolar fraction, spots of Vps1-Cgfp were solely found attached to vacuolar membranes, largely concentrated at vertices. Bars, 5  $\mu$ m. (c) A cytosolic fraction and two vacuole fractions taken from the vacuole isolation were slot blotted onto a membrane and immunoblotted with antibodies against CPY (used as a vacuolar marker) and GFP (Vps1-Cgfp). Both CPY and Vps1-Cgfp were detected in the vacuolar fractions, but not in the cytoplasmic fraction (dotted box).

#### 3.2.4. Overexpression of Vps1 results in vacuole tubulation whilst overexpression of Dnm1 results in vacuole fission

In order to achieve functional overexpression of Vps1, an untagged Vps1 construct was developed. Surprisingly, overexpression of Vps1 in wild type cells resulted in vacuoles becoming extensively tubulated in about 40% of the cells examined (Figure 3.12 a, b). As mentioned above, salt treatment resulted in very small vacuoles in *vps1 $\Delta$* , but not in *vps1 $\Delta$  dnm1 $\Delta$*  (Figure 3.9 g) suggesting that Vps1 and Dnm1 cooperate to fragment vacuoles. Thus, Vps1 was overexpressed in *dnm1 $\Delta$*  which resulted in more than 60% cells having tubular vacuoles which were also more extensive (Figure 3.12 a, b). Expressing Vps1 in a *vps1 $\Delta$*  background also resulted in vacuole tubulation (Figure 3.12 a, b).

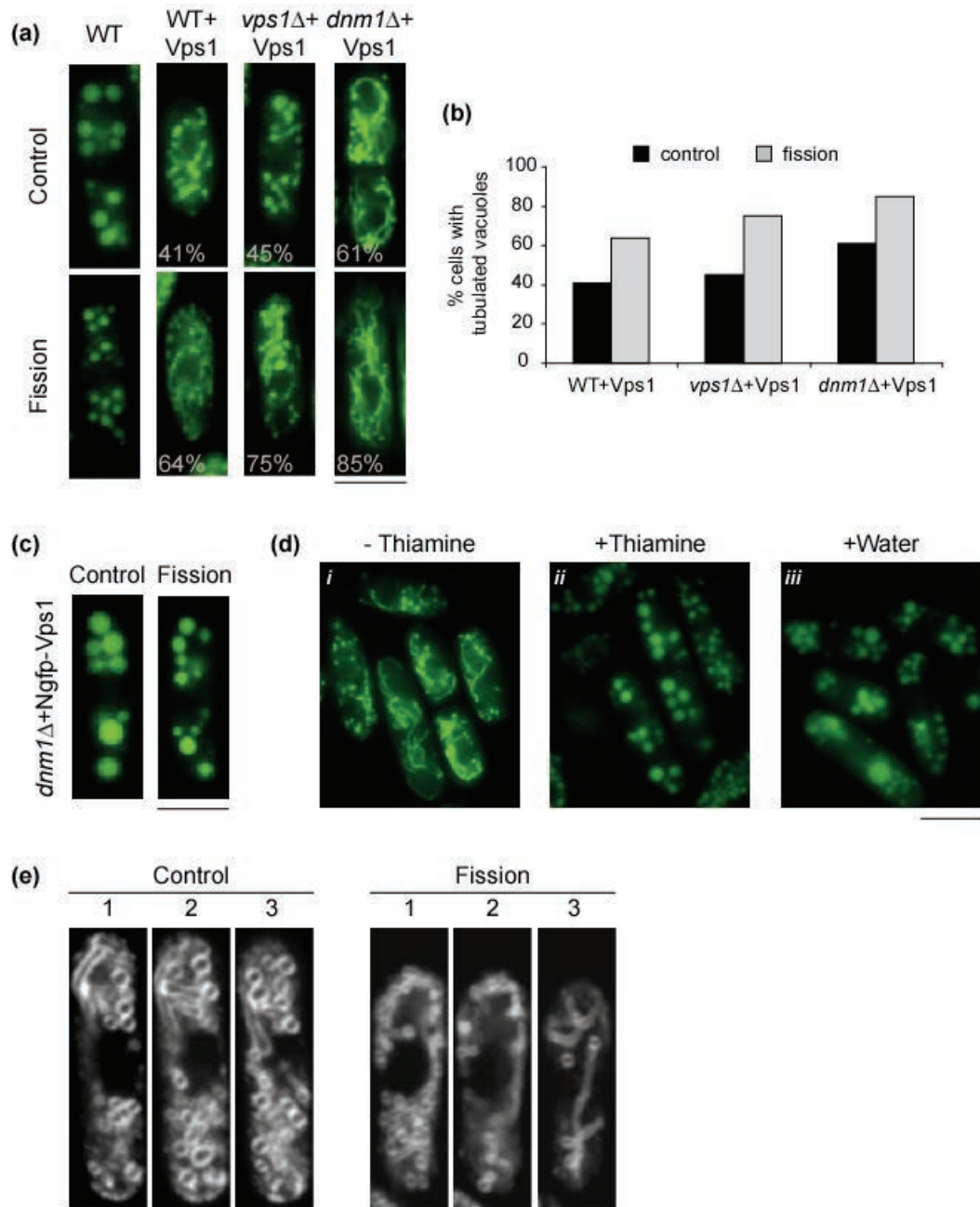


**Figure 3.12. Vps1 induces vacuole tubulation.** (a) CDCFDA-labelling of vacuoles following overexpression of Vps1 in different genetic backgrounds, with and without vacuole fission. Numbers indicate the percentage of cells showing the tubulated phenotype which was defined as the presence of at least two tubules. Vacuoles appeared tubulated in all cases but most strikingly in *dnm1*Δ. Induction of fission enhanced the phenotype. On average 100 cells were counted in each condition. (b) Graph showing the percentage of cells with tubulated vacuoles in each condition. (c) Overexpression of the non-functional Ngfp-Vps1 did not induce vacuole tubulation. (d) (i) Control cells expressing Vps1 in the absence of thiamine. (ii) Normal vacuole morphology was restored following the addition of 60 μM thiamine for 22 hrs to shut off expression of the Vps1 plasmid, or (iii) by incubation in water for 1 hr to induce vacuole fusion. (d) Confocal images of *dnm1*Δ cells overexpressing Vps1 and stained with FM4-64. Inducing fission caused the tubular vacuoles to become longer and thinner. Three z-sections are shown. Bars, 5 μm.

In all cases, the extent of tubulation was increased following the induction of fission (64% of cells in the wild type, 75% in *vps1Δ* and 85% in *dnm1Δ*) (Figure 3.12 b). No tubulation was observed following overexpression of the non-functional Ngfp-Vps1 (Figure 3.12 c). To ensure that the tubular vacuole phenotype was directly due to the overexpression of Vps1, 60  $\mu$ M thiamine was added to the growth medium and incubated for 22 hr to shut off Vps1 expression (under the control of the *nmt1* thiamine-repressible promoter). Suppression of Vps1 expression resulted in the tubular vacuoles reverting to their normal spherical shape (Figure 3.12 d). The tubular phenotype could also be reversed by transferring cells to water for 1 hr in order to induce fusion (Figure 3.12 d).

Confocal microscopy of *dnm1Δ* cells overexpressing Vps1 and stained with FM4-64 clearly showed that the vacuoles were tubular, with a diameter of approximately 0.4  $\mu$ m (Figure 3.12 e) (See Movie 2). Inducing fission by adding 0.4 M NaCl resulted in a further reduction in diameter of the tubular vacuoles to 0.3  $\mu$ m (Figure 3.12 e). Tubular vacuoles still had normal function, reflected by the endocytic uptake of FM4-64 (Figure 3.12 e) and CDCFDA staining (Figure 3.12 a), as well as by the normal response to the fusion and fission signals (Figure 3.12 d, e). In order to confirm that the Vps1-induced tubules were not just an artifact due to CDCFDA or FM4-64 staining, wild type and *dnm1Δ*+Vps1 cells were visualised by electron microscopy. As can be seen in Figure 3.13, vacuoles in the wild type appear as spherical unstained compartments, whereas in *dnm1Δ* cells elongated, tubular vacuoles are present.

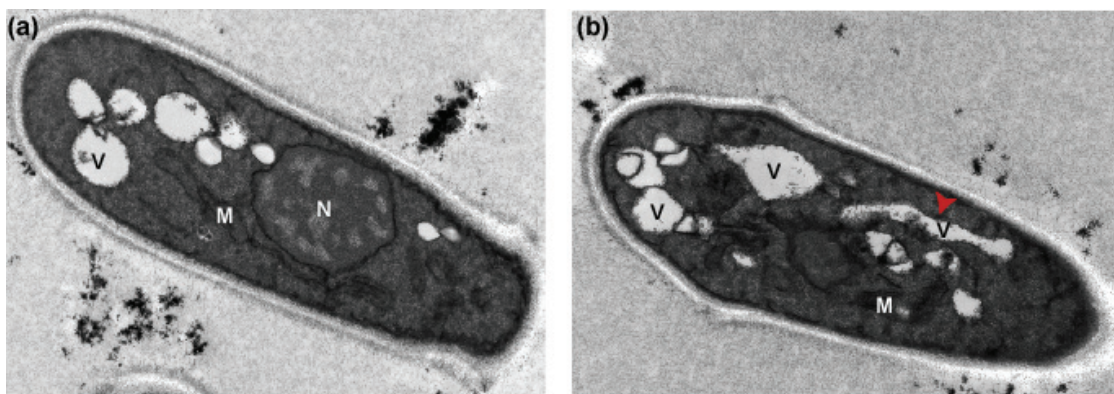


**Figure 3.13. Tubular vacuoles.** Electron micrographs showing (a) spherical vacuoles in the wild type and (b) tubular vacuoles (red arrowhead) in a *dnm1Δ* cell overexpressing Vps1. V: Vacuole, N: Nucleus, M: Mitochondria. Bar, 2  $\mu$ m.

The striking feature of the Vps1 overexpression experiments was the fact that Vps1 tubulates vacuole membranes but does not induce them to undergo fission. Therefore, it is possible that another dynamin serves this function. Since genetic studies indicate the cooperative interaction of Vps1 and Dnm1 (Jourdain *et al.*, 2008), it was examined whether Dnm1 overexpression induced vacuole fission. For this, an N-terminal GFP-tagged Dnm1 construct was made, as well as an untagged version.

Overexpression of both Ngfp-Dnm1 and untagged Dnm1 resulted in a reduction in vacuole diameter from 0.8  $\mu\text{m}$  to 0.5  $\mu\text{m}$  (Figure 3.14 a-d, control). The latter vacuoles were often incompletely stained with CDCFDA and contained a non-fluorescent (i.e., non acidic) invagination (Figure 3.14 b, c). Such vacuole profiles were not observed in *vps1* $\Delta$  cells overexpressing Dnm1 (Figure 3.14 d). The abnormal vacuoles induced by Dnm1 overexpression were less efficient at fusion (mean internal diameter wild type = 1.9  $\mu\text{m}$ ; Dnm1 overexpression = 1.2  $\mu\text{m}$ ) (Figure 3.14 a-d, fusion), but underwent fission in response to salt exposure more efficiently than wild type cells (Figure 3.14 a-d, fission), and were too small to be measured accurately. Thus, Dnm1 plays a role in vacuole fission. This is supported by the fact that *dnm1* $\Delta$  cells occasionally have vacuoles with a “dumbbell” profile, suggesting a fission defect. These incompletely divided “dumbbell” shaped vacuoles were observed both by CDCFDA staining (Figure 3.14 e) and electron microscopy (Figure 3.14 f).

### 3.2.5. Tubular vacuoles are microtubule and actin dependent

The tubular vacuoles observed following Vps1 overexpression were dynamic, on occasions curling back on themselves like a frond (See Movie 3). It is possible that a tubular network of vacuoles requires spatial regulation of its motility and morphology. In order to investigate this, both the microtubule and actin cytoskeletons were perturbed and the effects on the vacuole system were monitored by fluorescence microscopy. Incubating *dnm1* $\Delta$  cells overexpressing Vps1 (which had the most extensive tubular network) with 1.5  $\mu\text{M}$  TBZ (the anti-microtubule drug) caused the tubular vacuoles to revert back to their normal spherical shape (Figure 3.15 a), whereas the tubular phenotype persisted in control cells treated in the same way with DMSO (Figure 3.15 a). Microtubule immunofluorescence using the TAT-1 antibody



revealed that microtubules in TBZ-treated cells were completely depolymerised, whilst in DMSO-treated cells they remained intact (Figure 3.15 a).

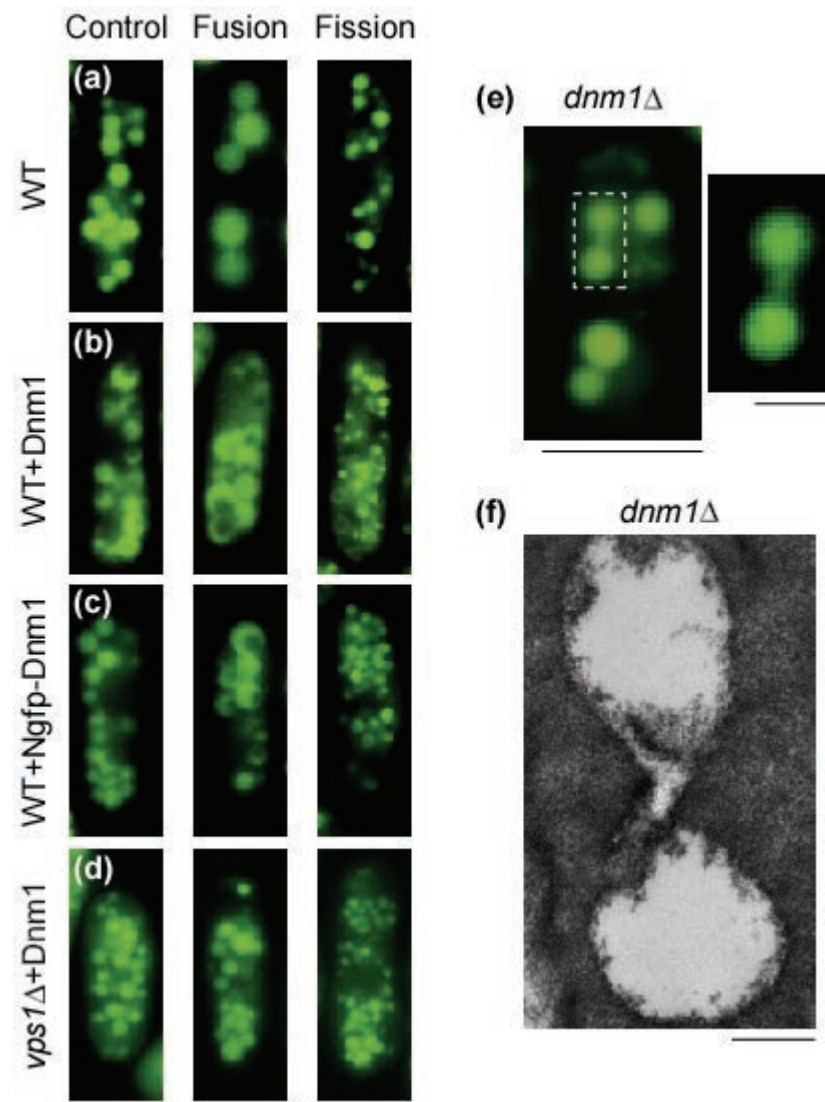


**Figure 3.14. Dnm1 induces vacuole fission.** Overexpression of Dnm1 results in the formation of small vacuoles which fuse less efficiently and fragment more. Vacuoles in (a) wild type, (b) WT+Dnm1, (c) WT+Ngfp-Dnm1 and (d) *vps1Δ*+Dnm1 cells were labelled with CDCFDA and incubated in either EMM (control), water, to examine vacuole fusion, or salt, to observe fission. Bar, 5  $\mu$ m. Note that in individual vacuoles, the CDCFDA staining is often incomplete. (e) Incompletely divided “dumbbell” shaped vacuoles are occasionally seen in *dnm1Δ*. Bars, 5  $\mu$ m and 2  $\mu$ m. (f) Electron micrograph of a “dumbbell” shaped vacuole in *dnm1Δ*. Bar, 200 nm.

As an alternative approach, Vps1 was overexpressed in the cold-sensitive *nda3-KM311* microtubule mutant (Umesono *et al.*, 1983). These cells were grown at the permissive temperature of 36°C and then shifted to the restrictive temperature of 20°C for at least 5 hr. At the restrictive temperature, *nda3-KM311* cells lack interphase

microtubules and only 5% of the cells had tubulated vacuoles, while under conditions promoting vacuole fission 17% were tubulated (Figure 3.15 b), as opposed to 41% and 64% respectively in the wild type. Together, the TBZ and *nda3-KM311* results (Figure 3.17) confirm a role for microtubules in the regulation of tubular vacuoles in fission yeast.

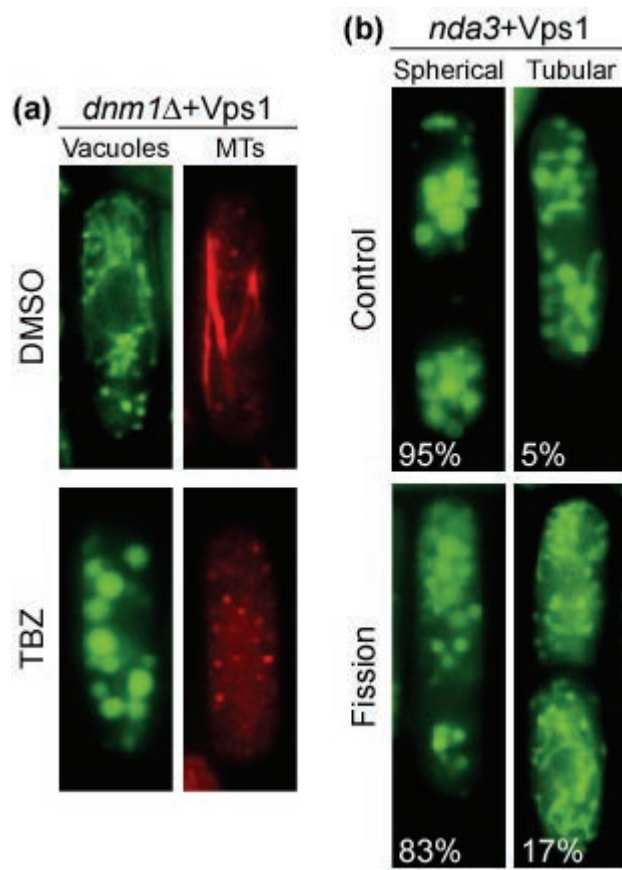


**Figure 3.15. Tubular vacuoles are microtubule-dependent.** (a) *dnm1Δ* cells overexpressing Vps1 were incubated for 15 min with 1.5  $\mu$ M TBZ or with the equivalent concentration of DMSO as a control. Vacuoles were stained with CDCFDA and complete microtubule (MTs) depolymerisation was verified by immunofluorescence using the TAT-1 antibody. (b) Vacuoles in *nda3-KM311* cells overexpressing Vps1 were labelled with CDCFDA and incubated with either EMM (control) or salt (to observe fission). Numbers indicate the percentage of cells showing normal spherical vacuoles or tubular vacuoles. On average 100 cells were counted in each condition. Bar, 5 $\mu$ m.

The actin cytoskeleton was perturbed in *dnm1Δ* cells overexpressing Vps1 by incubating with 65  $\mu$ M Latrunculin A (the anti-actin drug). This also caused the tubular vacuoles to revert back to their normal spherical shape (Figure 3.16 a). Once again, in control cells treated with DMSO there was no change in the tubular phenotype (Figure 3.16 a). Actin immunofluorescence using rhodamine-phalloidin confirmed that in control cells treated with DMSO, both actin patches and cables were visible, whereas in cells treated with Lat-A the actin cytoskeleton was completely abolished (Figure 3.16 a). To corroborate this result, Vps1 was overexpressed in mutants affecting the actin cytoskeleton, such as *myo52Δ* (Mulvihill *et al.*, 2001) and



*for3Δ* (Feierbach and Chang, 2001). These cells were grown at the permissive temperature of 25°C and then shifted to the restrictive temperature of 36°C for at least 5 hrs. At the restrictive temperature, only 11% of *for3Δ* and 10% of *myo52Δ* cells overexpressing Vps1 had tubular vacuoles (Figure 3.16 b, c), while under conditions promoting vacuole fission 26% were tubulated in *for3Δ* and 36% in *myo52Δ* (Figure 3.16 b, c).

As can be seen in Figure 3.17, the percentages of cells with tubulated vacuoles are much smaller under circumstances in which the microtubule or actin cytoskeletons have been disrupted, indicating that they have a role in regulating tubular vacuoles in fission yeast.

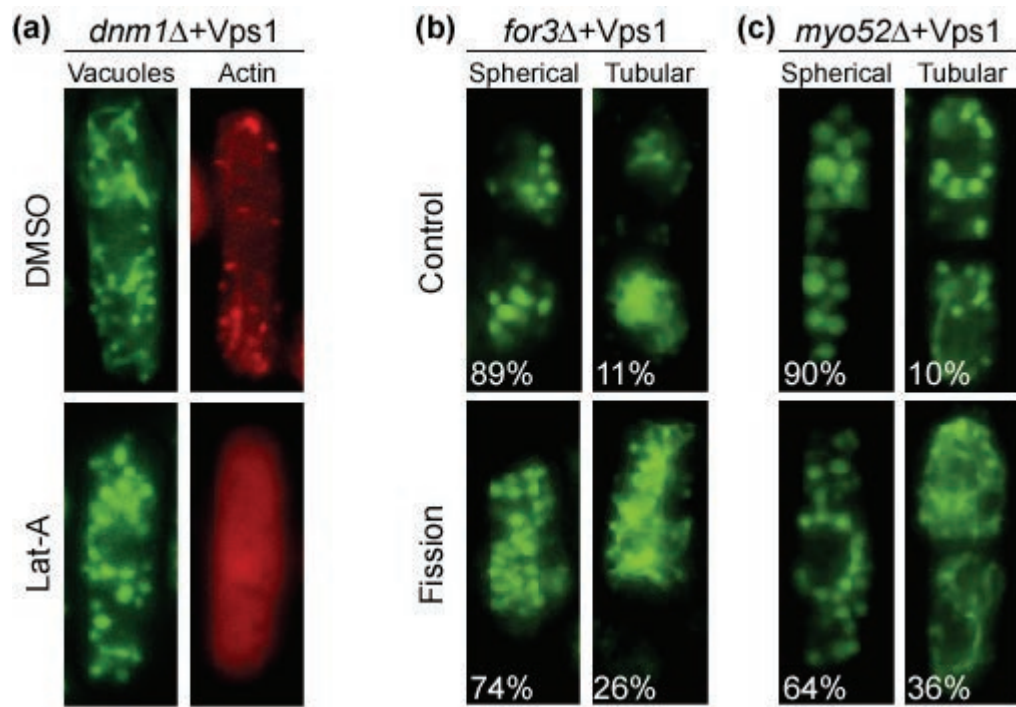


**Figure 3.16. Tubular vacuoles are actin-dependent.** (a) *dnm1Δ* cells overexpressing Vps1 were incubated for 15 min with 65 μM Lat-A or with the equivalent concentration of DMSO as a control. Vacuoles were stained with CDCFDA and actin was visualised by rhodamine-phalloidin staining. Vacuoles in *for3Δ* (b) and *myo52Δ* (c) cells overexpressing Vps1 were labelled with CDCFDA and incubated with either EMM (control) or salt (to observe fission). Numbers indicate the percentage of cells showing normal spherical vacuoles or tubular vacuoles. On average 100 cells were counted in each condition. Bar, 5μm.

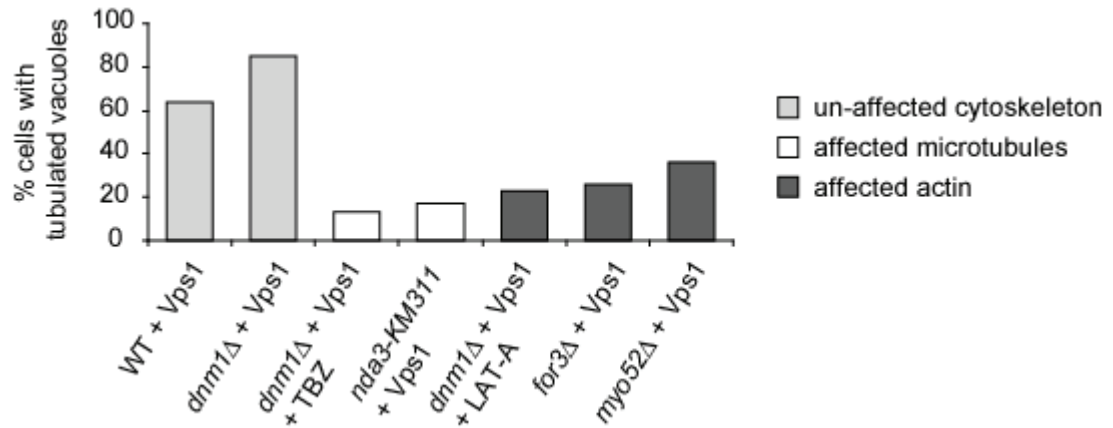


**Figure 3.17. A disrupted cytoskeleton reduces the formation of tubular vacuoles.** Graph showing the percentage of cells with tubulated vacuoles in conditions affecting either the actin or microtubule cytoskeleton.

### 3.2.6. Vps1 GTPase activity is required for vacuole morphology

In order to determine whether GTPase activity is essential for Vps1 function, a Vps1 construct lacking the entire GTPase domain ( $\Delta 1-251a.a$ ) was developed. Overexpression of Vps1-noGTP in wild type and *dnm1Δ* cells did not result in the formation of tubular vacuoles (Figure 3.18), indicating that GTPase activity is required for vacuole tubulation by Vps1. This could be due to lack of GTP binding or GTP hydrolysis. To investigate the requirement of GTP hydrolysis for Vps1 activity, *dnm1Δ* cells overexpressing Vps1 (which had the most extensive tubular vacuoles) were incubated with 100  $\mu$ M GTP $\gamma$ S, a non-hydrolysable form of GTP, either before or after inducing vacuole fission. In the control, 25% of cells presented spherical vacuoles while the remaining 75% had tubular vacuoles (Figure 3.19). Incubating cells with 100  $\mu$ M GTP $\gamma$ S for 45 min either before or after fission resulted in a reduction of cells with tubular vacuoles to 53% and 25%, respectively (Figure 3.19). After treatment with GTP $\gamma$ S, cells were washed several times and incubated in medium for 45 min which resulted in the recovery of tubular vacuoles (72% and 75%) (Figure 3.19). Together, these results indicate that GTP hydrolysis, and not GTP binding, is necessary for formation and maintenance of tubular vacuoles by Vps1.

As GTP hydrolysis is required for Vps1 vacuole tubulation, the next step was to examine whether GTP hydrolysis is also required for normal vacuole fission. Both wild type and *vps1Δ* cells were incubated with 100  $\mu$ M GTP $\gamma$ S for 45 min before

inducing vacuole fission. As can be seen in Table 3.2, when fission was induced in the absence of GTP $\gamma$ S vacuole size decreased from 0.89 to 0.69  $\mu$ m in the wild type and from 0.65 to 0.47  $\mu$ m in *vps1* $\Delta$ . However, when fission was induced in the presence of GTP $\gamma$ S, vacuole size did not decrease (0.81  $\mu$ m in the wild type and 0.57  $\mu$ m in *vps1* $\Delta$ ). Thus, normal vacuole fission by the dynamin-related proteins Vps1 and Dnm1 requires GTP hydrolysis.

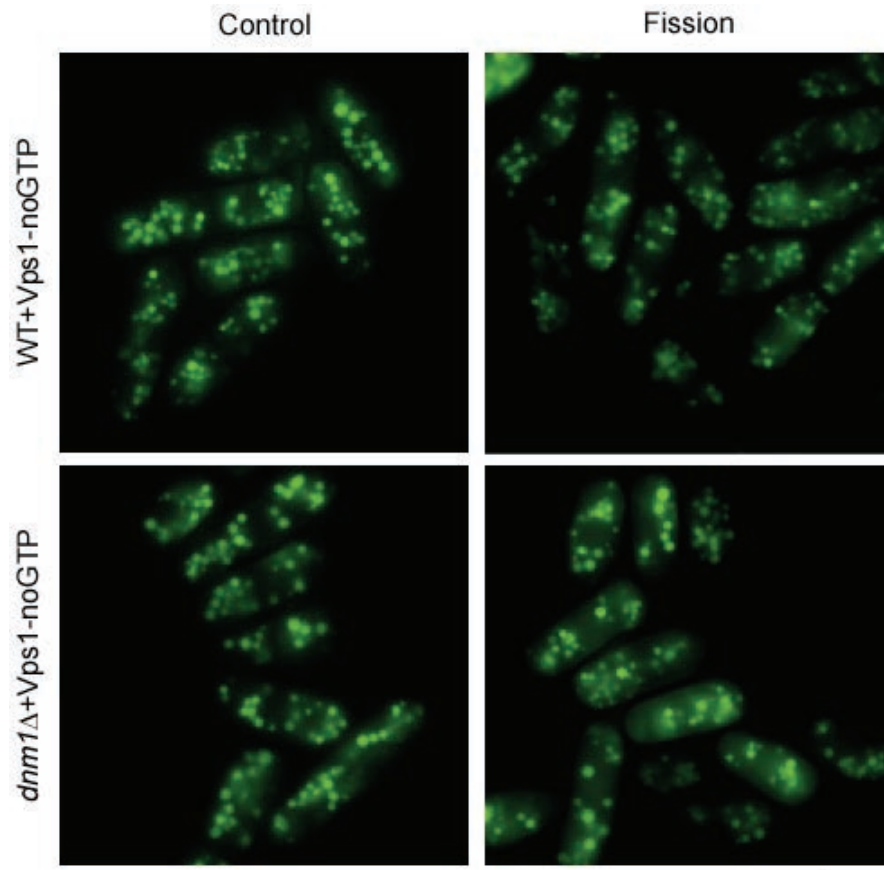


**Figure 3.18. Vps1 GTPase activity is required for vacuole tubulation.** CDCFDA-labelling of vacuoles (with and without fission) in wild type and *dnm1* $\Delta$  cells overexpressing a dominant-negative form of Vps1 which lacks the GTPase domain. Bar, 5  $\mu$ m.

**Table 3.2.** Mean vacuole diameter in cells treated with GTP $\gamma$ S

	Wild type	<i>vps1</i> $\Delta$
<b>Control (no fission)</b>	0.89 $\mu$ m	0.65 $\mu$ m
<b>Fission without GTP<math>\gamma</math>S</b>	0.69 $\mu$ m	0.47 $\mu$ m
<b>Fission with GTP<math>\gamma</math>S</b>	0.81 $\mu$ m	0.57 $\mu$ m

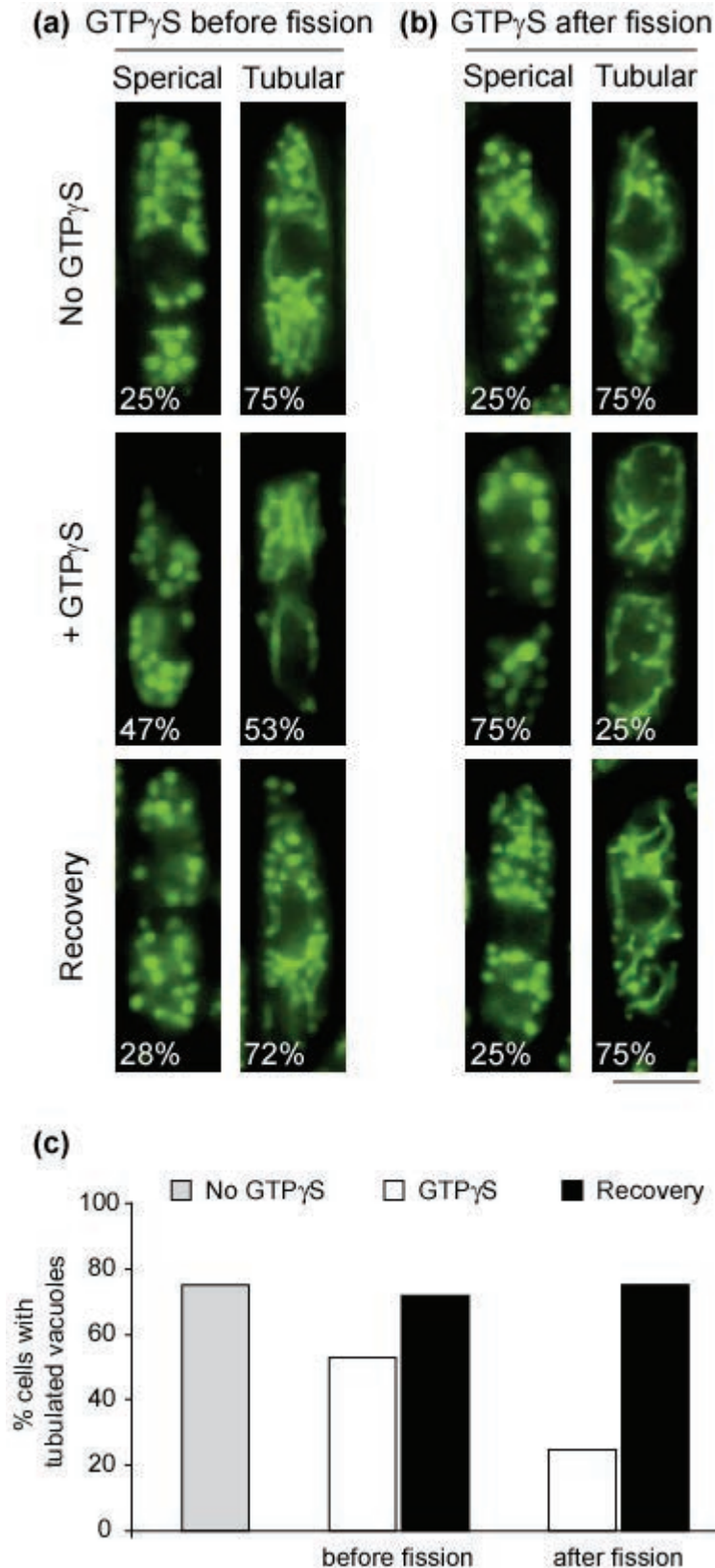


**Figure 3.19. GTP $\gamma$ S blocks tubule formation.** *dnm1* $\Delta$  cells overexpressing Vps1 were stained with CDCFDA for 30 min and incubated with 100  $\mu$ M of GTP $\gamma$ S for 45min either **(a)** before inducing fission or **(b)** after fission. For recovery, cells were washed several times and incubated in medium for 45 min. Numbers indicate the percentage of cells showing normal spherical vacuoles or tubular vacuoles.

Between 100 and 150 cells were counted in each condition. Bar, 5 $\mu$ m. **(c)** Graph showing the percentage of cells with tubulated vacuoles. Adding GTP $\gamma$ S either before or after fission reduces the percentage of cells with tubular vacuoles (compare white bar to grey bar). Recovery, after washing cells free of GTP $\gamma$ S, results in reversion back to the tubular phenotype (compare black bars to grey bar).

## **4. DISCUSSION**

---

#### 4.1. Vps1 has different functions in *S. pombe* and *S. cerevisiae*

---

The fission yeast *vps1* gene was first identified in an analysis of the *S. pombe* genome for homologues of budding yeast *VPS* (vacuolar protein sorting) genes (Takegawa *et al.*, 2003). Vps1 is 63% identical to its budding yeast counterpart, its homology extending throughout the protein except for a 22 amino acid deletion in the GTPase domain of the fission yeast protein. This study demonstrates that although very close to its budding yeast counterpart, Vps1 does not share functional homology in many cellular roles.

The fission yeast *vps1* deletion strain was completely viable even though Vps1 has been reported to be involved in several important cellular processes. In budding yeast, Vps1p was identified in screens for genes required for vacuolar protein sorting (Rothman and Stevens, 1986; Raymond *et al.*, 1992; Bonangelino *et al.*, 2002). In *S. pombe* however, *vps1* $\Delta$  cells were not defective in vacuolar protein processing. The conversion of CPY from the proenzyme to the mature form in *vps1* $\Delta$  was only minorly less efficient than in wild type. Neither was CPY secreted, a common fate of incorrectly processed enzymes (Bonangelino *et al.*, 2002). Thus, despite its name, Vps1 in fission yeast is not concerned with maintaining internal vacuole function. Vps1p in budding yeast has also been shown to be required for normal actin cytoskeleton organization and endocytosis (Yu and Cai, 2004). Budding yeast *vps1* $\Delta$  cells were found to have a depolarised actin cytoskeleton and defective bud site selection (Yu and Cai, 2004). In fission yeast however, deleting *vps1* had no effect on cell shape or size and both rhodamine-phalloidin staining and Crn1-GFP localisation were normal. The Lat-A sensitivity results were inconclusive, but the fact that the *vps1* $\Delta$  *for3* $\Delta$  double mutant had the same phenotype as *for3* $\Delta$  alone indicated that the absence of Vps1 did not worsen the actin phenotype. Taken together, these results suggest that Vps1 in fission yeast is not involved in the organization or function of the actin cytoskeleton. In addition to this, *vps1* $\Delta$  fission yeast cells also exhibited a normal rate of endocytosis, which is an actin-based process (Gachet and Hyams, 2005). This was similar to Dlp1, the mammalian homologue of Vps1, which has also been shown to have no effect on endocytosis (Pitts *et al.*, 1999).

## 4.2. Vps1 is involved in vacuole fission and fusion

---

Vacuoles are dynamic organelles that undergo fission and fusion in response to the environmental conditions (Bone *et al.*, 1998). Maintaining membrane homeostasis requires the coordination of mechanisms controlling these events and dynamins, or dynamin-related proteins such as Vps1, are likely candidates in this process. As in budding yeast (Peters *et al.*, 2004; Vizeacoumar *et al.*, 2006), fission yeast cells lacking Vps1 had a larger number of small vacuoles. Deletion of the *vps1* homologue of *Aspergillus nidulans*, *vpsA*, also results in vacuole fragmentation (Tarutani *et al.*, 2001) indicating a conserved role for this dynamin-related protein in vacuole fusion and fission, at least in fungi. In fission yeast, reduced vacuole diameter in *vps1Δ* cells was observed in minimal medium but was not so noticeable in rich medium. Whether the expression of the *vps1Δ* vacuole phenotype is dependent upon the nutritional status of the cells or differences in the osmotic strength or pH of the two types of medium is unknown. Initially, *VPS1* was not identified in a genome-wide screen of deletion strains having vacuole fusion or fission phenotypes (Seeley *et al.*, 2002) and it is possible that this phenotype too is dependent on the growth medium or strain background. However, budding yeast Vps1p was later on found to play a role in vacuole fission as *vps1Δ* vacuoles exposed to salt did not undergo fragmentation (Peters *et al.*, 2004). In contrast, *S. pombe* cells lacking Vps1 were more efficient in vacuole fission. Treatment of cells with salt, to induce vacuole fission, saw an *in vivo* reduction in vacuole diameter in both wild type and *vps1Δ* but the efficiency of the latter was greater, indicating that, similar to its budding yeast counterpart (Peters *et al.*, 2004), Vps1 in fission yeast has role in vacuole fission, although the molecular mechanism may differ.

Budding yeast Vps1p has also been shown to be essential for vacuole fusion in a cell-free system (Peters *et al.*, 2004). The vacuolar fusion defect of fission yeast *vps1Δ* was demonstrated when cells were transferred to water. In this *in vivo* fusion assay *vps1Δ* fused vacuoles were only about half the size of those in the wild type. Vps1 is therefore not essential for vacuole fusion but the process is more efficient in its presence. The inability of *vps1Δ* cells to adapt their vacuole size, depending on the environmental conditions, may be an explanation for the temperature sensitivity of *vps1Δ* cells at 36°C, as the vacuoles are unable to respond to temperature induced

stress. In conclusion, Vps1 in fission yeast is required for both vacuole fusion and fission. As the balance between these two vacuole processes needs to be maintained in order to prevent futile cycles of fusion and fission, Vps1 activity must be regulated by binding other proteins or by post-translational modification. For example, in budding yeast, Vam3p binds Vps1p, which is then released at a critical stage during the fusion process by Sec18p (Peters *et al.*, 2004).

In accordance with its role at the vacuole, GFP-tagged Vps1 was localised to the vacuolar membrane in both live cells and isolated vacuoles. Since other vacuole fusion factors are similarly localised (Wang *et al.*, 2003) and since oligomerised Vps1 has been shown to be associated with the vacuolar membrane in budding yeast (Peters *et al.*, 2004), it can be concluded that this result indeed reflects the correct association of Vps1 with vacuoles in *S. pombe*, although whether this is exclusive to fused vacuoles is unknown.

### **4.3. Dnm1 acts together with Vps1**

---

In peroxisome biogenesis, Vps1 acts in tandem (Kuravi *et al.*, 2006) or in parallel (Jourdain *et al.*, 2008) with Dnm1 and Dnm1 acts in concert with yet another DRP, Mgm1/OPA1 in achieving mitochondrial fission (Shaw and Nunnari, 2002; Guillou *et al.*, 2005). Both Vps1 and Dnm1 are homologues of the mammalian dynamin-like protein Dlp1 (Shin *et al.*, 1997), therefore it is possible that they cooperate in maintaining vacuole dynamics in *S. pombe*. Cells lacking Dnm1 were less efficient than wild type in vacuole fission and interestingly, the absence of Dnm1 abolished the increased fission index of *vps1Δ*, thus placing Dnm1 together with Vps1 in vacuole fission. The overexpression of Dnm1 resulted in a reduction in vacuole diameter and those vacuoles underwent vacuole fission more efficiently. Together, these results indicate that Dnm1 plays a role in vacuole fission. Dnm1 overexpression also resulted in less efficient vacuole fusion, which may be due to over fragmentation and not to a fusion defect *per se*. Dnm1 overexpression often resulted in abnormal vacuoles containing a non-fluorescent compartment within, which may be due to the invagination and scission of limiting membranes or due to remnant membrane fragments which arise by vacuole fusion (Wang *et al.*, 2002).



#### 4.4. Vps1 tubulates vacuoles

---

Overexpression of Vps1 caused striking vacuole tubulation. Tubular vacuoles are common in filamentous fungi (Shoji *et al.*, 2006), but they have never previously been reported in yeast, although tubular projections are seen during vacuole transport to the bud in *S. cerevisiae* (Weisman, 2006). Tubules had a diameter of 0.4  $\mu\text{m}$ , similar to tubular vacuoles present in filamentous fungi (Cole *et al.*, 1998). Vps1-induced tubulation was enhanced in *dnm1* $\Delta$  cells, further confirming that Vps1 and Dnm1 collaborate in vacuole membrane processes. Tubular vacuoles responded to the “fission signal” by becoming thinner and more extensive, which may be due to Vps1 GTPase activation. This is supported by an *in vitro* study in which liposomes tubulated by dynamin decreased in diameter upon GTP addition (Danino *et al.*, 2004).

#### 4.5. GTP hydrolysis by Vps1 is necessary for tubule formation and vacuole fission

---

Overexpression of a Vps1 mutant lacking its GTPase domain did not induce vacuole tubulation, indicating that GTPase activity is necessary for Vps1 function. Treating *dnm1* $\Delta$  cells overexpressing Vps1 with GTP $\gamma$ S, a non-hydrolysable form of GTP, either before or after vacuole fission, caused the tubular vacuoles to revert back to their normal spherical shape. Thus, GTP hydrolysis, but not GTP binding, is necessary for formation and maintenance of tubular vacuoles by Vps1. Vps1 recruited to the vacuole membrane may assemble into a stable helix and constrain the shape of the vacuole. GTP hydrolysis could then distort the helix away from its stable GTP-bound conformation, resulting in a lengthwise extension of the helix and subsequent vacuole tubulation, which would not occur in the presence of GTP $\gamma$ S. This idea is supported by the fact that lipid membranes tubulated *in vitro*, by purified dynamin, undergo twisting and supercoiling upon the addition of GTP, but not of GDP or GTP $\gamma$ S, which suggests a conformational change of the dynamin helix during GTP hydrolysis (Roux *et al.*, 2006). The degree of tubulation may be maintained by repeated cycles of Vps1 binding and release following GTP hydrolysis (Ramachandran and Schmid, 2008). If GTP $\gamma$ S is added to the cells after fission (i.e. after Vps1 release) this may block reassembly of Vps1 on the vacuole and thus

prevent further cycles of tubulation, therefore also resulting in an overall decrease in vacuole tubulation. Furthermore, GTP hydrolysis is needed for normal vacuole fission, as vacuoles in wild type cells do not fragment in the presence of GTP $\gamma$ S. Vacuole fission in *vps1* $\Delta$  cells was also blocked by GTP $\gamma$ S, leading to the hypothesis that vacuole scission by Dnm1 requires GTP hydrolysis as well.

#### **4.6. The microtubule and actin cytoskeletons regulate tubular vacuoles**

---

A tubular network of vacuoles requires spatial regulation of its motility and morphology. Tubular vacuoles in cells overexpressing Vps1 reverted back to their normal spherical shape when treated either with the anti-microtubule agent thiabendazole, or with the anti-actin drug Latrunculin-A. This also occurred when Vps1 was overexpressed in the microtubule mutant *nda3-KM311* (Umesono *et al.*, 1983), and in actin mutants *for3* $\Delta$  (Feierbach and Chang, 2001) and *myo52* $\Delta$  (Mulvihill *et al.*, 2001). However, the *for3* $\Delta$  and *myo52* $\Delta$  mutants are also defective in microtubule organization; thus the effects due to actin cannot be distinguished from those due to microtubules. These studies provide strong causal evidence that the microtubule cytoskeleton mediates the organisation of tubular vacuoles in fission yeast, with a possible involvement of the actin cytoskeleton. However, it was not possible to co-localise tubular vacuoles and microtubules, as CDCDFA (used to visualise vacuoles) did not resist fixation, hence a fluorescently tagged vacuole marker protein is necessary for this.

In the basidiomycete fungus, *Pisolithus tinctorius*, which has a very motile tubular network of vacuoles (Hyde and Ashford, 1997), it has been reported that tubular vacuole morphology and motility is regulated by microtubules but not by actin filaments (Hyde *et al.*, 1999). Also, in mammalian cells such as cultured human monocytes and mouse peritoneal macrophages, the maintenance of elongated, membrane-bound tubular lysosomes is dependent on intact microtubules (Swanson *et al.*, 1987). The integrity of the normal vacuole in budding yeast is also dependent upon the presence of microtubules (Guthrie and Wickner, 1988). Incubation of *S. pombe* wild type cells with TBZ, the anti-microtubule drug, significantly reduces

vacuole fusion (Mulvihill *et al.*, 2001); however, vacuoles are unaffected by the anti-actin drug, Latrunculin B (Mulvihill *et al.*, 2001). Additionally, vacuoles in *myo52Δ* cells do not undergo fusion, due to the disrupted microtubule network (Mulvihill *et al.*, 2001). Therefore, it can be concluded that the microtubule network regulates both normal and tubular vacuoles.

#### **4.7. A model for vacuole fission in fission yeast**

---

Here it is shown that Vps1 and Dnm1 dynamin-related proteins participate in vacuole fission in *S. pombe*. Although most of the genes involved in maintaining vacuole function in budding yeast are conserved in *S. pombe* (Takegawa *et al.*, 2003), the biology of the vacuolar compartment in the two yeasts is distinct. Whereas the vacuole is a low copy number organelle in budding yeast (i.e., the vacuole is essentially fused) (Weisman, 2006), *S. pombe* cells maintain multiple small, unfused vacuoles, the presence of large vacuoles interfering with the placement of the division site (Morishita and Shimoda, 2000). The proposed working model is that the morphological plasticity of the vacuole demonstrated here represents an exaggerated version of the normal fission mechanism for this membrane compartment in fission yeast, which proceeds by two distinct steps, each mediated by a different dynamin-related protein. It is proposed that Vps1 binds to the vacuole and induces membrane tubulation in order to provide a vacuole neck of the appropriate diameter for Dnm1 scission (Figure 4.1 a). This is similar to mitochondria, where rings of Dnm1 are tailored to fit the diameter of the constricted organelle (Ingerman *et al.*, 2005). Vps1 GTPase activity could influence the pitch of the Vps1 helix (Marks *et al.*, 2001), resulting in stretching and subsequent tubulation. In the absence of Vps1, Dnm1 is still able to fragment vacuoles but with no elongation of the vacuole neck, vacuoles are smaller (Figure 4.1 b). On the contrary, in the absence of Dnm1, vacuoles tubulate but do not fragment (Figure 4.1 c), occasionally resulting in dumbbell shaped vacuoles similar to those formed by the plant dynamin-related protein, phragmoplastin, at the cell plate (Verma, 2001). Vps1 overexpression results in an enhanced tubular phenotype as there is not enough Dnm1 to meet the demand for vacuole scission (Figure 4.1 d). The pathway described cannot be the only one that exists in *S. pombe* since a *vps1Δ dnm1Δ* double mutant still responds to fission and

fusion signals, albeit less efficiently than wild type. In filamentous fungi, vacuoles convert from spherical to tubular depending on growth conditions and position in the hypha, and have been found to be involved in nutrient transport (Shoji *et al.*, 2006). Fission yeast cells can also adopt a filamentous state that results in major changes in vacuole morphology (Sipiczki *et al.*, 1998) and the DRP-mediated fission pathway may be an adaption to such morphological flexibility.

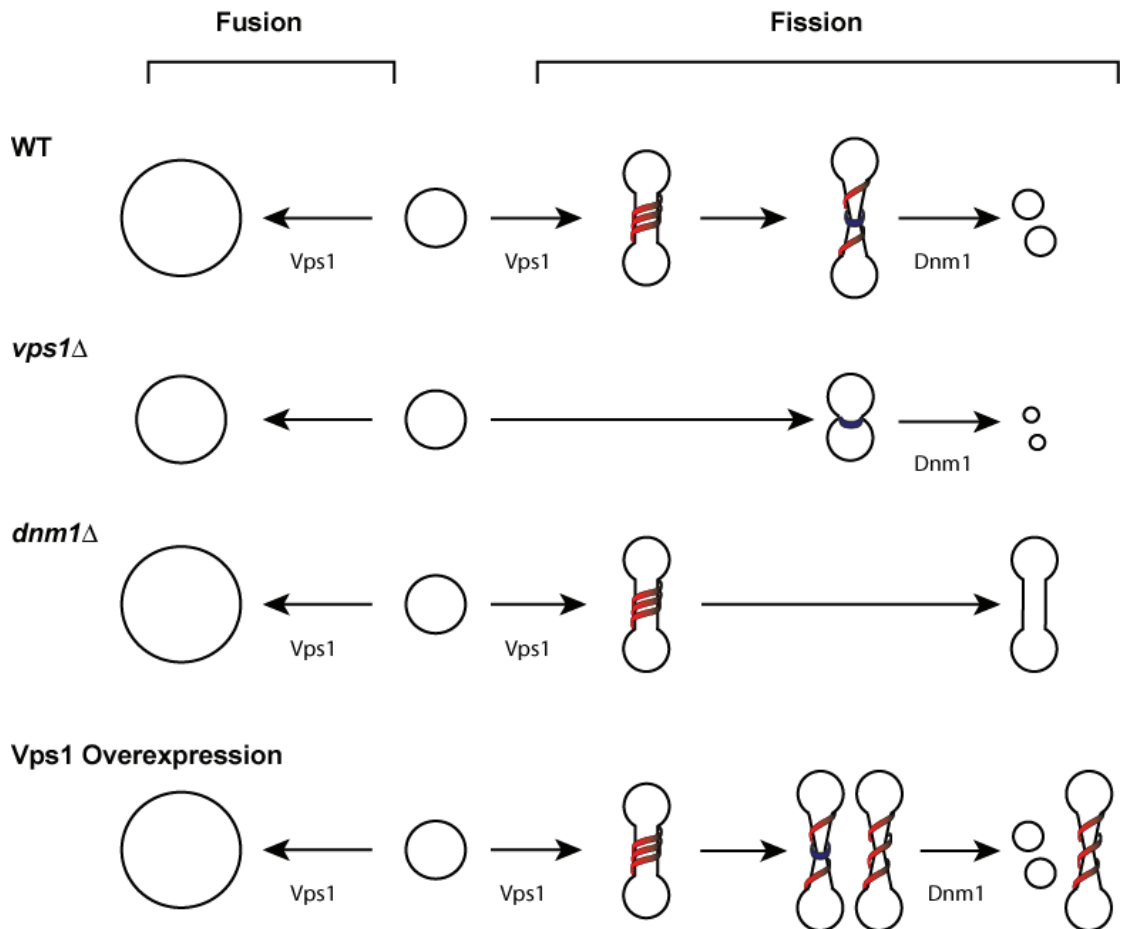


**Figure 4.1. A model for vacuole fission in fission yeast. (a)** Tubulation by Vps1 provides a vacuole neck of the appropriate diameter for fission by Dnm1 (blue). GTP hydrolysis by Vps1 may influence the pitch of the Vps1 helix. **(b)** In *vps1*Δ there is no elongation of the vacuole neck hence the Dnm1 fragmented vacuoles are smaller. **(c)** In *dnm1*Δ, vacuoles tubulate but do not fragment. **(d)** Vps1 overexpression results in an enhanced tubular phenotype as there is not enough Dnm1 to meet the demand.

## **5. CONCLUSIONS AND FUTURE PERSPECTIVES**

---

The dynamin-related protein Vps1 in fission yeast shares some common functions with Vps1p in budding yeast but also plays a number of cellular roles that are distinct. The differences reflect the early divergence of the two yeasts and the different strategies of fission versus budding as a mode of cell division. Put simply, the biology of the two yeasts and their cellular lifestyles are distinct and it is not surprising to find different strategies applied to common cellular functions. This is particularly true in the case of the maintenance of vacuole form and function where fission yeast maintains a large number of small vacuoles whilst budding yeast cells contain a small number of large vacuoles. Vacuoles in budding yeast are transported to the bud in an actomyosin dependent manner (the directed mode of organelle inheritance) whilst fission vacuoles are inherited by a simple partition process (the stochastic mode of organelle inheritance) (Warren and Wickner, 1996). Here, I have shown that vacuole fission also proceeds by distinct mechanisms.

This study proposes a new role for Vps1 in vacuole tubulation. Preliminary evidence suggests that Dnm1, rather than Vps1, is responsible for scission of the vacuole membrane. The evidence that Vps1 is involved in vacuole fission is compelling; however the role of Dnm1 in this process requires further study. Two dynamins are needed in fission yeast to fragment vacuoles, a situation which has never described. Demonstrating a physical interaction between Vps1 and Dnm1 may further support our model. GTP binding and hydrolysis is necessary for both Vps1 and Dnm1 function. These results extend the roles of these versatile GTPases in organelle biogenesis and offer new insights into the mechanism of membrane fission in fission yeast.

In this study, a role for Vps1 in vacuole fusion was also proposed. In *S. cerevisiae* it was found that Vps1p plays a role in vacuole fusion by interacting with the t-SNARE Vam3p (Peters *et al.*, 2004). *S. pombe* does not have a Vam3 homologue, so an interesting issue for further study is the vacuole fusion mechanism in fission yeast. The overexpression of Dnm1 suggested that this dynamin is also involved in fusion. Although further work is needed to confirm this finding, it poses the question of whether Dnm1 collaborates with Vps1 in vacuole fusion, as it does in vacuole fission.

Currently there is not much information regarding the regulation of dynamin-like

proteins such as Vps1. An intriguing question is what regulation mechanisms determine whether Vps1 acts in vacuole fusion or fission. SH3 domain-containing proteins are attractive candidates for regulators of Vps1 function, as they bind to and activate the GTPase activity of dynamin *in vitro*. In addition to regulation by effector molecules, Vps1 may also be regulated by post-translational modifications which may alter or favour its function. For instance, there are 22 putative Protein Kinase C or Casein Kinase II phosphorylation sites in fission yeast Vps1, as well as 4 myristoylation and 4 glycosylation sites.

In conclusion, although much work remains to be done to fully understand how Vps1 regulates the balance between fusion and fission, this study provides new insights into its role in vacuole fragmentation. A manuscript summarising these findings is currently under preparation for submission into *Traffic* (See Appendix 6.3).

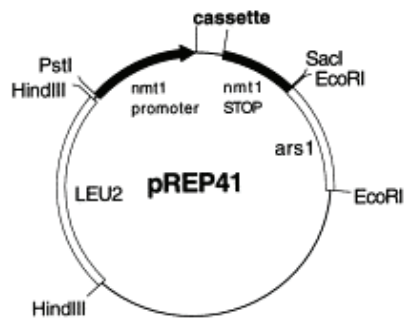
## **6. APPENDICES**

---

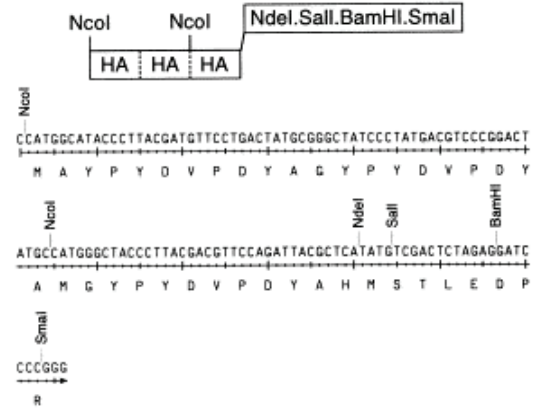


## 6.1. PLASMID MAPS

### 6.1.1. pREP41 Vector

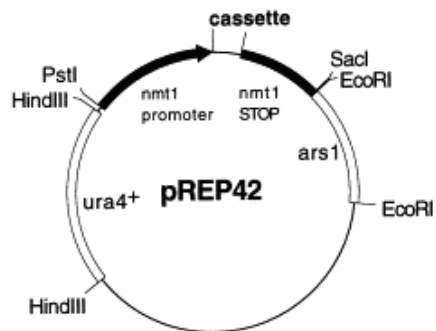


#### B pREP41/42HA N

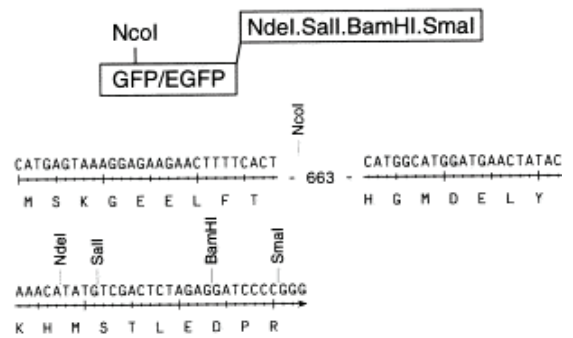


(Craven *et al.*, 1998)

### 6.1.2. pREP41-Ngfp Vector



#### A pREP41/42GFP/EGFP N



(Craven *et al.*, 1998)

## 6.2. STOCK SOLUTIONS

**Table 6.1 Salt Stock (50x)**

Per Litre	Final Concentration
52.5 g MgCl <sub>2</sub> ·6H <sub>2</sub> O	0.26 M
0.735 g CaCl <sub>2</sub> ·2H <sub>2</sub> O	4.99 mM
50 g KCl	0.67 M
2 g Na <sub>2</sub> SO <sub>4</sub>	14.1 mM

**Table 6.2. Vitamin Stock (1000x)**

Per Litre	Final Concentration
1 g pantothenic acid	4.20 mM
10 g nicotinic acid	81.2 mM
10 g inositol	55.5 mM
10 mg biotin	40.8µM

**Table 6.3. Mineral Stock (10,000x)**

Per Litre	Final Concentration
5 g boric acid	80.9 mM
4 g MnSO <sub>4</sub>	23.7 mM
4 g ZnSO <sub>4</sub> ·7H <sub>2</sub> O	13.9 mM
2 g FeCl <sub>2</sub> ·6H <sub>2</sub> O	7.40 mM
0.4 g molybdic acid	2.47 mM
1 g KI	6.02 mM
0.4 g CuSO <sub>4</sub> ·5H <sub>2</sub> O	1.60 mM
10 g citric acid	47.6 mM

**Table 6.4. Supplements added to the media**

Supplement	Stock concentration	Final concentration
Ampicillin	50 mg/ml	50 µg/ml
Geneticin	200 mg/ml	200 µg/ml
Adenine	3.5 g/l	75-225 mg/l
Uracil	3.5 g/l	75-225 mg/l
Leucine	12.5 g/l	225 mg/l
Thiamine	15 mM	15 µM, 30 µM

### **6.3. MANUSCRIPT**

---

**The dynamin-related proteins Vps1 and Dnm1 cooperate in  
vacuole tubulation and fission in fission yeast**

Sarah Röthlisberger, Isabelle Jourdain<sup>1</sup>, Chad Johnson,  
Kaoru Takegawa<sup>2</sup> & Jeremy S Hyams

Institute of Molecular Biosciences, Massey University  
Private Bag 11 222, Palmerston North, New Zealand

<sup>2</sup>Department of Life Sciences, Faculty of Agriculture  
Kagawa University, Miki-Cho, Kagawa 761-0795, Japan

<sup>1</sup>Corresponding author: [i.jourdain@massey.ac.nz](mailto:i.jourdain@massey.ac.nz)

Running title: Vacuole fission in fission yeast

## Summary

Dynamins are GTPases concerned with membrane tubulation and scission [1,2] although their precise mechanism of action remains to be resolved [3-5]. In the fission yeast, *Schizosaccharomyces pombe*, the dynamin-related proteins (DRPs) Vps1 and Dnm1 act redundantly in peroxisome biogenesis [6] but nothing is known about other cellular roles. Fission yeast cells contain ~20 small, spherical vacuoles that undergo fission or fusion in response to environmental signals [7]. Cells lacking Vps1 had smaller vacuoles with reduced capacity for fusion in response to hypotonic stress but enhanced fission in response to hypertonic conditions. The latter phenotype was abolished in cells lacking Dnm1. Overexpression of *dnm1* induced vacuole fragmentation, suggesting that Dnm1 has a direct role in vacuole membrane fission. Overexpression of *vps1* caused vacuole tubulation, an effect that was substantially enhanced in the absence of Dnm1. Spherical vacuoles were restored by repression of *vps1* expression or by induction of vacuole fusion. Vps1-GFP localised to the vacuolar membrane both in living cells and in isolated vacuoles. Our results are consistent with a model in which vacuole fission occurs in two steps, each involving a different DRP: the binding of Vps1 creates a tubule of an appropriate diameter for subsequent scission by Dnm1.

## Results and Discussion

### Loss of Vps1 affects vacuole size but not vacuole function

To determine the role of Vps1 in vacuole biogenesis in *S. pombe*, *vps1Δ* cells [6] were stained with either FM4-64, which stains the vacuolar membrane or CDCFDA which illuminates the vacuolar lumen [7-9]. Vacuole diameter was ~25% smaller in *vps1Δ* cells than in wild type (*vps1<sup>+</sup>*) in minimal medium (EMM; mean internal diameter *vps1<sup>+</sup>* = 0.8 μm; *vps1Δ* = 0.6 μm; Figure 1A, B). The difference was not as marked in rich medium (YE; mean internal diameter *vps1<sup>+</sup>* = 0.9 μm; *vps1Δ* = 0.8 μm) and all further experiments were carried out in EMM. Both large and small vacuoles are seen in budding yeast cells lacking Vps1 [10] whereas *Aspergillus nidulans* cells lacking the *vps1* homologue, *vpsA*, have small vacuoles [11]. Vps1 also appears to play a role

in vacuole size control in *S. pombe*.

*vps1Δ* was temperature sensitive for growth at 36°C (Figure 1C) and, unlike wild type, vacuoles showed no reduction in diameter when the growth temperature was raised to 36°C (Figure 1D). To investigate whether the temperature sensitive phenotype of *vps1Δ* reflected a defect in vacuole function, colony blots were carried out using an antibody to the vacuolar marker protein carboxypeptidase Y (CPY). No secretion of CPY was detected in either *vps1Δ* or wild type colonies (Figure 2A). By contrast, colonies of *vps34Δ*, which is defective in the delivery of CPY to the vacuole [12], showed intense staining. Further, the processing of CPY occurred at close to wild type efficiency in *vps1Δ* (Figure 2B) and both the rate of endocytic uptake of FM4-64 to the vacuole (Figure 2C) and the organisation of actin at the cell poles were indistinguishable to wild type. Thus, Vps1 appears to be primarily concerned with the maintenance of the vacuolar compartment and not its internal functions. Unlike budding yeast [13], Vps1 does not appear to have a role in the organisation of actin patches and endocytosis.

To assess the role of Vps1 in vacuole fission and fusion, we labelled *vps1Δ*, *dnm1Δ* and the *vps1Δ dnm1Δ* double mutant with FM4-64 or CDCFDA and induced vacuole fusion by resuspending cells in distilled water for 2 hrs and vacuole fission in 0.4 M NaCl or 1.0 M sorbitol for 10 min [7] (Figure 3A-D). Vacuole diameter was measured (Figure 3E) and a “fusion index” and “fission index” determined for each strain relative to a wild type value of 1.0 (Figure 3F,G). Wild type vacuoles roughly doubled in size by fusion and halved in size as the result of fission (Figure 3E). Whereas *vps1Δ* cells showed a reduced fusion index (0.6), *dnm1Δ* (0.97) and the *vps1Δ dnm1Δ* double mutant (0.93) showed values much closer to that of wild type (Figure 3F). By contrast, whilst *dnm1Δ* (0.7) and *vps1Δ dnm1Δ* (0.4) showed reduced fission efficiency, fission was enhanced in *vps1Δ* (1.27). This is almost certainly an underestimate because many vacuoles were too small to be measured accurately (Figure 3G). Interestingly, the increased fission index of *vps1Δ* was abolished in the absence of Dnm1. We conclude that, as in budding yeast [9],

Vps1 regulates the balance between vacuole fusion and fission but, unlike budding yeast, Vps1's role in fission also involves Dnm1.

### **Vps1 is present at the vacuole membrane**

If Vps1 has a role at the vacuolar membrane, it should be possible to demonstrate this cytologically. Accordingly, we expressed either N- or C-terminally GFP-tagged Vps1 constructs in both wild type and *vps1Δ* cells. Both GFP-Vps1 and Vps1-GFP were non-functional in terms of rescuing the vacuole and temperature sensitivity phenotypes of *vps1Δ* (data not shown). Both localise to peroxisome-sized cytoplasmic dots as well as showing strong cytoplasmic fluorescence [6]. Nevertheless, in cells containing fused vacuoles Vps1-GFP was observed close to, and in many cases following the contours of, the vacuolar membrane (Figure 4A). We next examined the association of Vps1-GFP with isolated vacuoles. Cells were stained with FM4-64 and vacuoles fused in distilled water prior to isolation and examination by fluorescence microscopy. As can be seen in Figure 4B, dots of Vps1 fluorescence, indicating the presence of Vps1 oligomers [10], were associated with the vertices, but not the adhering faces of the apposed vacuole membranes. Since other vacuole fusion factors are similarly localised [14] and since oligomerised Vps1 has been shown to be associated with the vacuolar membrane in budding yeast [10], we conclude that our results indeed reflect the correct association of Vps1 with vacuoles in *S.pombe*.

### **Overexpression of *vps1* results in vacuole tubulation whilst overexpression of *dnm1* results in vacuole fission**

The fact that salt treatment results in smaller vacuoles in *vps1Δ* than in *vps1Δ dnm1Δ* suggests that Vps1 and Dnm1 cooperate to fragment vacuoles. Overexpression of Vps1 in wild type cells under the control of the thiamine repressible *nmt1* promoter resulted in vacuoles becoming extensively tubulated in about 40% of the cells examined (Figure 5A). Although tubular vacuoles have never previously been reported in yeast (tubular projections are, however, seen during vacuole transport to the bud in *S. cerevisiae* [15]), they are common in filamentous fungi [16]. Overexpression of Vps1 in *dnm1Δ*

resulted in more than 60% cells having tubular vacuoles which were also more extensive (Figure 5A). In both cases, the extent of tubulation was increased following the induction of fission (Figure 5A) but did not occur following expression of the non-functional Vps1-GFP (data not shown). The tubular phenotype could be reversed by the addition of thiamine to the growth medium to suppress Vps1 expression (Figure 5B) or by transferring cells to water to induce fusion (Figure 5B). Tubules had a diameter of 0.4  $\mu\text{m}$ , strikingly similar to that of liposomes tubulated by dynamin *in vitro* [17] and of the tubular vacuoles present in filamentous fungi [18]. The addition of either 0.4 M NaCl or 1.0 M sorbitol resulted in a further reduction in diameter of the tubular vacuoles to 0.3  $\mu\text{m}$  (Figure 5C) which, thus, still respond to the “vacuole fission signal.”

*dnm1 $\Delta$*  vacuoles had a similar size distribution to wild type (Figure 3). Occasionally vacuoles with a “dumbbell” profile, suggesting a fission defect, were observed (Figure 5E). Overexpression of Dnm1 resulted in a reduction in vacuole diameter from 0.8 to 0.5  $\mu\text{m}$ . The latter vacuoles were often incompletely stained with CDCFDA and contained a non-fluorescent (i.e., non acidic) invagination (Figure 5D). Such vacuole profiles were not observed in *vps1 $\Delta$*  (Figure 5D) or following overexpression of GFP-Dnm1 or Dnm1-GFP which, like GFP-tagged Vps1 constructs, are non-functional (data not shown). The abnormal vacuoles induced by untagged Dnm1 overexpression fused less efficiently but underwent fission in response to salt more efficiently than wild type cells (compare Figures 5A and D). We conclude that Dnm1 plays a role in vacuole fission.

### **A model for vacuole fission in fission yeast**

In budding yeast, Vps1 participates in diverse cellular roles. These include growth and endocytosis at high temperature [19], sporulation [20] vacuolar protein sorting [21] secretion [22-24], actin organization [13] and peroxisome inheritance [25-27]. Recently, Vps1 was shown to maintain the balance between vacuole membrane fission and fusion [9], despite not having been identified during extensive screens for mutants with vacuole defects [28]. In



peroxisome biogenesis, Vps1 acts in tandem [26] or in parallel [6] with Dnm1 and Dnm1 acts in concert with yet another DRP, Mgm1/OPA1 in achieving mitochondrial fission [29,30]. Here we show that Dnm1 and Vps1 proteins participate in vacuole fission in *S. pombe*. Although most of the genes involved in maintaining vacuole function in budding yeast are conserved in *S. pombe* [7], the biology of the vacuolar compartment in the two yeasts is distinct. Whereas the vacuole is a low copy number organelle in budding yeast (i.e., the vacuole is essentially fused) [15], *S. pombe* cells maintain multiple small, unfused, vacuoles, the presence of large vacuoles interfering with the placement of the division site [31]. Our working model is that the morphological plasticity of the vacuole demonstrated here represents an exaggerated version of the normal fission mechanism for this membrane compartment in fission yeast which proceeds by two, distinct steps, each mediated by a different DRP; membrane tubulation by Vps1 and membrane scission by Dnm1 (Figure 6). In the case of mitochondria, rings of Dnm1 are tailored to fit the diameter of the organelle [32] and Vps1 may similarly provide an appropriately sized tubule for Dnm1 scission. In the absence of Vps1, Dnm1 is still able to fragment vacuoles but with no elongation of the vacuole neck, vacuoles are smaller. On the contrary, in the absence of Dnm1, vacuoles tubulate but do not fragment, although tubular vacuoles are still able to respond to the "fission signal". The pathway that we describe cannot be the only one that exists in *S. pombe* since a *vps1* $\Delta$  *dnm1* $\Delta$  double mutant still responds to fission and fusion signals, albeit less efficiently than wild type. In filamentous fungi, vacuoles convert from spherical to tubular depending on growth conditions, position in the hypha etc [16]. Fission yeast cells can also adopt a filamentous state that results in major changes in vacuole morphology [33] and the DRP-mediated fission pathway may be an adaptation to such morphological flexibility.

## Conclusions

Membrane tubulation and fission by dynamin family proteins has been extensively described, both *in vitro* [1] and *in vivo* [2]. Overexpression of Vps1 in fission yeast results in the formation of tubular vacuoles, a process that is

enhanced in the absence of Dnm1. Our results extend the roles of these versatile GTPases in organelle biogenesis and suggest that the fission yeast vacuole offers new insights into the mechanisms of membrane fission and fusion.

### **Acknowledgements**

We thank Pascale Belenguer, Paul Nurse, Fred Chang and Yannick Gachet for strains and plasmids. We gratefully acknowledge financial support from the Palmerston North Medical Research Foundation and a Massey University Masterate scholarship to SR.

### **Experimental procedures**

#### **Plasmid constructs**

The constructs used in this study are listed in Table S1. DNAs coding for Vps1 and Dnm1 were amplified by polymerase chain reaction (PCR) from wild type genomic DNA. Different sets of primers containing either *Bgl*III or *Nde*I restriction sites were obtained from Sigma-Proligo. Cloning into pREP41 and pREP41-Ngfp was achieved by using *Nde*I restriction sites, while *Bgl*III restriction sites were used to clone into pREP41-Cgfp. All constructs were verified by sequencing (Allan Wilson Centre, Palmerston North, New Zealand).

#### **Yeast strains and cultures**

The *S. pombe* strains used in this study are listed in Table S2. Media, growth, genetics and maintenance of strains were as described in [34]. *vps1::ura4* is described in [6] and *dnm1::KanMX6* was kindly provided by P.Belenguer [29]. Cells were cultured to mid-log phase at 25°C, unless stated. Cells expressing pREP41-N or –CGFP Vps1 or Dnm1 were first mini-cultured in the presence of 60µM thiamine, washed 3 times and large-cultured in medium minus thiamine for approx. 20 hrs. Cells expressing untagged dynamin plasmids were cultured in the continuous absence of thiamine to allow their maximum expression.

## Microscopy

Live cell imaging was performed in an imaging chamber (CoverWell, 20-mm diameter, 0.5-mm deep) (Molecular Probes) filled with 800  $\mu$ l of 2% agarose in EMM and sealed with a 22x22-mm glass coverslip. CDCFDA and FM4-64 (Molecular Probes) were dissolved in DMSO at a concentration of 1 mg/ml (1.89 mM and 1.64 mM, respectively). Stains were added to the cells at a final concentration of 1.89  $\mu$ M and 8.2  $\mu$ M, respectively, and incubated in the dark for at least 1 hr. The cells were washed in EMM before being applied to an imaging chamber. For fission experiments, the cells were further incubated 10 min in medium plus 0.4 M NaCl or 1.0 M sorbitol, before being applied on a chamber containing the same concentration of fission reagent. For fusion experiments, the cells were washed three times in sterile water and incubated several hours in water, before being applied to a chamber made of 2% agarose in water.

Endocytosis was monitored by following FM4-64 uptake over time. *vps1 $\Delta$*  and wild-type cells were mixed, wild-type cells being first stained with Hoechst [35] for latter recognition. FM4-64 was added to the cells and at various time points an aliquot was fixed in paraformaldehyde 3.3%. Cells were observed the same day. *Schizosaccharomyces pombe* cells were observed at room temperature using an Olympus IX 71 microscope with a x100 oil immersion lens. Pictures were captured with a Hamamatsu ORCA-ER C4742-80 digital charge-coupled device camera (Hamamatsu Corporation). For confocal microscopy, a Leica TCS SP5 microscope and a x63 oil immersion lens NA 1.4, were used. Counts and measurements were made using METAMORPH software (Molecular Devices Corporation) and downloaded to Microsoft Excel for analysis.

## Biochemistry

Vacuoles were isolated as previously described [36]. In brief, cells were pre-stained with FM4-64 and incubated a few hours in water to induce vacuolar fusion. Cells were spheroplasted in the presence of sorbitol, broken in a glass-teflon homogeniser and fractions separated on a discontinuous Ficoll gradient. After ultracentrifugation, fractions were collected from the 8 to 0% Ficoll

interface. FM4-64 staining allowed the visualisation of vacuoles. Vacuolar protein sorting was performed as described [36]. Vacuolar Carboxypeptidase Y (CPY) missorted to the medium was detected by colony blot assay as previously described in [37]. Cells were spotted onto an EMM plate in contact with a nitrocellulose membrane and incubated at 25°C for 2 days. After removing cells by washing, the nitrocellulose membrane was blotted with rabbit polyclonal antibodies against *S. pombe* Cpy1p (1:1000 dilution) [34], followed by horseradish peroxidase-conjugated anti-rabbit IgG antiserum (1:5000 dilution) (Promega), and the SuperSignal<sup>®</sup> West Pico Chemiluminescent Substrate (Pierce).

## References

- [1] Praefcke, G.J., and McMahon, H.T. (2004). The dynamin superfamily: universal membrane tubulation and fission molecules? *Nat Rev Mol Cell Biol.* 5, 133-47.
- [2] Verma, D.P., and Hong, Z. (2005). The ins and outs in membrane dynamics: tubulation and vesiculation. *Trends Plant Sci.* 10, 159-65.
- [3] Sever, S., Damke, H., and Schmid, S.L. (2000). Garrotes, springs, ratchets, and whips: putting dynamin models to the test. *Traffic.* 1, 385-392.
- [4] Roux, A., Uyhazi, K., Frost, A., and De Camilli, P. (2006). GTP-dependent twisting of dynamin implicates constriction and tension in membrane fission. *Nature.* 441, 528-531
- [5] Mear, J.A., Ray, P., and Hinshaw, J.E. (2007). A corkscrew model for dynamin constriction. *Structure.* 15, 1190-1202
- [6] Jourdain, I., Sontam, D., Johnson, C., Dillies, C., and Hyams, J.S. (2008). Dynamin-dependent biogenesis, cell cycle regulation and mitochondrial association of peroxisomes in fission yeast. *Traffic.* 9, 353-365.
- [7] Bone, N., Millar, J.B.A., Toda, T. and Armstrong, J. (1998). Regulated vacuole fusion and fission in *Schizosaccharomyces pombe*: an osmotic response dependent on MAP kinases. *Curr. Biol.* 8, 135–144.
- [8] Takegawa, K., Iwaki, T., Fujita, Y., Morita, T., Hosomi, A., and Tanaka N. (2003). Vesicle-mediated protein transport pathways to the vacuole in *Schizosaccharomyces pombe*. *Cell Struct Funct.* 28, 399-417

- [9] Gachet, Y., and Hyams, J.S. (2005). Endocytosis in fission yeast is spatially associated with the actin cytoskeleton during polarised cell growth and cytokinesis. *J. Cell Sci.* *118*, 4231-4242
- [10] Peters, C., Baars, T.L, Buhler, S., and Mayer, A. (2004). Mutual control of membrane fission and fusion proteins. *Cell.* *119*, 667-678.
- [11] Tarutani, Y., Ohsumi, K., Arioka, M., Nakajima H., and Kitamoto K. (2001). Cloning and characterization of *Aspergillus nidulans vpsA* gene which is involved in vacuolar biogenesis. *Gene.* *268*, 23-30
- [12] Takegawa, K., DeWald, D.B., and Emr, S.D. (1995). *Schizosaccharomyces pombe* Vps34p, a phosphatidylinositol-specific PI 3-kinase essential for normal cell growth and vacuole morphology. *J. Cell Sci.* *108*, 3745-3756.
- [13] Yu, X., and Cai, M. (2004). The yeast dynamin-related GTPase Vps1p functions in the organization of the actin cytoskeleton via interaction with Sla1p. *J Cell Sci.* *117*, 3839-3853.
- [14] Wang. L., Merz, A.J., Collins, K.M., and Wickner, W. (2003). Hierarchy of protein assembly at the vertex ring domain for yeast vacuole docking and fusion. *J Cell Biol.* *160*, 365-74.
- [15] Weisman L.S. (2006). Organelles on the move: insights from yeast vacuole inheritance. *Nat Rev Mol Cell Biol.* *7*, 243-252.
- [16] Shoji, J.Y., Arioka, M., and Kitamoto, K. (2006). Possible involvement of pleiomorphic vacuolar networks in nutrient recycling in filamentous fungi. *Autophagy.* *2*, 226-227.
- [17] Danino, D., Moon, K.H., and Hinshaw, J.E. (2004). Rapid constriction of lipid bilayers by the mechanochemical enzyme dynamin. *J Struct Biol.* *147*, 259-267
- [18] Cole, L., Orlovich, D.A., and Ashford, A.E. (1998). Structure, function, and motility of vacuoles in filamentous fungi. *Fungal Genet Biol.* *24*, 86-100.
- [19] Rothman, J.H., Raymond, C.K., Gilbert, T., O'Hara, P.J., and Stevens, T.H. (1990). A putative GTP binding protein homologous to interferon-inducible Mx proteins performs an essential function in yeast protein sorting. *Cell.* *61*, 1063-1074.
- [20] Yeh, E., Driscoll, R., Coltrera, M., Olins, A., and Bloom, K. (1991). A

dynamamin-like protein encoded by the yeast sporulation gene SPO15. *Nature*. 349, 713-715.

[21] Vater, C.A., Raymond, C.K., Ekena, K., Howald-Stevenson, I., and Stevens, T.H. (1992). The VPS1 protein, a homolog of dynamamin required for vacuolar protein sorting in *Saccharomyces cerevisiae*, is a GTPase with two functionally separable domains. *J Cell Biol.* 119, 773-786.

[22] Nothwehr, S.F., Conibear, E., and Stevens T.H. (1995). Golgi and vacuolar membrane proteins reach the vacuole in vps1 mutant yeast cell via the plasma membrane. *J Cell Biol.* 129, 35-46.

[23] Gurunathan, S., David, D., and Gerst, J.E. (2002). Dynamamin and clathrin are required for the biogenesis of a distinct class of secretory vesicles in yeast. *EMBO J.* 21, 602-614.

[24] Harsay, E., and Schekman, R. (2002). A subset of yeast vacuolar protein sorting mutants is blocked in one branch of the exocytic pathway. *J Cell Biol.* 156, 271-285.

[25] Hoepfner, D., van den Berg, M., Philippsen, P., Tabak, H.F., and Hettema E.H. (2001). A role for Vps1p, actin, and the Myo2p motor in peroxisome abundance and inheritance in *Saccharomyces cerevisiae*. *J Cell Biol.* 155, 979-990.

[26] Kuravi, K., Nagotu, S., Krikken, A.M., Sjollema, K., Deckers, M., Erdmann, R., Veenhuis, M., and van der Klei, I.J. (2006). Dynamamin-related proteins Vps1p and Dnm1p control peroxisome abundance in *Saccharomyces cerevisiae*. *J Cell Sci.* 119, 3994-4001.

[27] Vizeacoumar, F.J., Vreden, W.N., Fagarasanu, M., Eitzen, G.A., Aitchison, J.D., and Rachubinski, R.A. (2006). The dynamamin-like protein Vps1p of the yeast *Saccharomyces cerevisiae* associate with peroxisomes in a Pex19p-dependent manner. *J Biol Chem.* 281, 12817-12823.

[28] Seeley, E.S., Kato, M., Margolis, N., Wickner, W., and Eitzen, G. (2002). Genomic analysis of homotypic vacuole fusion. *Mol Biol Cell.* 13, 782-94.

[29] Guillou, E., Bousquet, C., Daloyau, M., Emorine, L.J., and Belenguer, P. (2005). Msp1p is an intermembrane space dynamamin-related protein that mediates mitochondrial fusion in a Dnm1p-dependent manner in *S. pombe*. *FEBS Lett.* 579, 1109-16.

[30] Shaw, J.M., and Nunnari, J. (2002). Mitochondrial dynamics and division

in budding yeast. *Trends Cell Biol.* 12, 178-184.

[31] Morishita, M., and Shimoda, C. (2000). Positioning of medial actin rings affected by eccentrically located nuclei in a fission yeast mutant having large vacuoles. *FEMS Microbiol Lett.* 188, 63-67.

[32] Ingerman, E., Perkins, E.M., Marino, M., Mears, J.A., McCaffery, J.M., Hinshaw, J.E., and Nunnari, J. (2005). Dnm1 forms spirals that are structurally tailored to fit mitochondria. *J Cell Biol.* 170, 1021-1027.

[33] Sipiczki, M., Takeo, K., and Grallert, A. (1998). Growth polarity transitions in a dimorphic fission yeast. *Microbiology* 144, 3475–3485

[34] Moreno, S., Klar, A., and Nurse, P. (1991). Molecular genetic-analysis of fission yeast *Schizosaccharomyces pombe*. *Meth Enzymol* 194, 795-823

[35] Alfa, C.E., Fantes, P., Hyams, J.S., Mcleod, M., and Warbrick, E. (1993). *Experiments With Fission Yeast: A Laboratory Course Manual*, (New York: Cold Spring Harbor Press) pp. 186.

[36] Tabuchi, M., Iwaihara, O., Ohtani, Y., Ohuchi, N., Sakurai, J., Morita, T., Iwahara, S., and Takegawa, K. (1997). Vacuolar protein sorting in fission yeast: cloning, biosynthesis, transport, and processing of carboxypeptidase Y from *Schizosaccharomyces pombe*. *J Bacteriol.* 179, 4179-4189.

[37] Iwaki, T., Hosomi, A., Tokudomi, S., Kusunoki, Y., Fujita, Y., Giga-Hama, Y., Tanaka, N., and Takegawa, K. (2006). Vacuolar protein sorting receptor in *Schizosaccharomyces pombe*. *Microbiology.* 152, 1523-1532.

### Figure legends

**Figure 1. Vps1 controls vacuole size.** A) *vps1Δ* has small vacuoles. Wild-type (WT) and *vps1Δ* cells were labelled with FM4-64 or CDCFDA. Bar, 5 μm. B) The inner diameter of wild type (WT) and *vps1Δ* FM4-64-stained vacuoles was measured in cells grown in rich (YE) and minimal (EMM) medium. The difference between wild-type and *vps1Δ* vacuoles is more obvious in EMM. Results are the mean of at least two independent experiments. C) *vps1Δ* is temperature sensitive at 36°C. D) Time course of vacuole size in wild type (filled circles) and *vps1Δ* cells (open circles) at 36°C. Cells were grown at the permissive temperature and shifted to 36°C. Vacuoles were stained with FM4-64 and their diameter measured. Unlike wild type vacuoles, *vps1Δ* vacuole

size did not decrease at 36°C.

**Figure 2. Vps1 has no role in vacuolar protein sorting, endocytosis or actin patch organisation.**

A) Colony blots showing that, like wild type, *vps1Δ* does not secrete CPY into the growth medium. *vps34Δ* was used as a positive control. B) *vps1Δ* has close to normal CPY processing. Wild type and *vps1Δ* strains were pulsed-labelled with Express35<sup>S</sup> for 15 min and cold chased for 30 min. The positions of the precursor (proCPY) and the mature (mCPY) forms of CPY are indicated. C) The endocytic uptake of FM4-64 was compared in wild type and *vps1Δ* cells. Crn1-GFP actin patches are similarly polarized to the cell poles in wild type and *vps1Δ* cells. Bar, 5 μm.

**Figure 3. The dynamin-related proteins Vps1 and Dnm1 are involved in vacuole fusion and fission.**

Vacuoles in wild type (WT; A), *vps1Δ* (B), *dnm1Δ* (C) and *vps1Δ dnm1Δ* cells (D) were labelled with FM4-64 and incubated in either EMM (control), water, to examine vacuole fusion, or salt, to observe fission. Bar, 5 μm. Vacuole diameter was measured in each condition (E-G). Fusion and fission indices were normalised to wild type = 1.0. The higher the index, the higher the fusion or fission process. Results are the mean of at least two independent experiments. Values for *vps1Δ* are showed as dotted lines as both are likely to be underestimates due to the presence of many vacuoles that were too small to measure accurately.

**Figure 4. In wild type cells, Vps1-GFP localises to the vacuole membrane.**

A) Live cells stained with FM4-64. Vps1-GFP is cytoplasmic but also localises to dots, whose size varies with the level of expression, around vacuoles. B) Isolated vacuoles pre-stained with FM4-64. Within the vacuolar fraction, spots of Vps1-GFP were solely found attached to vacuolar membranes, largely concentrated at vertices. Bars, 5 μm.

**Figure 5. Vps1 induces vacuole tubulation and Dnm1 induces vacuole fission**

A) CDCFDA-labeling of vacuoles following overexpression of Vps1 in different



genetic backgrounds. Numbers indicate the percentage of cells showing the tubulated phenotype which was defined as the presence of at least two tubules. Vacuoles appear tubulated in all cases but most strikingly in *dnm1Δ*. Induction of fission enhances the phenotype. B) (a) Control cells expressing Vps1 in the presence of thiamine. Normal vacuole morphology was restored following the addition of 60 μM thiamine for 22 hrs to shut off expression of the Vps1 plasmid (b), or by incubation in water for 1 hr to induce vacuole fusion (c). C) Confocal images of *dnm1Δ* cells overexpressing Vps1 and stained with FM4-64. Three z sections are shown. D) Overexpression of Dnm1 in various strains results in the formation of small vacuoles which fuse less and fragment more. Note that in individual vacuoles, the CDCFDA staining is often incomplete. E) Incompletely divided “dumbbell” shaped vacuoles are occasionally seen in *dnm1Δ*. Bars, 5 μm.

**Figure 6. A model for vacuole fission in fission yeast**

Tubulation by Vps1 (red) provides a vacuole of appropriate diameter for fission by Dnm1 (blue). Non-functional alleles of Vps1 do not cause membrane tubulation. Hence, the pitch of the Vps1 helix could reflect the GTP-bound form of the protein [1].

**Supplementary table 1.** List of plasmids used in this study

Stock #	Plasmid	Source
V7	pREP41	Y. Gachet
V8	pREP41-Ngfp	Y. Gachet
V9	pREP41-Cgfp	Y. Gachet
V64	pREP41-Vps1 (untagged)	This study
V67	pREP41-Ngfp-Vps1	This study
V37	pREP41-Vps1-Cgfp	This study
V65	pREP41-Dnm1 (untagged)	This study
V66	pREP41-Ngfp-Dnm1	This study
V44	pREP41-Dnm1-Cgfp	This study

**Supplementary table 2.** List of strains used in this study

Strain	Genotype	Source
MU141	<i>leu1.32, h-</i>	P. Nurse
MU88	<i>vps1::ura4, ura4-D18, leu1.32, h-</i>	Lab stock
MU155	<i>vps1::ura4, ura4-D18, leu1.32, ade6-M210, h+</i>	Lab stock
MU48	<i>Crn1-gfp ::KanMX6, ura4-D18, leu1.32, ade6-</i>	F. Chang
MU167	<i>Crn1-gfp ::KanMX6, ura4-D18, leu1.32, h+</i>	Lab stock
MU157	<i>vps1::ura4, Crn1-gfp ::KanMX6, ura4-D18, leu1.32, h-</i>	This study
MU145	<i>dnm1::kanMX6, ura4-D18, leu1.32, ade6-M210, h+</i>	P. Belenguer
MU205	<i>dnm1::kanMX6, leu1.32, h+</i>	This study
MU159	<i>vps1::ura4, dnm1::kanMX6, leu1.32, h+</i>	This study

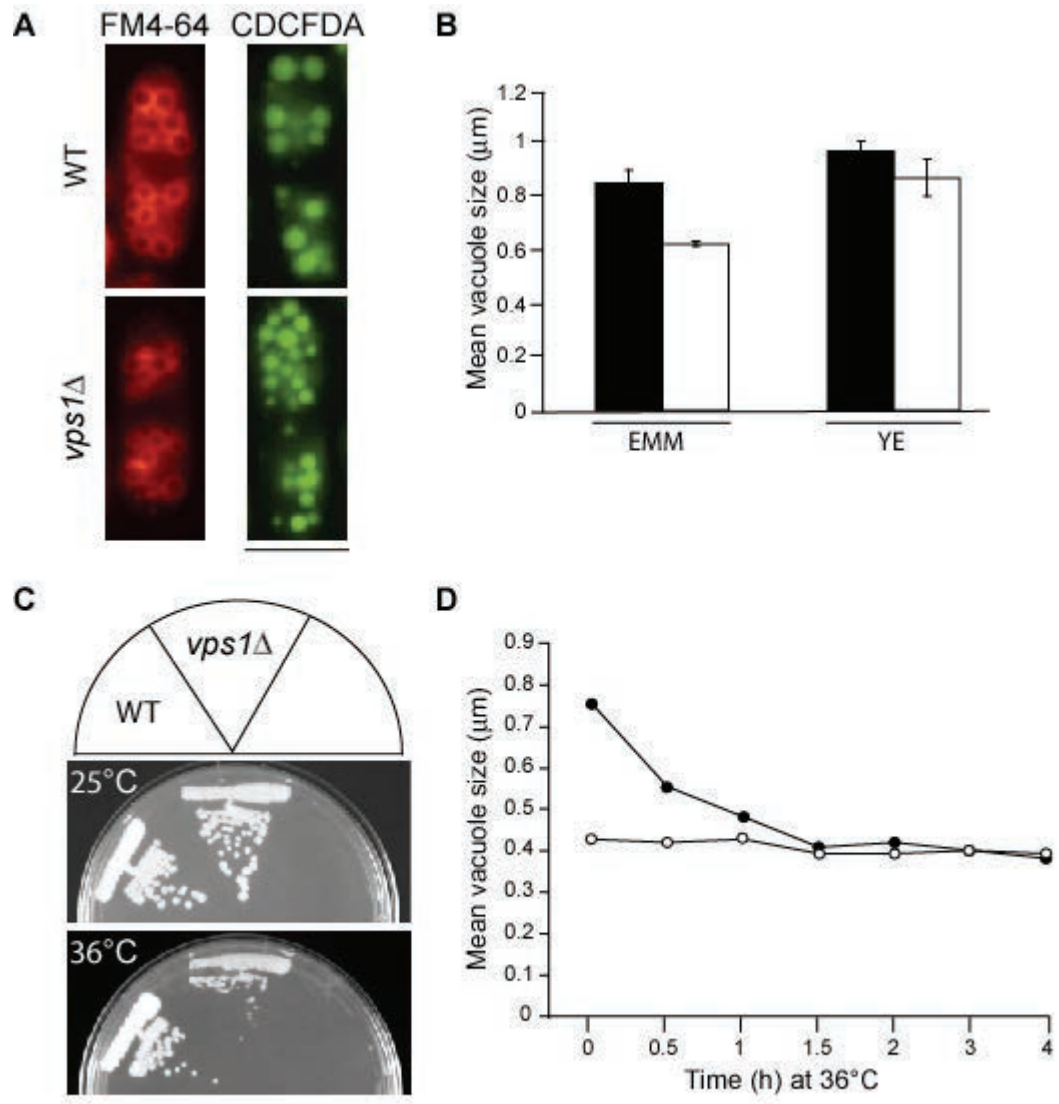


Figure 1. Rothlisberger *et al.*

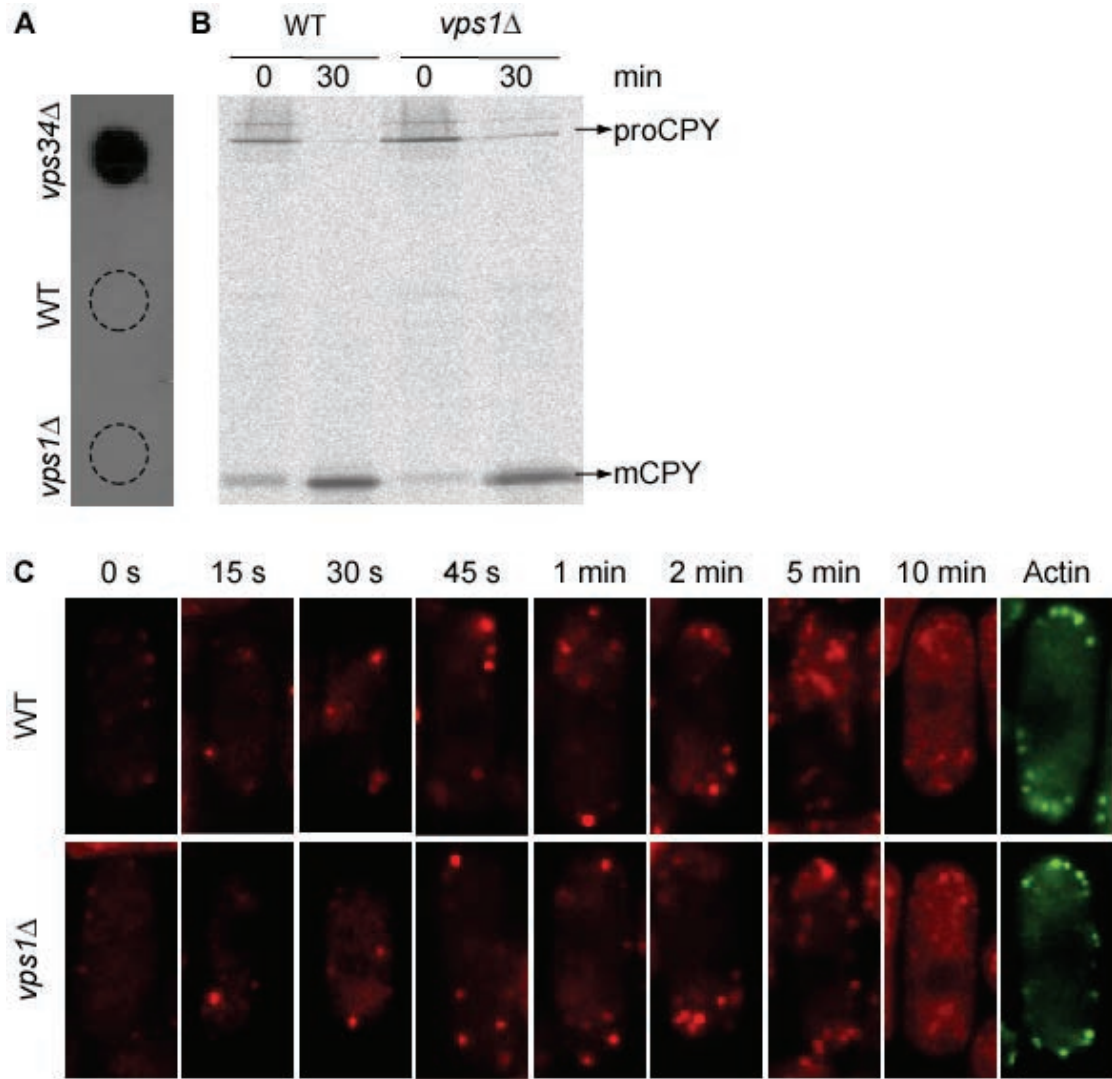


Figure 2. Rothlisberger *et al.*

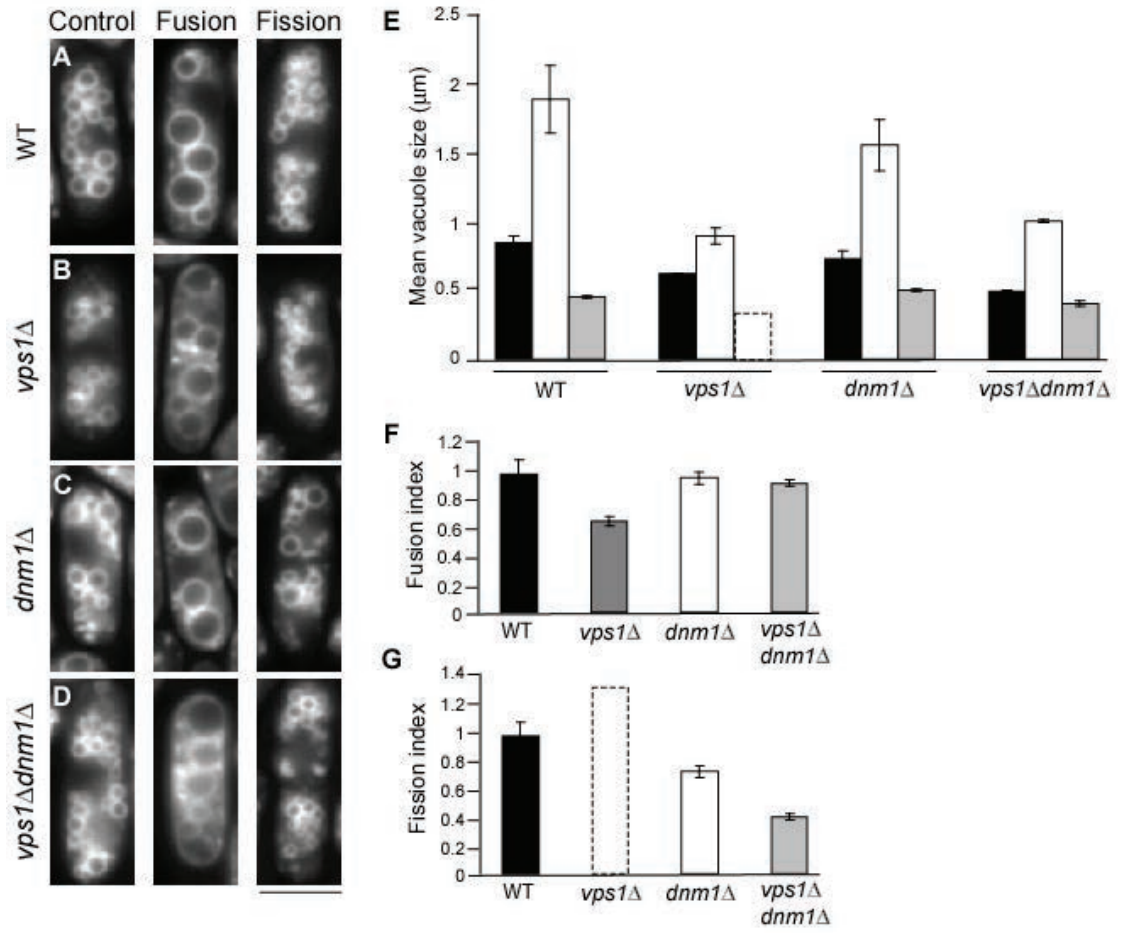


Figure 3. Rothlisberger *et al.*

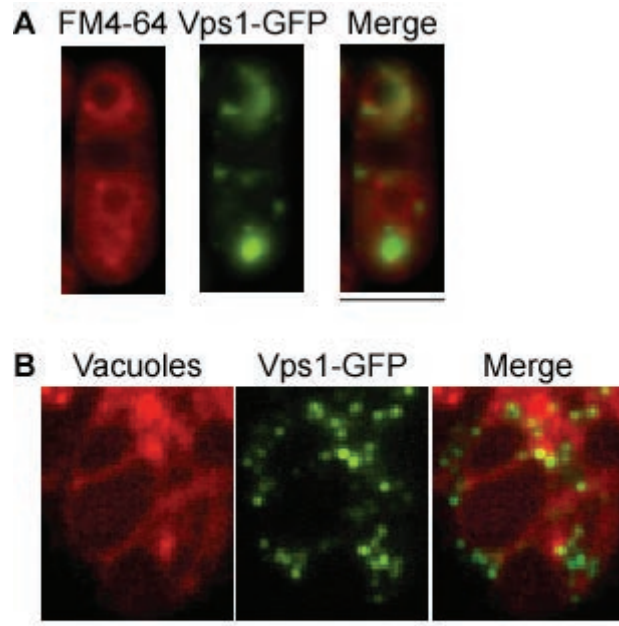
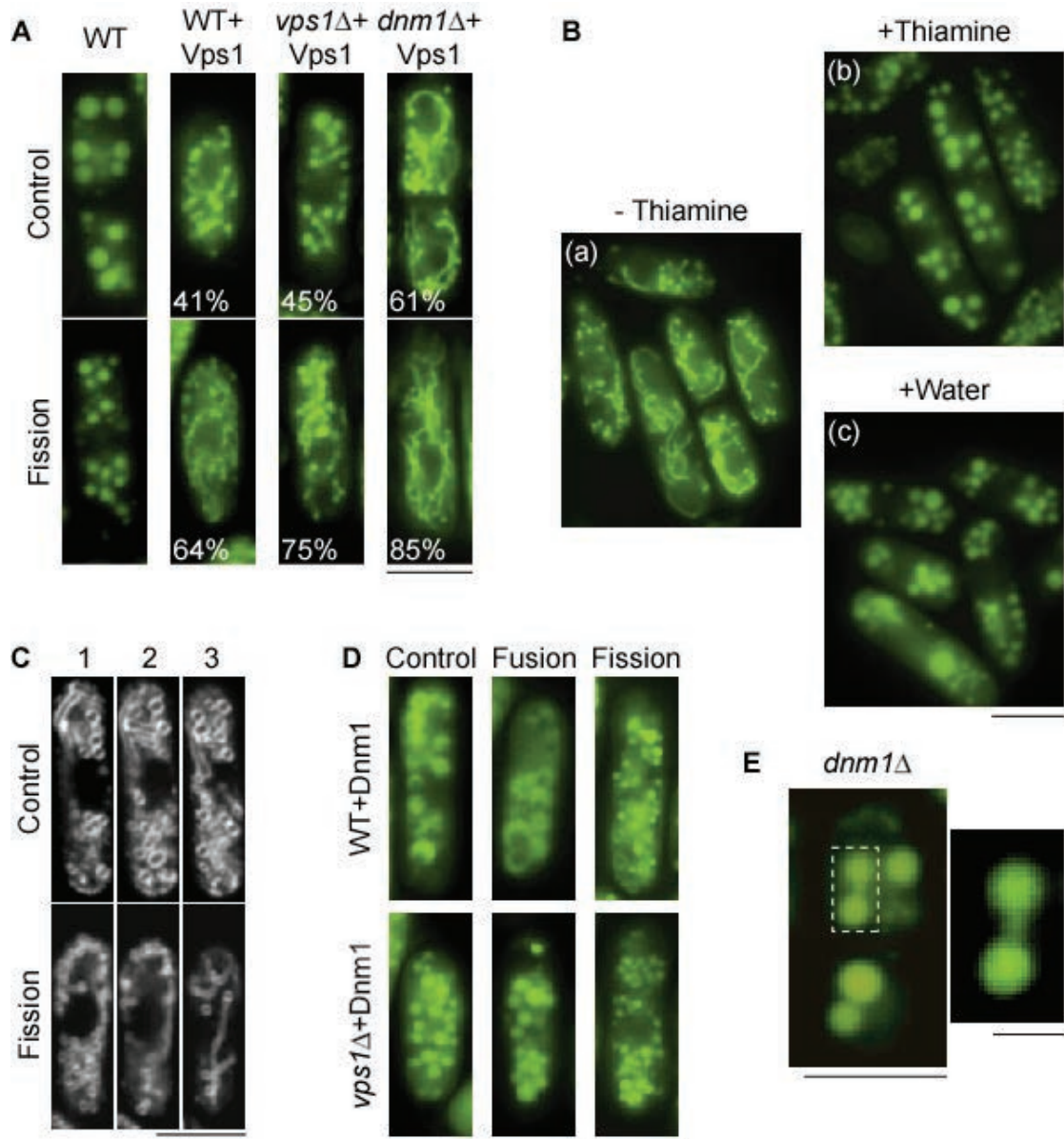


Figure 4. Rothlisberger *et al.*

Figure 5. Rothlisberger *et al.*

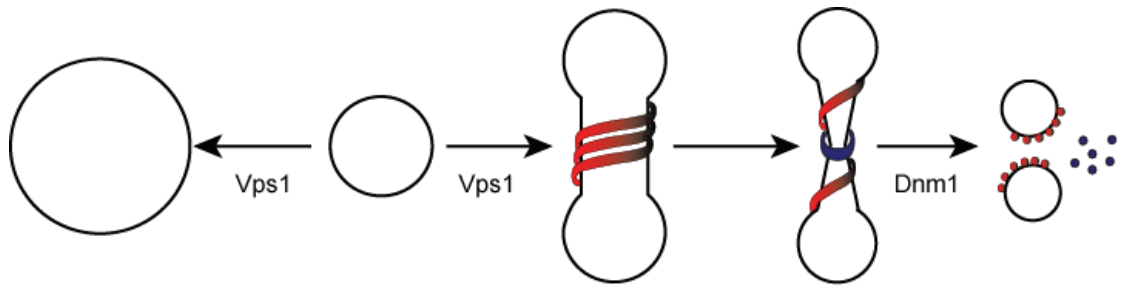


Figure 5. Rothlisberger *et al.*



## 7. BIBLIOGRAPHY

---

Alfa, C.E., Gallagher, I.M., and Hyams, J.S. (1993). Antigen localization in fission yeast. *Methods Cell Biol.* 37, 201-222.

Bard, F., and Malhotra, V. (2006). The Formation of TGN-to-Plasma-Membrane Transport Carriers. *Annual Review of Cell and Developmental Biology* 22, 439-455.

Bhar, D., Karren, M.A., Babst, M., and Shaw, J.M. (2006). Dimeric Dnm1-G385D Interacts with Mdv1 on Mitochondria and Can Be Stimulated to Assemble into Fission Complexes Containing Mdv1 and Fis1. *J Biol Chem* 281, 17312-17320.

Bleazard, W., McCaffery, J.M., King, E.J., Bale, S., Mozdy, A., Tieu, Q., Nunnari, J., and Shaw, J.M. (1999). The dynamin-related GTPase Dnm1 regulates mitochondrial fission in yeast. *Nat Cell Biol* 1, 298-304.

Bonangelino, C.J., Chavez, E.M., and Bonifacino, J.S. (2002). Genomic screen for vacuolar protein sorting genes in *Saccharomyces cerevisiae*. *Mol. Biol. Cell* 13, 2486-2501.

Bone, N., Millar, J.B.A., Toda, T., and Armstrong, J. (1998). Regulated vacuole fusion and fission in *Schizosaccharomyces pombe*: an osmotic response dependent on MAP kinases. *Current Biology* 8, 135-144.

Cao, H., Garcia, F., and McNiven, M.A. (1998). Differential Distribution of Dynamin Isoforms in Mammalian Cells. *Mol. Biol. Cell* 9, 2595-2609.

Castagnetti, S., Behrens, R., and Nurse, P. (2005). End4/Sla2 is involved in establishment of a new growth zone in *Schizosaccharomyces pombe*. *J Cell Sci* 118, 1843-1850.

Cobbett, C.S. (2000). Phytochelatins and Their Roles in Heavy Metal Detoxification. *Plant Physiol.* 123, 825-832.

Cole, L., Orlovich, D.A., and Ashford, A.E. (1998). Structure, Function, and Motility of Vacuoles in Filamentous Fungi. *Fungal Genetics and Biology* 24, 86-100.

Coue, M., Brenner, S.L., Spector, I., and Korn, E.D. (1987). Inhibition of actin polymerization by latrunculin A. *FEBS Letters* 213, 316-318.

Craven, R.A., Griffiths, D.J.F., Sheldrick, K.S., Randall, R.E., Hagan, I.M., and Carr, A.M. (1998). Vectors for the expression of tagged proteins in *Schizosaccharomyces pombe* *Gene* 221, 59-68.

Damke, H., Baba, T., Warnock, D.E., and Schmid, S.L. (1994). Induction of Mutant Dynamin Specifically Blocks Endocytic Coated Vesicle Formation. *The Journal of Cell Biology* 127, 915-934.

Damke, H., Binns, D.D., Ueda, H., Schmid, S.L., and Baba, T. (2001). Dynamin GTPase Domain Mutants Block Endocytic Vesicle Formation at Morphologically Distinct Stages. *Molecular Biology of the Cell* 12, 2578-2589.

Danino, D., Moon, K.H., and Hinshaw, J.E. (2004). Rapid constriction of lipid bilayers by the mechanochemical enzyme dynamin. *J Struct Biol* 147, 259-267.

David, C., McPherson, P.S., Mundigl, O., and De Camilli, P. (1996). A role of amphiphysin in synaptic vesicle endocytosis suggested by its binding to dynamin in nerve terminals. *Proceedings of the National Academy of Sciences* 93, 331-335.

Dever, T.E., Glynias, M.J., and Merrick, W.C. (1987). GTP-binding domain: three consensus sequence elements with distinct spacing. *Proc. Natl. Acad. Sci. USA*. 84, 1814-1818.

Feierbach, B., and Chang, F. (2001). Roles of the fission yeast formin for3p in cell polarity, actin cable formation and symmetric cell division. *Current Biology* 11, 1656-1665.

Forsburg, S.L., and Rhind, N. (2006). Basic methods for fission yeast. *Yeast* 23, 173-183.

Fukushima, N.H., Brisch, E., Keegan, B.R., Bleazard, W., and Shaw, J.M. (2001). The GTPase Effector Domain Sequence of the Dnm1p GTPase Regulates Self-Assembly and Controls a Rate-limiting Step in Mitochondrial Fission. *Mol. Biol. Cell* 12, 2756-2766.

Gachet, Y., and Hyams, J.S. (2005). Endocytosis in fission yeast is spatially associated with the actin cytoskeleton during polarised cell growth and cytokinesis. *J Cell Sci* 118, 4231-4242.

Gammie, A.E., Kurihara, L.J., Vallee, R.B., and Rose, M.D. (1995). DNM1, a dynamin-related gene, participates in endosomal trafficking in yeast. *J Cell Bio* 130, 553-566.

Guillou, E., Bousquet, C., Daloyau, M., Emorine, L.J., and Belenguer, P. (2005). Msp1p is an intermembrane space dynamin-related protein that mediates mitochondrial fusion in a Dnm1p-dependent manner in *S. pombe*. *FEBS Letters* 579, 1109-1116.

Gurunathan, S., David, D., and Gerst, J.E. (2002). Dynamin and clathrin are required for the biogenesis of a distinct class of secretory vesicles in yeast. *EMBO Journal* 21, 602-614.

Guthrie, B.A., and Wickner, W. (1988). Yeast vacuoles fragment when microtubules are disrupted. *J Cell Bio* 107, 115-120.

Harsay, E., and Schekman, R. (2002). A subset of yeast vacuolar protein sorting mutants is blocked in one branch of the exocytic pathway. *J. Cell Biol.* 156, 271-286.

Henley, J.R., Cao, H., and McNiven, M.A. (1999). Participation of dynamin in the biogenesis of cytoplasmic vesicles. *FASEB J.* 13, 243S-247.

Herskovits, J.S., Shpetner, H.S., Burgess, C.C., and Vallee, R.B. (1993). Microtubules and Src homology 3 domains stimulate the dynamin GTPase via its C terminal domain. *PNAS*, 11468-11472.

Hinshaw, J.E. (1999). Dynamin Spirals. *Current Opinion in Structural Biology* 9, 260-267.

Hoepfner, D., Berg, M.v.d., Philippsen, P., Tabak, H.F., and Hettema, E.H. (2001). A role for Vps1p, actin, and the Myo2p motor in peroxisome abundance and inheritance in *Saccharomyces cerevisiae*. *The Journal of Cell Biology* 155, 979-990.

Hyde, G.J., and Ashford, A.E. (1997). Vacuole motility and tubule-forming activity in *Pisolithus tinctorius* hyphae are modified by environmental conditions. *Protoplasma* 198, 85-92.

Hyde, G.J., Davies, D., Perasso, L., Cole, L., and Ashford, A.E. (1999). Microtubules, But Not Actin Microfilaments, Regulate Vacuole Motility and Morphology in Hyphae of *Pisolithus tinctorius*. *Cell Motility and the Cytoskeleton* 42, 114-124.

Ingerman, E., Perkins, E.M., Marino, M., Mears, J.A., McCaffery, J.M., Hinshaw, J.E., and Nunnari, J. (2005). Dnm1 forms spirals that are structurally tailored to fit mitochondria. *J Cell Bio* 170, 1021-1027.

Iwaki, T., Hosomi, A., Tokudomi, S., Kusunoki, Y., Fujita, Y., Giga-Hama, Y., Tanaka, N., and Takegawa, K. (2006). Vacuolar protein sorting receptor in *Schizosaccharomyces pombe*. *Microbiology* 152, 1523-1532.

Jones, S.M., Howell, K.E., Henley, J.R., Cao, H., and McNiven, M.A. (1998). Role of dynamin in the formation of transport vesicles from the trans-Golgi network. *Science* 279, 573-577.

Jourdain, I., Sontam, D., Johnson, C., Dillies, C., and Hyams, J.S. (2008). Dynamin-Dependent Biogenesis, Cell Cycle Regulation and Mitochondrial Association of Peroxisomes in Fission Yeast. *Traffic* 9, 1-13.

Katzmann, D.J., and Odorizzi, G.E., S. D. (2002). Receptor downregulation and multivesicular-body sorting. *Nat Rev Mol Cell Biol* 3, 893-905.

Kim, Y., Chattopadhyay, S., Locke, S., and Pearce, D.A. (2005). Interaction among Btn1p, Btn2p, and Ist2p Reveals Potential Interplay among the Vacuole, Amino Acid Levels, and Ion Homeostasis in the Yeast *Saccharomyces cerevisiae*. *Eukaryotic Cell* 4, 281-288.

Klionsky, D.J., and Ohsumi, Y. (1999). Vacuolar import of proteins and organelles from the cytoplasm. *Annu Rev Cell Dev Biol* 15, 1-32.

Koch, A., Schneider, G., Luers, G.H., and Schrader, M. (2004). Peroxisome elongation and constriction but not fission can occur independently of dynamin-like protein 1. *J Cell Sci* 117, 3995-4006.

Koch, A., Thiemann, M., Grabenbauer, M., Yoon, Y., McNiven, M.A., and Schrader, M. (2003). Dynamin-like Protein 1 Is Involved in Peroxisomal Fission. *J. Biol. Chem.* 278, 8597-8605.

Kosaka, T., and Ikeda, K. (1983a). Possible temperature-dependent blockage of synaptic vesicle recycling induced by a single gene mutation in *Drosophila*. *J Neurobiol.* 14, 207-225.

Kosaka, T., and Ikeda, K. (1983b). Reversible blockage of membrane retrieval and endocytosis in the garland cell of the temperature-sensitive mutant of *Drosophila melanogaster*, shibirets1. *J. Cell Biol.* 97, 499-507.

Kuravi, K., Nagotu, S., Krikken, A.M., Sjollem, K., Deckers, M., Erdmann, R., Veenhuis, M., and van der Klei, I.J. (2006). Dynamin-related proteins Vps1p and Dnm1p control peroxisome abundance in *Saccharomyces cerevisiae*. *J Cell Sci* 119, 3994-4001.

- Lauvrak, S.U., Torgersen, M.L., and Sandvig, K. (2004). Efficient endosome-to-Golgi transport of Shiga toxin is dependent on dynamin and clathrin. *J Cell Sci* *117*, 2321-2331.
- Legesse-Miller, A., Massol, R.H., and Kirchhausen, T. (2003). Constriction and Dnm1p Recruitment Are Distinct Processes in Mitochondrial Fission. *Mol. Biol. Cell* *14*, 1953-1963.
- Marks, B., Stowell, M.H.B., Vallis, Y., Mills, I.G., Gibson, A., Hopkins, C.R., and McMahon, H.T. (2001). GTPase activity of dynamin and resulting conformation change are essential for endocytosis. *Nature* *410*, 231-235.
- Marks, J., and Hyams, J.S. (1985). Localization of F-actin through the cell division cycle of *Schizosaccharomyces pombe*. *Eur. J. Cell Biol.* *39*, 27-32.
- Maudrell, K. (1990). *nmt1* of fission yeast. A highly transcribed gene completely repressed by thiamine. *J. Biol. Chem.* *265*, 10857-10864.
- Moreno, S., Klar, A., and Nurse, P. (1991). Molecular Genetic Analysis of Fission Yeast *Schizosaccharomyces pombe*. *Methods in Enzymology* *194*, 795-823.
- Morishita, M., and Shimoda, C. (2000). Positioning of medial actin rings affected by eccentrically located nuclei in a fission yeast mutant having large vacuoles. *FEMS Microbiol Lett.* *188*, 63-67.
- Morita, T., and Takegawa, K. (2004). A simple and efficient procedure for transformation of *Schizosaccharomyces pombe*. *Yeast* *21*, 613-617.
- Muhlberg, A.B., Warnock, D.E., and Schmid, S.L. (1997). Domain structure and intramolecular regulation of dynamin GTPase. *EMBO Journal* *16*, 6676-6683.
- Mulvihill, D.P., Pollard, P.J., Win, T.Z., and Hyams, J.S. (2001). Myosin V-mediated vacuole distribution and fusion in fission yeast. *Current Biology* *11*, 1124-1127.

Naylor, K., Ingerman, E., Okreglak, V., Marino, M., Hinshaw, J.E., and Nunnari, J. (2006). Mdv1 Interacts with Assembled Dnm1 to Promote Mitochondrial Division. *J. Biol. Chem.* *281*, 2177-2183.

Nothwehr, S.F., Conibear, E., and Stevens, T.H. (1995). Golgi and vacuolar membrane proteins reach the vacuole in *vps1* mutant yeast cells via the plasma membrane. *J Cell Biol* *129*, 35-46.

Obar, R.A., Collins, C.A., Hammarback, J.A., Shpetner, H.S., and Vallee, R.B. (1990). Molecular cloning of the microtubule-associated mechanochemical enzyme dynamin reveals homology with a new family of GTP-binding proteins. *Nature* *347*, 256-261.

Otsuga, D., Keegan, B.R., Brisch, E., Thatcher, J.W., Hermann, G.J., Bleazard, W., and Shaw, J.M. (1998). The dynamin-related GTPase, Dnm1p, controls mitochondrial morphology in yeast. *J Cell Bio* *143*, 333-349.

Pelham, R.J., and Chang, F. (2001). Role of actin polymerization and actin cables in actin-patch movement in *Schizosaccharomyces pombe*. *Nat Cell Biol* *3*, 235-244.

Peters, C., Baars, T.L., Buhler, S., and Mayer, A. (2004). Mutual control of membrane fission and fusion proteins. *Cell* *119*, 667-678.

Pitts, K.R., McNiven, M.A., and Yoon, Y. (2004). Mitochondria-specific function of the dynamin family protein DLP1 is mediated by its C-terminal domains. *J Biol Chem* *279*, 50286-50294.

Pitts, K.R., Yoon, Y., Krueger, E.W., and McNiven, M.A. (1999). The Dynamin-like Protein DLP1 Is Essential for Normal Distribution and Morphology of the Endoplasmic Reticulum and Mitochondria in Mammalian Cells. *Mol. Biol. Cell* *10*, 4403-4417.

Praefcke, G.J., and McMahon, H.T. (2004). The dynamin superfamily: universal membrane tubulation and fission molecules? *Nat Rev Mol Cell Biol.* *5*, 133-147.

Ramachandran, R., and Schmid, S.L. (2008). Real-time detection reveals that effectors couple dynamin's GTP-dependent conformational changes to the membrane. *The Embo Journal* *27*, 27-37.

Raymond, C.K., Howald-Stevenson, I., Vater, C.A., and Stevens, T.H. (1992). Morphological classification of the yeast vacuolar protein sorting mutants: evidence for a prevacuolar compartment in class E vps mutants. *Mol. Biol. Cell* *3*, 1389-1402.

Rothman, J.H., Raymond, C.K., Gilbert, T., O'Hara, P.J., and Stevens, T.H. (1990). A putative GTP binding protein homologous to interferon-inducible Mx proteins performs an essential function in yeast protein sorting. *Cell* *61*, 1063-1074.

Rothman, J.H., and Stevens, T.H. (1986). Protein sorting in yeast: Mutants defective in vacuole biogenesis mislocalize vacuolar proteins into the late secretory pathway. *Cell* *47*, 1041-1051.

Roux, A., Uyhazi, K., Frost, A., and De Camilli, P. (2006). GTP-dependent twisting of dynamin implicates constriction and tension in membrane fission. *Nature* *441*, 528-531.

Samuels, A.L., Giddings, T.H., Jr., and Staehelin, L.A. (1995). Cytokinesis in tobacco BY-2 and root tip cells: a new model of cell plate formation in higher plants. *J. Cell Biol.* *130*, 1345-1357.

Schmid, S.L., McNiven, M.A., and De Camilli, P. (1998). Dynamin and its partners: a progress report. *Curr Opin Cell Biol.* *10*, 504-512.

Seeley, E.S., Kato, M., Margolis, N., Wickner, W., and Eitzen, G. (2002). Genomic Analysis of Homotypic Vacuole Fusion. *Mol. Biol. Cell* *13*, 782-794.

Sesaki, H., and Jensen, R.E. (1999). Division versus Fusion: Dnm1p and Fzo1p Antagonistically Regulate Mitochondrial Shape. *J. Cell Biol.* *147*, 699-706.



Sesaki, H., Southard, S.M., Hobbs, A.E., and Jensen, R.E. (2003). Cells lacking Pcp1p/Ugo2p, a rhomboid-like protease required for Mgm1p processing, lose mtDNA and mitochondrial structure in a Dnm1p- dependent manner, but remain competent for mitochondrial fusion. *Biochem Biophys Res Commun* 308, 276-283.

Shaw, J.M., and Nunnari, J. (2002). Mitochondrial dynamics and division in budding yeast. *Trends Cell Biology* 12, 178-184.

Shin, H.-W., Shinotsuka, C., Torii, S., Murakami, K., and Nakayama, K. (1997). Identification and Subcellular Localization of a Novel Mammalian Dynamin-Related Protein Homologous to Yeast Vps1p and Dnm1p. *J. Biochem* 122, 525-530.

Shoji, J.Y., Arioka, M., and Kitamoto, K. (2006). Possible involvement of pleiomorphic vacuolar networks in nutrient recycling in filamentous fungi. *Autophagy* 2, 226-227.

Shupliakov, O., Löw, P., Grabs, D., Gad, H., Chen, H., David, C., Takei, K., Camilli, P.D., and Brodin, L. (1997). Synaptic vesicle endocytosis impaired by disruption of dynamin-SH3 domain interactions. *Science* 276, 259-263.

Sipiczki, M., Takeo, K., and Grallert, A. (1998). Growth polarity transitions in a dimorphic fission yeast. *Microbiology* 144, 3475-3485.

Smirnova, E., Griparic, L., Shurland, D.-L., and van der Bliek, A.M. (2001). Dynamin-related Protein Drp1 Is Required for Mitochondrial Division in Mammalian Cells. *Mol. Biol. Cell* 12, 2245-2256.

Smirnova, E., Shurland, D.-L., Newman-Smith, E.D., Pishvaee, B., and van der Bliek, A.M. (1999). A Model for Dynamin Self-assembly Based on Binding Between Three Different Protein Domains. *J. Biol. Chem.* 274, 14942-14947.

Smirnova, E., Shurland, D.-L., Ryazantsev, S.N., and van der Bliek, A.M. (1998). A Human Dynamin-related Protein Controls the Distribution of Mitochondria. *J. Cell Biol.* 143, 351-358.

Spector, I., Shochet, N.R., Kashman, Y., and Groweiss, A. (1983). Latrunculins: novel marine toxins that disrupt microfilament organization in cultured cells. *Science* *219*, 493-495.

Stowell, M.H., Marks, B., Wigge, P., and McMahon, H.T. (1999). Nucleotide-dependent conformational changes in dynamin: evidence for a mechanochemical molecular spring. *Nat Cell Biol* *1*, 27-32.

Swanson, J., Bushnell, A., and Silverstein, S.C. (1987). Tubular Lysosome Morphology and Distribution within Macrophages Depend on the Integrity of Cytoplasmic Microtubules. *Proceedings of the National Academy of Sciences* *84*, 1921-1925.

Sweitzer, S.M., and Hinshaw, J.E. (1998). Dynamin Undergoes a GTP-Dependent Conformational Change Causing Vesiculation *Cell* *93*, 1021-1029

Tabuchi, M., Iwaihara, O., Ohtani, Y., Ohuchi, N., Sakurai, J., Morita, T., Iwahara, S., and Takegawa, K. (1997). Vacuolar protein sorting in fission yeast: cloning, biosynthesis, transport, and processing of carboxypeptidase Y from *Schizosaccharomyces pombe*. *J. Bacteriol.* *179*, 4179-4189.

Takegawa, K., DeWald, D.B., and Emr, S.D. (1995). *Schizosaccharomyces pombe* Vps34p, a phosphatidylinositol-specific PI 3-kinase essential for normal cell growth and vacuole morphology. *J Cell Sci* *108*, 3745-3756.

Takegawa, K., Iwaki, T., Fujita, Y., Morita, T., Hosomi, A., and Tanaka, N. (2003). Vesicle-mediated protein transport pathways to the vacuole in *Schizosaccharomyces pombe*. *Cell Structure and Function* *28*, 399-417.

Takei, K., Haucke, V., Slepnev, V., Farsad, K., Salazar, M., Chen, H., and De Camilli, P. (1998). Generation of coated intermediates of clathrin-mediated endocytosis on protein-free liposomes. *Cell* *94*, 131-141.

Takei, K., McPherson, P.S., Schmid, S.L., and De Camilli, P. (1995). Tubular membrane invaginations coated by dynamin rings are induced by GTP-gamma S in nerve terminals. *Nature* 374, 186-190.

Tarutani, Y., Ohsumi, K., Arioka, M., Nakajima, H., and Kitamoto, K. (2001). Cloning and characterization of *Aspergillus nidulans* vpsA gene which is involved in vacuolar biogenesis. *Gene* 268, 23-30.

Tournier, S., Gachet, Y., Buck, V., Hyams, J.S., and Millar, J. (2004). Disruption of Astral Microtubule Contact with the Cell Cortex Activates a Bub1, Bub3, and Mad3-dependent Checkpoint in Fission Yeast. *Molecular Biology of the Cell* 15, 3345–3356.

Tuma, P.L., and Collins, C.A. (1994). Activation of dynamin GTPase is a result of positive cooperativity. *J. Biol. Chem.* 269, 30842-30847.

Umesono, K., Toda, T., Hayashi, S., and Yanagida, M. (1983). Cell division cycle genes *nda2* and *nda3* of the fission yeast *Schizosaccharomyces pombe* control microtubular organization and sensitivity to anti-mitotic benzimidazole compounds. *J Mol Bio* 168, 271-284.

Vater, C.A., Raymond, C.K., Ekena, K., Howald-Stevenson, I., and Stevens, T.H. (1992). The VPS1 protein, a homolog of dynamin required for vacuolar protein sorting in *Saccharomyces cerevisiae*, is a GTPase with two functionally separable domains. *J. Cell Biol.* 119, 773-786.

Verma, D.P., and Hong, Z. (2005). The ins and outs in membrane dynamics: tubulation and vesiculation. *. Trends Plant Sci.* 10, 159-165.

Verma, D.P.S. (2001). Cytokinesis and building of the cell plate in plants. *Annu. Rev. Plant Physiol. Plant Mol. Biol.* 52, 751-784.

Vida, T.A., and Emr, S.D. (1995). A new vital stain for visualizing vacuolar membrane dynamics and endocytosis in yeast. *J. Cell Biol.* 128, 779-792.

Vizeacoumar, F.J., Vreden, W.N., Fagarasanu, M., Eitzen, G.A., Aitchison, J.D., and Rachubinski, R.A. (2006). The Dynamin-like Protein Vps1p of the Yeast *Saccharomyces cerevisiae* Associates with Peroxisomes in a Pex19p-dependent Manner. *J. Biol. Chem.* *281*, 12817-12823.

Wang, L., Merz, A.J., Collins, K.M., and Wickner, W. (2003). Hierarchy of protein assembly at the vertex ring domain for yeast vacuole docking and fusion. *Journal of Cell Biology* *160*, 365-374.

Wang, L., Seeley, E.S., Wickner, W., and Merz, A.J. (2002). Vacuole fusion at a ring of vertex docking sites leaves membrane fragments within the organelle. *Cell* *108*, 357-369.

Warnock, D.E., Hinshaw, J.E., and Schmid, S.L. (1996). Dynamin Self-assembly Stimulates Its GTPase Activity. *J. Biol. Chem.* *271*, 22310-22314.

Warren, G., and Wickner, W. (1996). Organelle inheritance. *Cell* *84*, 395-400.

Weisman, L.S. (2006). Organelles on the move: insights from yeast vacuole inheritance. *Nat Rev Mol Cell Biol* *7*, 243-252.

Wilsbach, K., and Payne, G.S. (1993). Vps1p, a member of the dynamin GTPase family, is necessary for Golgi membrane protein retention in *Saccharomyces cerevisiae*. *EMBO Journal* *12*, 3049-3049.

Wong, E.D., Wagner, J.A., Scott, S.V., Okreglak, V., Holewinski, T.J., Cassidy-Stone, A., and Nunnari, J. (2003). The intramitochondrial dynamin-related GTPase, Mgm1p, is a component of a protein complex that mediates mitochondrial fusion. *J. Cell Biol.* *160*, 303-311.

Yoon, Y., Pitts, K.R., and McNiven, M.A. (2001). Mammalian Dynamin-like Protein DLP1 Tubulates Membranes. *Mol. Biol. Cell* *12*, 2894-2905.

Yoshida, Y., and Takei, K. (2005). Stimulation of Dynamin GTPase Activity by Amphiphysin Methods in *Enzymology* 404, 528-537

Yu, X., and Cai, M. (2004). The yeast dynamin-related GTPase Vps1p functions in the organization of the actin cytoskeleton via interaction with Sla1p. *J Cell Sci* 117, 3839-3853.

Zhang, Z., Hong, Z., and Verma, D.P.S. (2000). Phragmoplastin Polymerizes into Spiral Coiled Structures via Intermolecular Interaction of Two Self-assembly Domains. *J. Biol. Chem.* 275, 8779-8784.